Interaction Properties of hnRNP-U Family Proteins

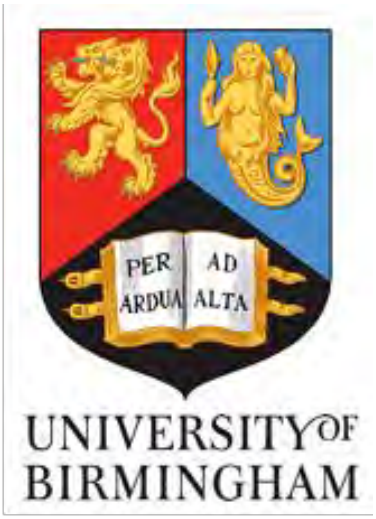

Submitted by Kenny Pratt

[redacted]

This project is submitted in partial fulfilment of the requirements for the award of the MRes

Supervisors: Dr Roger Grand & Dr Grant Stewart

Abstract

The efficient repair of DNA damage through highly co-ordinated repair pathways, such as homologous recombination (HR), is critical for cell viability. In addition to heterogenous nuclear ribonuclearproteins (hnRNPs) exhibiting influences through controlling the expression levels of DNA repair proteins via their mRNA processing activities, hnRNPs have recently been shown to have roles within the DNA damage response (DDR). Previous studies have shown hnRNP-U-like1 (hnRNP-UL1) and hnRNP-U-like2 (hnRNP-UL2) to interact with the NBS1 subunit of the MRN complex, p53, CtIP and BLM, all of which have essential roles in the DDR.

Within this study, interactions between the hnRNP-U-like proteins and p53, CtIP and BLM were confirmed both *in vitro* and *in vivo*. Binding of p53 was mapped to a BBS-RGG domain fragment of hnRNP-UL1, whilst CtIP and BLM required interactions beyond the extent of the BBS-RGG domain fragment despite showing that these domains were critical for interaction. Regions at the N-terminal and C-terminal ends of BLM were shown to be required for binding to hnRNP-UL1 and –UL2, with the BBS-RGG domain of hnRNP-UL1 being essential for these interactions. The hnRNP-ULs were also shown to interact with one another and also with various other hnRNPs *in vivo*, whilst a novel interaction between PARP and the hnRNP-ULs was also identified. This observation, along with the confirmation of the protein-protein interactions of various other studies, which reveal a link between hnRNP-U-like proteins and DNA damage response proteins, have verified the extensive associations and potential roles of hnRNP-U-like proteins within the DDR.

Acknowledgements

I would like to thank Dr Roger Grand and Dr Grant Stewart for their help, advice and guidance, both in the laboratory and in the writing of this project. I would also like to thank Dr Andrew Turnell, Paul Minshal and Ellis Ryan for their continual support.

List of Contents

List of Figures and Tables

Chapter One:

Introduction

1.1 Heterogenous Nuclear Ribonuclearproteins (hnRNPs)

Heterogenous nuclear ribonuclearproteins (hnRNPs) are a large family of diverse proteins and whilst exhibiting overlap in structure and function, they do not necessarily exhibit extensive homology to one another [1]. They exist as complexes of both protein and RNA, and reside largely in the cell nucleus. They were first characterised functionally by their roles in mRNA metabolism [2]. Pre-mRNA molecules require processing to become mature mRNA, involving packaging, processing, export and localisation to production sites in the cytoplasm. This is largely executed by complexes of hnRNPs. In recent years they have been implemented in a far wider range of cellular activities, including the DNA damage response, which is the focus of this study [1]. During hnRNP's mRNA processing they facilitate RNA binding through complementary nucleotide interactions to their own sequence-specific RNAs. hnRNPs involvement in other cellular activities, such as DNA repair, has also shown their protein-binding capabilities. This direct protein-protein binding of human hnRNP-U-L1 and hnRNP-U-L2 was explored during this study.

1.2 hnRNP-UL1 and –UL2

hnRNP-UL1 was originally known as E1B-AP5 (adenovirus early region 1B-associated protein 5) due to its interaction with the adenovirus E1B-55 kDa protein during the course of lytic infection [3]. Its naming as hnRNP-UL1 and also the naming of hnRNP-UL2, unsurprisingly relates to its significant homology to hnRNP-U (SAF-A) [3,4]. hnRNP-UL1 and -UL2 share 43% total homology to one another, with significant homology across various domains of the protein (Figure 1.2). The SAP (SAF-A/B, Acinus and PIAS) domain is a DNA binding domain, whilst the SPRY (SPIa/Ryanodine receptor domain) has no known function of yet [5]. The RGG is a common domain amongst hnRNPs and is characterized by closely spaced clusters of Arg-Gly-Gly tripeptide repeats with interspersed aromatic (Phe, Tyr) residues. It was originally thought that the RGG box was solely involved in RNA-binding, however, within hnRNP-A1 and -G it is found in combination with other RNA-binding elements suggesting other possible roles [6]. Of greater interest to this study were the BBS (BRD7-binding site) domain, the RGG (arginine and glycine-rich region) box, and the PP (proline-rich region) region as they had already been implicated in some protein interactions. The availability of defined fragments of hnRNP-UL1 containing these regions allowed the assessment of their importance in protein interactions.

The role of hnRNP-UL1 in mRNA processing and transport were outlined earlier [3]. In more recent years it has been found to have roles in the DNA damage response (DDR). HnRNP-UL1 has been shown to interact with p53, BRD7, CtIP and BLM [7,8,9,4]. It is direct protein-protein interactions with DNA damage response proteins that were investigated within this study.

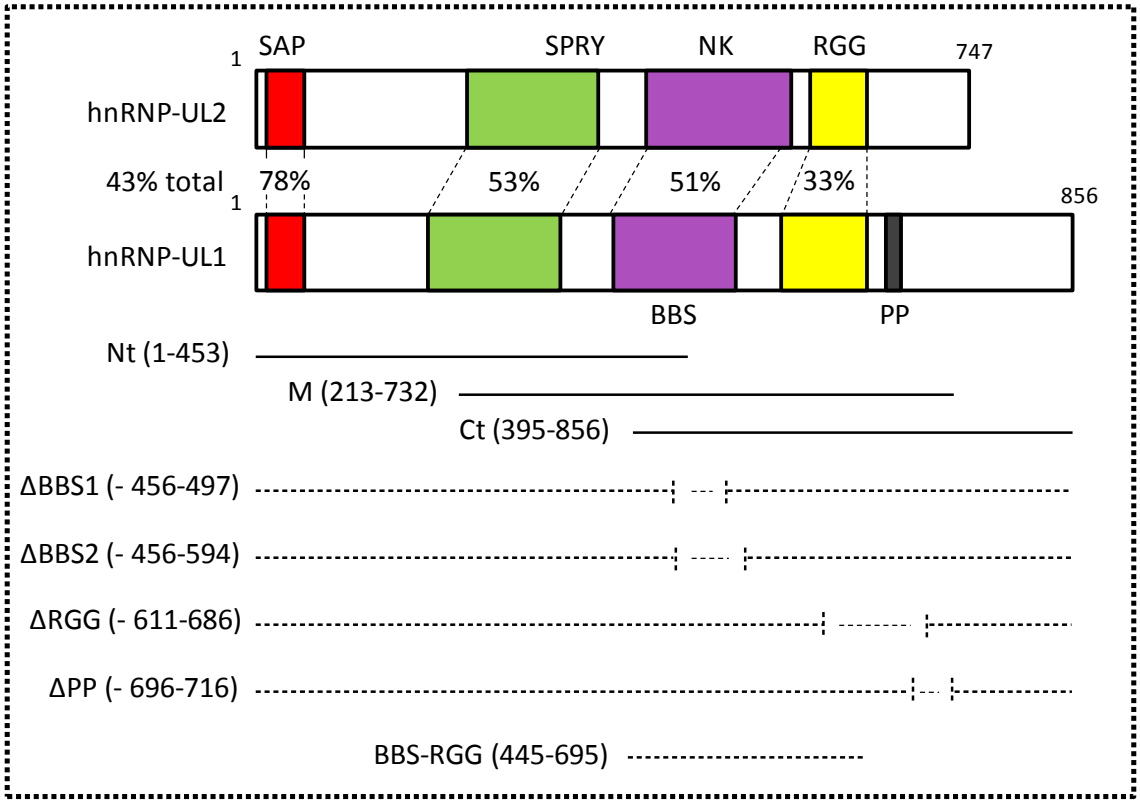

Figure 1.2 – Structure of hnRNP-UL1 and -UL2 and its Domains. A schematic representation of the full length (WT) hnRNP-U-like proteins and the various fragments expressed via *in vitro* translation or used for GST-pulldown experiments. SAP, SAF-A/B, Acinus and PIAS motif; SPRY, SPIa/Ryanodine receptor domain; NK, putative nucleoside/nucleotide kinase domain; BBS, BRD7-binding site; RGG, arginine and glycine-rich region, RNA and ssDNA binding; PP, proline-rich region; Nt, N-terminal fragment; M, middle fragment; Ct, C-terminal fragment. Percentages of amino acid homology are indicated (total and for coloured domains). Nt, M, Ct, ΔBBS1, ΔBBS2, ΔRGG, ΔPP and BBS-RGG refer to hnRNP-UL1 deletion mutants (adapted from [4]).

1.3 The DNA Damage Response

DNA is continuously coming under a barrage of attack from both endogenous and exogenous sources causing varied types of damage, including single-strand lesions, double-strand breaks and inter-strand crosslinks. Cells have a complex network of repair mechanisms to address such damage [10]. If repair is not undertaken efficiently, genomic instability can arise which may result in tumorigenesis. p53 has been termed ‘the guardian of the genome’

and is an extensively studied tumour suppressor protein. DNA damage is one of a number of upstream activators of p53, which when activated can mediate cell cycle arrest and DNA repair [11].

Critical regulators of DNA damage response (DDR) pathways are the PI3K (phosphatidylinositol 3 kinase) proteins, ATM (ataxia telangiectasia) and ATR (ataxia telangiectasia and RAD3-related) proteins, and their activation can trigger activities such as cell cycle inhibition, DNA repair or apoptosis, depending on the severity of the DNA damage. Simplistically, ATM is activated in response to double-stranded DNA breaks (DSBs) commonly caused by ionising radiation (IR), cellular stress and prolonged stalling of replication forks. ATR is activated in response to single-stranded DNA lesions induced by ultra-violet (UV) radiation [10].

The focus of this investigation is repair to double-strand breaks (DSBs), the most highly cytotoxic DNA lesions. DSBs are commonly repaired via two mechanisms; homologous recombination (HR) and non-homologous end joining (NHEJ). The cell's choice of repair mechanism is dependent upon the stage of the cell cycle as HR requires a section of homologous DNA in order to complete error-free repair. However, the sister chromatids required for such repair are only available during the S and G2 phases of the cycle. During other phases of the cell cycle NHEJ must be employed which is error-prone meaning the DNA sequence is often altered/mutated during repair [12].

To repair a DSB by HR, a cascade of tightly controlled protein signalling pathways must be activated to, firstly, recognise the DNA break, recruit repair factors and then execute accurate repair. Within the initial response to a DSB by HR, a distinct focal point around the location of the break is created and is often referred to as Ionizing Radiation-Induced Foci (IRIF) [13]. The MRN complex plays a critical role as it is the initial sensor of DSBs and through its intrinsic capacity to bind DNA it is able to recruit and stimulate ATM [14]. ATM is then activated by autophosphorylation at S1981. A large number of other proteins contribute to cell-cycle arrest, DNA repair and apoptosis (Figure 1.3a). One such protein is the histone H2AX, whose phosphorylation mediates interaction with the scaffold protein MDC1. MDC1 acts as a hub for many proteins involved in the DDR to attach and form repair foci, including the ubiquitin ligases RNF8, RNF168 and BRCA1 [15].

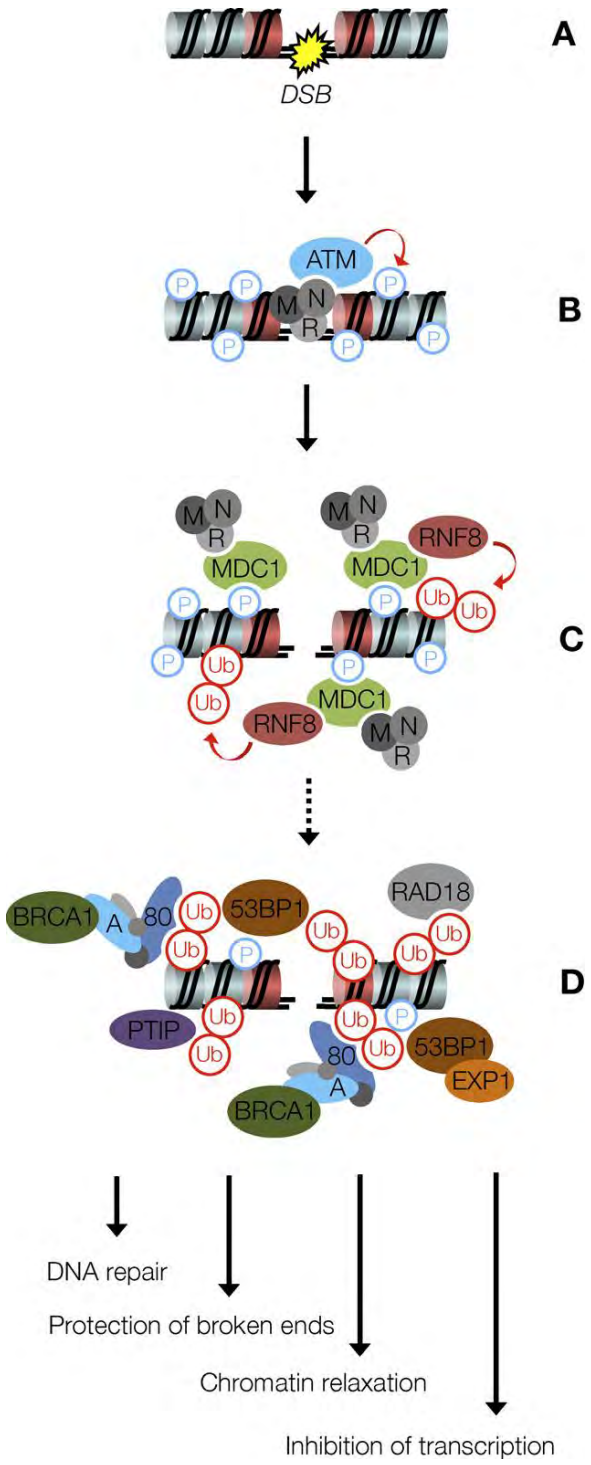

Figure 1.3a – The Early Responses to DSBs Resulting in the Highly Hierarchical Assembly of IRIF. The DSB is sensed by the MRN (MRE11-RAD50-NBS1) complex, which recruits the ATM kinase (A) resulting in turn in the recruitment of the scaffold protein MDC1 via phosphorylation of the histone H2AX. MDC1 recruits many proteins including the ubiquitin ligase RNF8, which ubiquitylates histones (C) to further recruit a second wave of repair factors such as 53BP1, the BRCA1 A complex and so on. The assembly of these repair proteins controls various DNA and chromatin transactions, ultimately leading to repair of the DSB. P: phosphate, M: MRE11, N: NBS1, R: RAD50, Ub: Ubiquitin, A: Abraxas (ABRA1), 80: Rap80, EXP1: EXPAND1 [16].

1.4 DNA End Resection During HR (Homologous Recombination)

Following the initial response to DSBs and accumulation of such repair foci, DNA end resection of the DSB is required to reveal ssDNA, which triggers ATR-dependent checkpoint signalling and DSB repair by HR [17]. This is essential in the recruitment of the homologous region of the complementary sister DNA strand upon which the error-free repair by HR is based. Once the ends of the break are resected, ssDNA is bound by the RPA protein complex, which subsequently recruits the Rad51 recombinase forming a nucleoprotein filament. Rad51 is responsible for the recruitment of the complementary sister strand, resulting in the

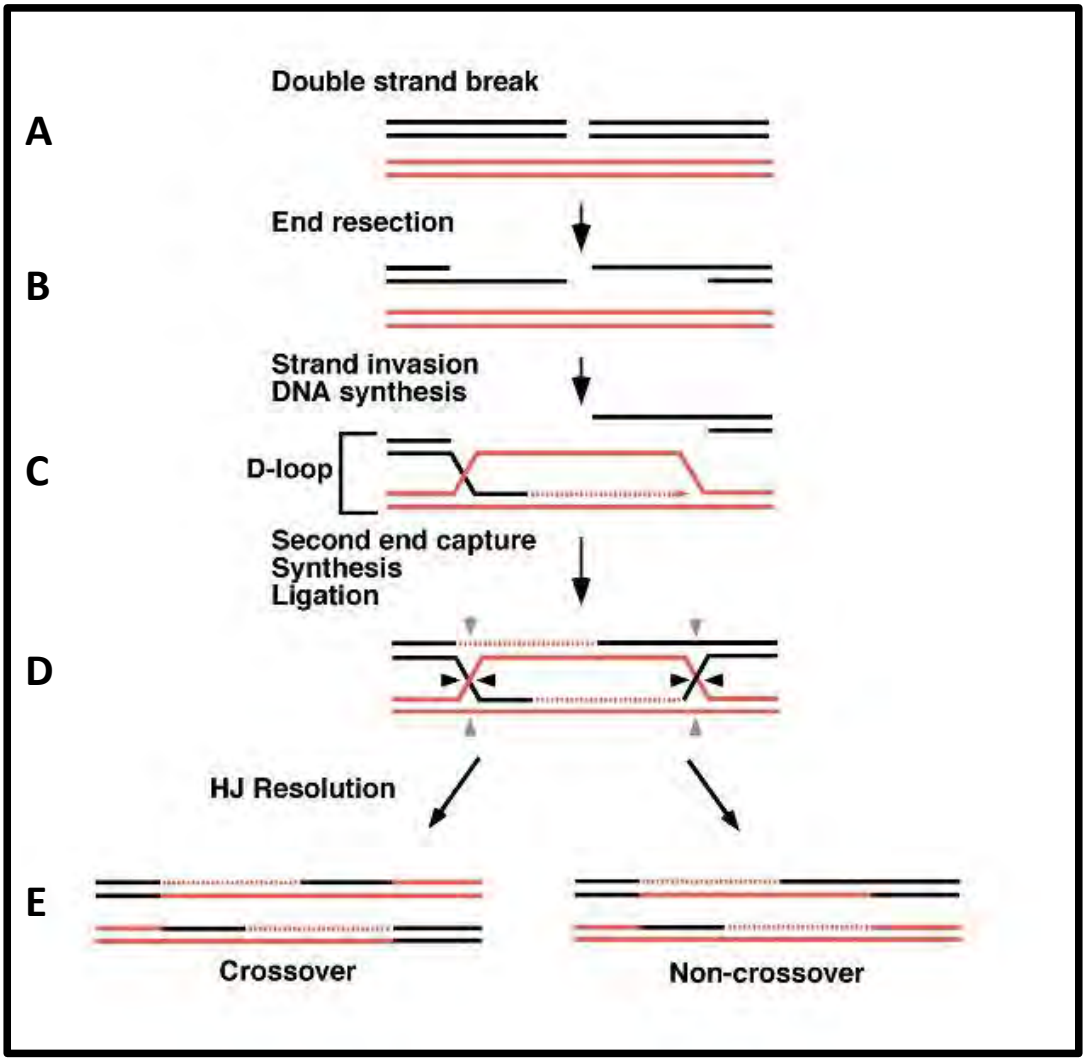

Figure 1.3b – The DNA Formations and Processing During DSB Repair by HR. A DSB occurs and repair foci form (A), followed by end resection (B) and the strand invasion by the recruited complementary sister DNA strand. DNA synthesis follows creating D-loop structures (C). Ligation of the DNA ends causes the formation of Holliday junctions (HJ) (D). Finally, these are junctions are resolved, which can result in the exchange (crossover) of DNA between sister chromatids (E) (adapted from [18]).

formation of displacement-loops (D-loops) and Holliday junctions (Figure 1.3b). A new strand is then synthesised by DNA polymerase, the two ends joined by a DNA ligase to repair the DSB and finally, the intermediate HJ structures are resolved [18].

1.5 CtIP in DNA End Resection

DNA end resection is carried out by a series of enzymes including nucleases and helicases. The C-terminal-binding protein interacting protein (CtIP), as the name suggests, was originally identified for its capability to bind CtBP (C-terminal-binding protein) [19]. CtIP is an endonuclease and through its interaction with the MRN complex (which also has its own exo- and endo-nuclease activity) it is able to mediate DSB end resection [17]. As well as interacting with the MRN complex, CtIP is known to be one of the phosphorylation targets of ATM and also binds to BRCA1 during responses to DSBs [20]. It is clear that CtIP is essential for resection and therefore efficient repair by HR. Studies have also shown that the phosphorylation of CtIP by ATM at serine residue 327 mediates the interaction with BRCA1 and this subsequently controls choice of the DSB repair pathway (either HR or NHEJ) depending on stage of the cell cycle [21,22].

1.6 BLM (Bloom Syndrome Protein) in DNA End Resection

Another protein central to DNA end resection and recombination is the Bloom Syndrome protein (BLM). BLM is a member of the RecQ family of DNA helicases. It is able to unwind dsDNA in the 3' to 5' direction and its role within sites of DSB repair stems from its affinity for recombination intermediates, such as D-loops and Holliday junctions [23]. BLM is recruited to repair foci and co-localises with γ-H2AX, clearly showing involvement in the DDR [24].

RecQ helicases are thought to possess both pro-recombinase and anti-recombinase activities. The prevention of excessive HR is indeed critical in avoiding genome rearrangements that may harm the cell. BLM was first recognized for its anti-recombinase activity [25]. Mutations in (i.e. loss of function of) BLM lead to the extremely rare, autosomal recessive disease Bloom Syndrome (BS). Of the 240 cases identified worldwide, symptoms include severe growth retardation, photosensitivity, immunodeficiency, fertility problems, and predisposition to cancer, as would be expected with a defect in DNA repair pathways [26]. Due to loss of the anti-recombinase activity of BLM, levels of HR increase

ultimately leading to genetic instability [27]. Further evidence of anti-recombinase activity is shown through its interaction with Rad51, subsequently inhibiting polymerisation of Rad51 required for location of the complementary sister chromatid [24]. Recent evidence, alluding to BLM's pro-recominogenic roles, has shown that it interacts directly with the 5' to 3' dsDNA exonuclease, Exo1, resulting in stimulation of its resection activity [28]. BLM has also been shown to have roles within the later stages of HR as it forms a complex with Topoisomerase IIIα, which is able to resolve Holliday junctions in the correct manner reducing the number of potentially harmful crossover events [29].

1.7 hnRNPs in DNA Damage Repair (DDR)

In recent years, more and more evidence has accumulated which implicates hnRNPs in coordinating repair pathways both through protein-protein interactions and the regulation of transcription of repair and stress response mRNA [1]. Given the extensive roles of hnRNPs in mRNA processing it is unsurprising that they play a pivotal role in repair pathways by controlling the expression levels of DNA repair proteins. More unexpected is their regulation by direct interaction with proteins involved in repair processes. Many examples of this have now been recognised. Firstly, roles within NHEJ pathway have been suggested through hnRNP-B1's interaction and inhibition of DNA-dependent protein kinase (DNA-PK) and hnRNP-C1/C2's interaction with the Ku antigen (Ku) [30,31]. hnRNP-K was shown to be phosphorylated in response to DSBs by ATM and to act as a co-factor to p53 for transcriptional control of DNA repair factors [32]. p53 has also been shown to interact with hnRNP-UL1, the hnRNP of main focus to this study [7]. In direct relation to DSB repair pathways, hnRNP A1, A18, A2/B1, C1/C2, K and P2 have been shown to be involved in regulating the choice between HR and NHEJ [1].

1.8 hnRNP-UL1 and –UL2 in the DDR

The evidence for hnRNP-UL1's involvement in the DDR is very strong. It has been shown to interact with a C-terminal region of p53 and to reduce p53's activities as a transcription factor [7]. RPA70 and RPA32 are principle components of the RPA complex which binds ssDNA during HR. hnRNP-UL1 was found to bind directly to RPA70 and RPA32, and during adenovirus infection was required for phosphorylation of H2AX [33].

Previous work completed in conjunction with our laboratory was published whilst this study was on-going [4]. It showed that both hnRNP-UL1 and –UL2 bound to NBS1 of the

MRN complex. The interaction was shown to be between the C-terminus of NBS1 and the middle portion of hnRNP-UL1 (specifically the BBS-RGG region). The study also highlighted hnRNP-UL1's requirement in stimulating DNA end resection and for effective HR repair. When RNA was depleted in cells, the interdependent recruitment of hnRNP-UL1 and –UL2 (i.e. as part of the same complex) to sites of DNA damage was observed. The contribution of hnRNP-UL1 to ATR-dependent signalling during DNA repair by promoting DSB resection was also alluded to. This influence was mediated downstream of MRN and CtIP by the recruitment of BLM to sites of laser-induced or camptothecin (CPT)-induced damage [4]. The study also showed association of hnRNP-UL1 with BLM. Such direct protein-protein interactions with proteins involved in the DDR was the focus of this study.

1.9 Aims

Therefore, based on the previous work discussed above the principle aims of this study were:

1. To investigate the protein-protein interactions of hnRNP-UL1 and –UL2 with proteins involved in the DDR.
2. To further characterise the known interactions of hnRNP-UL1 with p53 and BLM.
3. To try to identify novel interacting partners of hnRNP-UL1 and –UL2.

Chapter Two:

Materials and Methods

2. Materials and Methods

2.1 Tissue Culture Techniques

2.1.1 Maintenance of Human Cell Lines

Cell lines were maintained in a 5% CO_2 incubator at 37ºC (Table 2.1). Cell lines were sustained in Dulbecco's modified Eagle's medium (DMEM) (Sigma), supplemented with 7% v/v foetal calf serum (FCS) (PAA Laboratories).

Table 2.1 Human Cell Lines Used in the Study.

Cell line	ATCC number	Additional Information
U20S	HTB-96	Human epithelial osteosarcoma cell line (origin = bone).
Hela	CCL-2	Human epithelial adenocarcinoma cell line (origin = cervix). Contains human papilloma virus.
DLD-1	CCL-221	Human epithelial osteosarcoma cell line (origin = bone).

2.1.2 Human Cell Culture

The passage of adherent cell lines was achieved by washing twice with PBS (phosphate buffered saline) (Sigma), trypsinisation using 5 mls of 0.05% trypsin-ethylenediaminetetraacetic acid (EDTA) (Invitrogen) and incubated at 37ºC until cells lost adherence to the tissue culture dish. 10 mls of media was added deactivating the trypsin, followed by centrifugation at 1,400 revolutions per minute (rpm) at room temperature for 4 minutes and the cell pellet resuspended media and replated at required density.

2.2 Protein Chemistry Techniques

2.2.1 Harvesting Human Adherent Cells

For harvesting cells for Glutathione S-Transferase (GST) pulldown or co-immunoprecipitation assays, media was removed and cells washed twice in cold 0.15M saline. Cells were scraped from the surface of the tissue culture dish, resuspended in cold saline and centrifuged at 1,500 rpm at 4ºC for 4 minutes. For GST pulldown the cell pellet was resuspended in buffer A (PBS/2mMEDTA/1%Triton X100). For co-immunoprecipitation the cell pellet was resuspended in NETN buffer (0.15M NaCl / 2mM

EDTA / 1%NP40 / 40mM Tris (pH 7.4)). The cells were then homogenised using a Wheaton-Dounce hand homogeniser and sonicated twice to disrupt cell membranes and DNA. The lysate was cleared via centrifugation at 3,000 rpm at 4ºC for 5 minutes. The supernatant was centrifuged twice more, once at 13,000 rpm, 4ºC for 5 minutes and then again at 45,000 rpm, 4ºC for 30 minutes and in each case the pellet discarded.

2.2.2 Sodium Dodecyl Sulphate-Polyacrylamide Gel Electrophoresis (SDS-PAGE)

Proteins were separated according to molecular weight via SDS-PAGE. 10% polyacrylamide gels were made using the following components: 30% w/v acrylamide (37:5:1 BIS-acrylamide) (Severn Biotech), 0.1M Tris (Melford)/ 0.1M Bicine (pH8.3) (Severn Biotech), 0.1% SDS (Severn Biotech), 0.3% N, N, N', N'-Tetramethylethylenediamine (TEMED) (Severn Biotech), 0.6% ammonium persulphate (APS) (Sigma) and deionised water. Gels were cast in an assembled apparatus and wells filled with running buffer (0.1M Tris/ 0.1M Bicine (pH8.3) and 0.1% w/v SDS). Cell lysate, GST-pulldown and co-immunoprecipitation samples were prepared for running on polyacrylamide gels by adding an equal amount of Laemmli sample buffer (25% v/v glycerol (BDH Laboratories), 5% β-mercaptoethanol, 2% w/v SDS, 0.01% w/v bromophenol blue (BDH Laboratories) and 65mM Tris (pH 6.8)). Samples were then heated at 95ºC for 5 minutes, centrifuged at 13,000rpm for 1 minute, and loaded in to the gel wells along with a molecular weight marker. Gels were typically run overnight at 8-15mA for 16 hours.

2.2.3 Visualisation of *In Vivo* Proteins Separated by SDS-PAGE

The protein quality of SDS-PAGE run samples was assessed by staining the polyacrylamide gels for 1 hour in 0.1% w/v Coomassie brilliant blue R-250 (Sigma) in 25% methanol (Sigma), 10% acetic acid (Fisher Scientific). Gels were then destained in rapid Coomassie destain (acetic acid/methanol/water (1:3:6 v/v ratio)) overnight, and assessed after destaining was deemed sufficient.

2.2.4 Visualisation of *In Vitro* Translated Proteins Separated by SDS-PAGE

The radioactive, [^{35}S]-labelled *in vitro* translated proteins (see Section 2.5.1) were visualised by placing the gels in 1M sodium salicylate (Sigma), drying them under vacuum at 80ºC for 2 hours and exposure to autoradiography film (Kodak) for a suitable time period.

2.2.5 Visualisation of Proteins on Nitrocellulose Membranes

Proteins transferred from polyacrylamide gels on to nitrocellulose membranes were stained with Ponceau-S Stain consisting of 0.1% Ponceau-S (Sigma) and 3% trichloroacetic acid (TCA) (BDH Laboratories) for 30 seconds. Nitrocellulose membranes were then thoroughly washed with deionised water for visualisation and then further washed in Tris-Buffered Saline Tween-80 (TBST) (1% Tween-80 (Sigma), 0.15M NaCl (Sigma), 50 mM Tris, HCl pH 7.4 (Fisher Scientific)) to remove the remaining stain.

2.2.6 GST Pulldown Assay

These assays were utilised to assess direct protein-protein interactions. Cell lysates as prepared in section 2.2.1 were incubated with 25µg GST-fusion proteins (Table 2.2.6) and left rotating at 4ºC (this time period was overnight for cell lysates and 3 hours for incubation with ^{35}S-labelled in vitro translated proteins). 50µl of resuspended glutathione-agarose beads (Sigma) were added and incubated for 90 minutes at 4ºC on a rotator to allow protein-protein complexes to bind to the beads. Samples were then centrifuged at 3,000rpm, 4ºC for 1 minute and supernatant discarded. Samples were then washed 4 times in buffer A and once in buffer B (2mM EDTA (Sigma) in PBS), any residual buffer was removed and 60µl of 25mM glutathione pH 8.2 (BDH Laboratories) was added and left to incubate for 1 hour at 4 ºC under gentle agitation. Samples were then centrifuged at 13,000rpm, 4ºC for 1 minute and the supernatant retained in a fresh Eppendorf tube. A further 30µl of glutathione was added to the beads and incubated at 4ºC for a further 30 minutes. The samples were centrifuged again at 13,000rpm, 4ºC for 1 minute and the supernatant pooled with the previous one. 25µl of Laemmli sample buffer was added to each sample, heated at 95ºC for 5 minutes, centrifuged at 13,000rpm for 1 minute and loaded on to a 10% SDS-polyacrylamide gel (Section 2.2.2).

Table 2.2.6 - GST-fusion Proteins Used in this Study. Indicated are the GST-fusion proteins used in this study, the amino acid lengths they incorporate and their source.

GST-fusion protein	Incorporating	Source
GST-hnRNP-UL1	hnRNP-UL1 wild-type fragment aa 1-856	Produced prior to this study
GST-hnRNP-UL1-BBSRGG	hnRNP-UL1 fragment aa 445-695	Produced prior to this study
GST- hnRNP-UL1-673	hnRNP-UL1 fragment aa 1-673	Produced prior to this study
GST- hnRNP-UL2	hnRNP-UL2 wild-type fragment aa 1-747	Produced prior to this study
GST-p53	p53 wild-type fragment aa 1-393	Produced prior to this study
GST-CtIP	CtIP wild-type fragment aa 1-897	Produced prior to this study
GST-BLM wt	BLM wild-type fragment aa 1-1417	Produced prior to this study
GST-BLM fragment 1	BLM fragment aa 1-212	Produced prior to this study and during this study
GST- BLM fragment 2	BLM fragment aa 191-660	Produced prior to this study
GST- BLM fragment 3	BLM fragment aa 621-1041	Produced prior to this study and during this study
GST- BLM fragment 4	BLM fragment aa 1001-1417	Produced prior to this study

2.3 Immunological Techniques

2.3.1 Western Blotting

Following fractionation of proteins by SDS-PAGE, proteins were transferred on to nitrocellulose membrane via the following method. Transfer cassettes were assembled containing the following layers: a sponge, Whatmann 3MM blotting paper, nitrocellulose

membrane (Pall corporation), SDS-PAGE gel, Whatmann blotting paper and a sponge (all equipment was pre-immersed in transfer buffer containing 20% v/v methanol, 0.19M glycine and 0.05M Tris). The cassette was then placed in a transfer tank filled with transfer buffer and a 280mA current applied for 6 hours. Membranes were blocked by placement in 5% skimmed dried milk (Marvel) in TBST for 30 minutes. Primary antibodies (Table 2.3.1a) were diluted in 5% skimmed dried milk in TBST and incubated with the membranes overnight at 4ºC under gentle agitation. The membranes were then washed 3 times for 15 minutes in TBST. Membranes were then incubated with secondary antibodies (Table 2.3.1b) conjugated to horseradish peroxidise (HRP) in 5% skimmed dried milk in TBST for 2 hours at room temperature. Membranes were washed again in TBST 6 times for 5 minutes each time. Enhanced chemiluminescence (ECL) reagent (Millipore or GE Healthcare) was added for 1 minute and the blot exposed to autoradiography film (Kodak) for a suitable time period.

Table 2.3.1a – Primary Antibodies Used in this Study. Indicated are the primary antibodies used in this study, their antigens, dilution, use, species of origin and source.

Antibody	Antigen	Dilution	Use	Species	Company/Source
BLM	BLM	1 in 500	WB, IP	Goat	Bethyl
hnRNP-U	hnRNP-U	1 in 1000	WB	Goat	SantaCruz
hnRNP-H	hnRNP-H	1 in 1000	WB	Goat	SantaCruz
hnRNP-K	hnRNP-K	1 in 1000	WB	Rabbit	SantaCruz
hnRNP-UL1	hnRNP-UL1	1 in 1000	WB, IP	Rabbit	Produced ‘in house’
PARP	PARP	1 in 1000	WB	Mouse	SantaCruz
CtIP	CtIP	1 in 1000	WB, IP	Mouse	Richard Baer
D01 (p53)	p53	1 in 1000	WB, IP	Mouse	David Lane

(N.B. WB – Western blot; IP – immunoprecipitation)

Table 2.3.1b – Secondary Antibodies Used in this Study. Indicated are the secondary antibodies used in this study, their antigens, dilution, use, species of origin and source.

Antibody	Antigen	Dilution	Use	Species	Company/Source
Mouse	Mouse IgG	1 in 2000	WB	Goat	Dako Laboratories
Rabbit	Rabbit IgG	1 in 3000	WB	Swine	Dako Laboratories
Goat	Goat IgG	1 in 2000	WB	Rabbit	Dako Laboratories

(N.B. WB – Western blot)

2.3.2 – Co-Immunoprecipitation (CoIP)

Cell lysate, as prepared in Section 2.2.1, was incubated with 5-20µl of primary antibody (Table 2.4.1a) on rotation at 4ºC overnight. Samples were then centrifuged at 45,000rpm, 4ºC for 30 minutes and the pellet discarded to remove proteins that had become insoluble overnight. 40µl of Protein G-agarose beads (Sigma) were added to samples and rotated at 4ºC for 90 minutes. The samples were then centrifuged at 3,000rpm, 4ºC for 1 minute and supernatant discarded. After 4 washes of the samples in NETN buffer and removal of the supernatant each time, 50µl of Laemmli sample buffer was added, heated at 95ºC for 5 minutes, centrifuged at 13,000rpm for 1 minute and resolved by SDS-PAGE.

2.4 Molecular Biology Techniques

2.4.1 *In Vitro* Translation Protein Production

The TNT Coupled Reticulocyte Lysate Systems kit (Promega Corporation) was used to produce proteins with [^{35}S]-labelled, radioactive methionine incorporated within them. The components listed in Table 2.5.1 were added to a sterile 1.5ml Eppendorf tube. The volume was made up to 50µl with sterile distilled water and incubated at 30ºC for 90 minutes. 3µl aliquots were then subjected to SDS-PAGE, the gels placed in 1M sodium salicylate (Sigma), dried and exposed to autoradiography film for a suitable time period to assess the quality of proteins produced. The remainder of the sample were frozen until required.

Table 2.4.1 – Reaction Mixture Required for *In Vitro* Translation Protein Production.

Component	Volume added (µl)
TNT Rabbit Reticulocyte Lysate	25
TNT Reaction buffer	2
TNT RNA Polymerase	1
Amino acid mixture (minus methionine) 1mM	1
[35S]-labelled methionine (1,000Ci/mmol at 10MCi/ml)	2
RNasin Ribonuclease Inhibitor (40µg/µl)	1
DNA template (0.5µg/µl)	2

2.4.2 GST-Fusion Protein Production

10mls of Luria Bertani (LB)-broth (10g/L tryptone (Fischer Scientific), 10g/L NaCl and 5g/L yeast extract (Fischer Scientific)) supplemented with 100µg/ml ampicillin (Sigma) was inoculated with BL21 E. Coli transformed with gene constructs (Table 2.4.2), and left in an orbital incubator at 37ºC overnight. 5mls of LB-broth culture was then added to 500mls of LB-broth supplemented with 100µg/ml ampicillin, and grown at 220rpm, 37ºC until cultures reached an optical density of 0.6-0.7 absorbency units at a wavelength of 600nm. 0.5mM isopropyl –D-1thiogalactopyranoside (IPTG) (Sigma) was then added to the cultures and grown for a further 3 hours at 30ºC, 220 rpm. Following incubation, cultures were centrifuged at 6,000rpm for 15 minutes, supernantants discarded and pellets frozen at -80ºC until required.

The pellets were resuspended in 30mls of Buffer A (2mM EDTA, 1% Triton X100 (Sigma) in PBS) and sonicated twice for 30 seconds (1 minute interval), then centrifuged at 18,000rpm for 5 minutes and the pellet discarded. The supernatant (bacterial cell lysate) was further centrifuged at 18,000rpm for 30 minutes and the pellet discarded. 2mls of PBS:glutathione-agarose beads (50:50) were added to the supernatant and rotated for 3 hours at 4ºC. Samples were then centrifuged at 1,500rpm for 5 minutes, 1ml of PBS:glutathione-agarose beads (50:50) added to the supernatant and rotated at 4ºC for a further hour. The pelleted beads were washed three times in 50mls of Buffer A, centrifuging at 2,000rpm for 5 minutes at 4ºC each time. A wash was then completed in 50 mls of Buffer B. To the beads, 2mls of 25mM glutathione (pH8.2) was added and rotated at 4ºC for 1 hour. This was followed by centrifugation at 2,000 rpm for 5 minutes and supernatant retained. Supernatants

were then subjected to dialysis at 4ºC overnight via placement in to dialysis tubing surrounded by a buffer containing 150Mm NaCl, 25mM Tris (pH7.5) and 1mM dithiothreitol (DTT) (Sigma).

Table 2.4.2 – Gene Expression Constructs Used for GST-Fusion Protein Production.

Gene	Vector	Source
BLM Fragment 1 (aa 1-212)	pGEX-4T-1	Dr Sengupta [34]
BLM Fragment 3 (aa 621-1041)	pGEX-4T-1	Dr Sengupta

2.4.3 – Preparation of Samples for Mass Spectrometry

GST-pulldown samples were prepared as in section 2.2.7 until the final wash with buffer B (2mM EDTA (Sigma) in PBS) and any residual buffer was removed. 20µl of SDS buffer (50mM ammonium bicarbonate, 8M Urea, and 5% SDS) and 5µl of 50mM DTT solution was added to the beads before heating at 56ºC for 1 hour. 10µl of 100mM iodoacetamide solution (Sigma) was added and left at room temperature for 30 mins, before subsequent addition of 5µl Laemmli sample buffer. Samples were centrifuged at 3,000rpm for 1 minute and the supernatants subjected to SDS-PAGE at 200V for an appropriate time period, along with high molecular weight marker (Fermentas) on pre-cast 4-20% polyacrylamide gels. The running buffer was composed of 20ml NUPAGE MOPS SDS Running Buffer (x20) (Invitrogen) in 500ml sterile water). The gel was stained overnight in Colloidal Coomassie blue (0.1% Coomassie blue G250, 20% methanol, 1.6% orthophosphoric acid, 8% ammonium persulphate).

The gel was destained in 1% acetic acid (BDH) before sectioning control and sample lanes in to 15-20 gel pieces, placing them in sterile Eppendorf tubes and adding 200µl 50% acetonitrile 50mM NH_4HCO_3 (Sigma) and incubating at 37ºC for 45 minutes under gentle agitation. Three washes were made in 200µl 10% acetonitrile 50mM NH_4HCO_3 for 15 minutes at room temperature, before drying the gel sections. 20µl trypsin (Roche) was then added to samples for 1 hour at 37ºC to digest proteins within the gel sections. 20µl 10% acetonitrile 50mM NH_4HCO_3 was added and samples left overnight.

Supernatants were collected and remaining gel sections incubated in 30µl 3% formic acid at 37ºC for 1 hour. The subsequent supernatant was then added to the previous one, the addition of 3% formic acid and 1 hour incubation at 37ºC repeated and combined supernatants stored at -20ºC until samples were analysed by mass spectrometry.

Chapter Three:

Results

3.1 – p53, CtIP and BLM Interact with [^{35}S]-Labelled hnRNP-UL1 and hnRNP-UL2 *In Vitro*

Previous studies had shown hnRNP-UL1 and –UL2 to associate with various proteins with crucial roles within the DNA damage response, including p53, CtIP and BLM [7,4]. To further investigate the interactions of hnRNP-ULs with these proteins, GST pulldown assays were performed. GST-fusion proteins were incubated with [^{35}S]-labelled *in vitro* translated forms of hnRNP-UL1, -UL2, and also various fragments of hnRNP-UL1. The resulting protein complexes formed were isolated using glutathione-agarose beads. After separation by SDS-PAGE protein bands were visualised by autoradiography. This showed that hnRNP-UL1 and –UL2 interacted directly with p53, CtIP and BLM *in vitro* (Figure 3.1). p53 was included as a positive control since it had previously been shown to interact directly with hnRNP-UL-1 [7].

Use of various [^{35}S]-labelled fragments of hnRNP-UL1 (shown in Figure 1.2) allowed the assessment of which regions/domains of the protein were required for binding to p53, CtIP and BLM. The autoradiographs shown in Figure 3.1 B-D were subjected to densitometric scanning in an attempt to quantitate the interaction (shown in Figure 3.1 D). The middle (M) and C-terminal (Ct) regions exhibited interaction with each of the three proteins, whilst the N-terminal region of hnRNP-UL1 showed no interaction. Deletion of the RGG domain severely perturbed the ability of hnRNP-UL1 to bind the three proteins, as did the larger deletion (ΔBSS2) of the BBS domain. However, a BBS-RGG domain fragment alone failed to show significant interaction with CtIP or BLM whilst binding to p53. This suggests regions of hnRNP-UL1 other than the BBS and RGG domains are required for binding CtIP and BLM. Deletion of the polyproline-rich (PP) region also reduced binding more significantly with CtIP and BLM than with p53. Finally, it is shown that hnRNP-UL2 binds p53 with two-fold better efficiency than both CtIP and BLM (Figure 1.1).

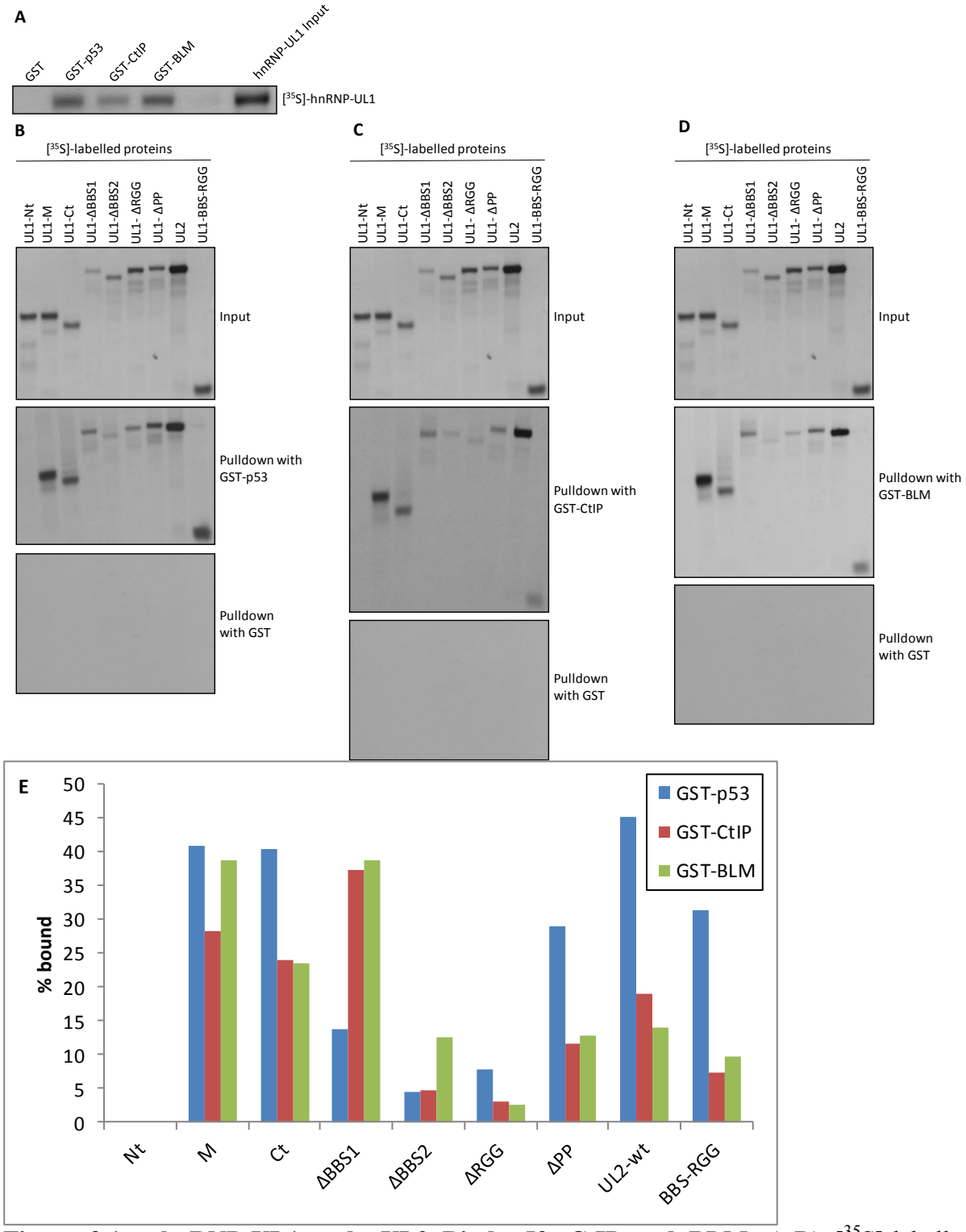

Figure 3.1 – hnRNP-UL1 and –UL2 Bind p53, CtIP and BLM. A-D) [^{35}S]-labelled proteins were incubated with the indicated GST fusion proteins and protein complexes formed isolated with glutathione-agarose beads, before subsequent elution with glutathione. The eluted proteins were fractionated by SDS-polyacrylamide gel electrophoresis and revealed by autoradiography. In **B**, **C** and **D** the upper panel shows inputs, the central panel the bound protein and the lower panel protein bound to GST. **E)** Densitometric scanning was used to quantify the proportion of each of the proteins bound to the indicated GST-fusion protein (these data are derived from the autoradiographs shown in **B-D**).

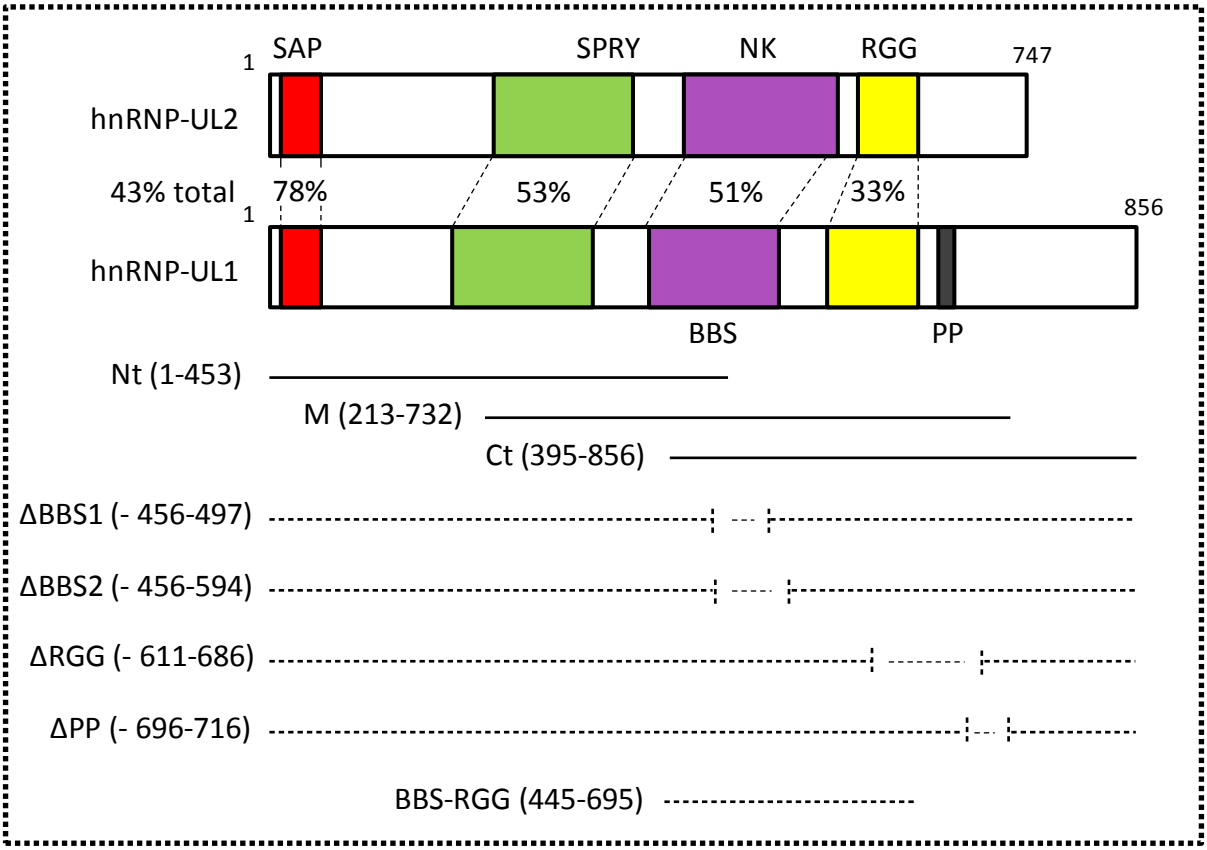

Figure 1.2 – Structure of hnRNP-UL1 and -UL2 and its Domains. A schematic representation of the full length (WT) hnRNP-U-like proteins and the various fragments expressed via *in vitro* translation or used for GST experiments. SAP, SAF-A/B, Acinus and PIAS motif; SPRY, SPIa/Ryanodine receptor domain; NK, putative nucleoside/nucleotide kinase domain; BBS, BRD7-binding site; RGG, arginine and glycine-rich region, RNA and ssDNA binding; PP, proline-rich region; Nt, N-terminal fragment; M, middle fragment; Ct, C-terminal fragment. Percentages of amino acid homology are indicated (total and for coloured domains). Nt, M, Ct, ΔBBS1, ΔBBS2, ΔRGG, ΔPP and BBS-RGG refer to hnRNP-UL1 deletion mutants (adapted from [4]).

3.2 – The N-Terminal and C-Terminal Regions of BLM Interact with [^{35}S]-Labelled hnRNP-UL Proteins *In Vitro*

To further assess the binding of the BLM helicase with hnRNP-UL1, GST pulldowns were performed using GST-BLM fragments (shown in Figure 3.2a). Various GST-BLM fragments were expressed in *E. coli* (Table 2.5.2), purified and resolved by SDS-PAGE. SDS-PAGE gels were then stained with Coomassie Blue to assess the purity of the GST-fusion proteins produced (Figure 3.2b). Other GST-fusion proteins were already available within the laboratory. GST-fusion proteins were incubated with [^{35}S]-labelled *in vitro* translated forms of hnRNP-UL1, -UL2, and the various fragments of hnRNP-UL1 described in Figure 1.2. The resulting protein complexes formed were isolated using attachment of the GST moiety to glutathione-agarose beads. After separation by SDS-PAGE protein bands were visualised by

autoradiography, showing that hnRNP-UL1 and –UL2 interacted with BLM fragments 1 and 4 *in vitro* (Figure 3.2c(A)).

Once again, use of various [^{35}S]-labelled fragments of hnRNP-UL1 allowed the assessment of which regions/domains of the protein interacted with BLM fragments 1 and 4. Whilst loss of the BBS, RGG and PP domains/regions significantly reduced the binding of hnRNP-UL1, loss of the BBS domain appeared to affect the binding of BLM fragment 4 significantly more than fragment 1 (Figure 3.2c (B-D)). BLM fragment 1 exhibited very efficient binding to the BBS-RGG domain fragment alone, whilst BLM fragment 4 did not. This suggests that whilst the BLM fragment 4 critically requires the BBS and RGG domains for binding, they do not permit significant interaction alone.

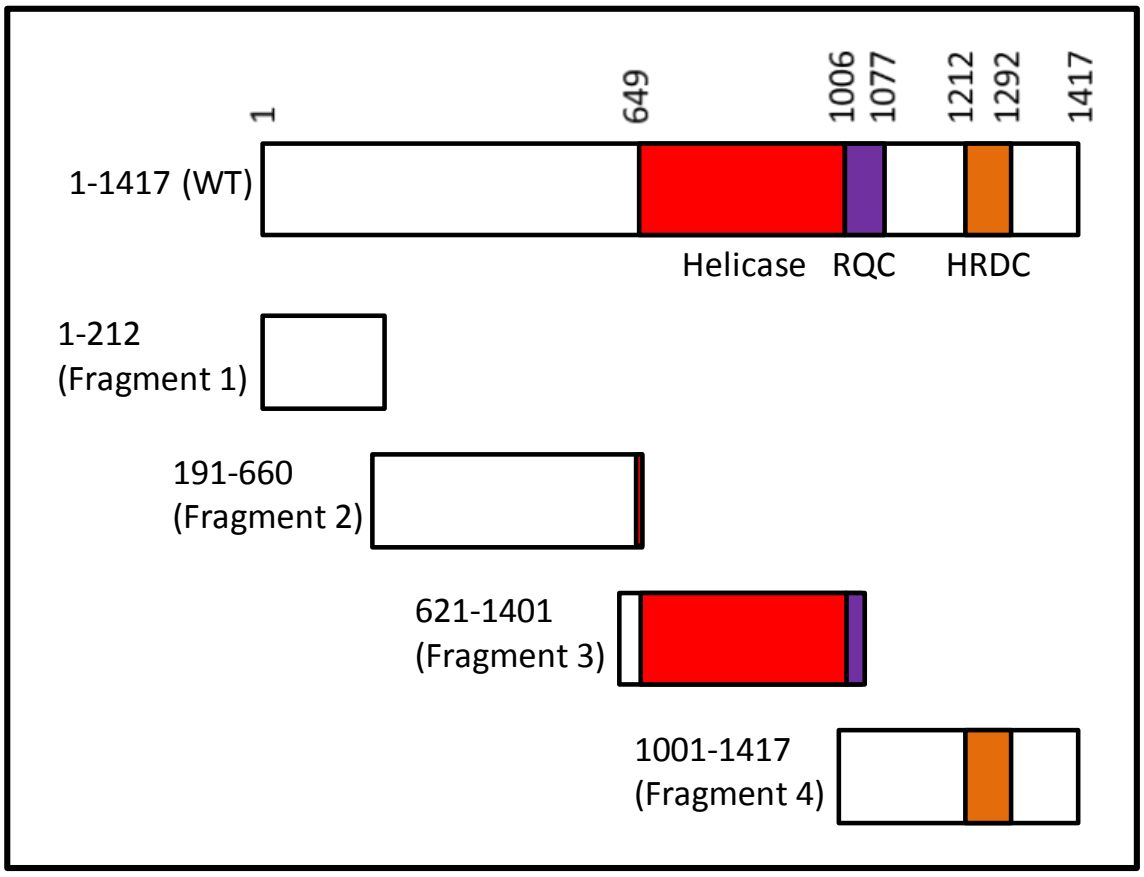

Figure 3.2a – Structure of BLM and its Domains. A schematic representation of BLM and the GST-BLM fragments (numbered 1-4) used in this study. Amino acid numbers are indicated above the full length (WT) BLM and various domains below. RQC, RecQ carboxy-terminal; HRDC, Helicase and Rnase D C-terminal (adapted from [35]).

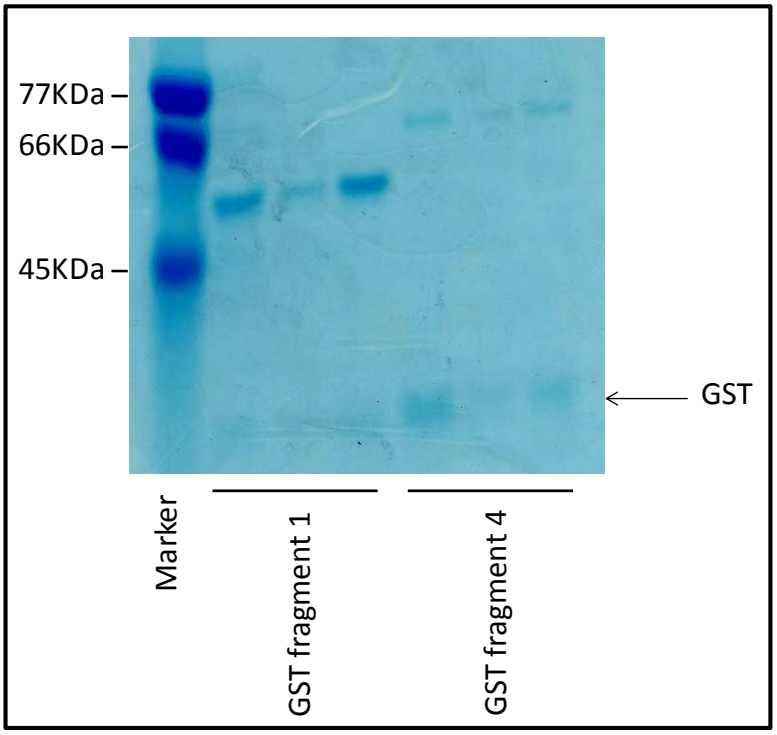

Figure 3.2b – Assessment of the Protein Purity of the GST-BLM Fragments Produced in this Study. The required plasmid DNA constructs were transformed in to BL21 *E. Coli* to produce the indicated GST-fusion proteins. The proteins were purified using gluitathione agarose, resolved by SDS-PAGE, Coomassie Blue stained and subsequently destained to assess protein purity. The 3 tracks for each fragment show different elutions from the glutathione agarose as described in the Methods section.

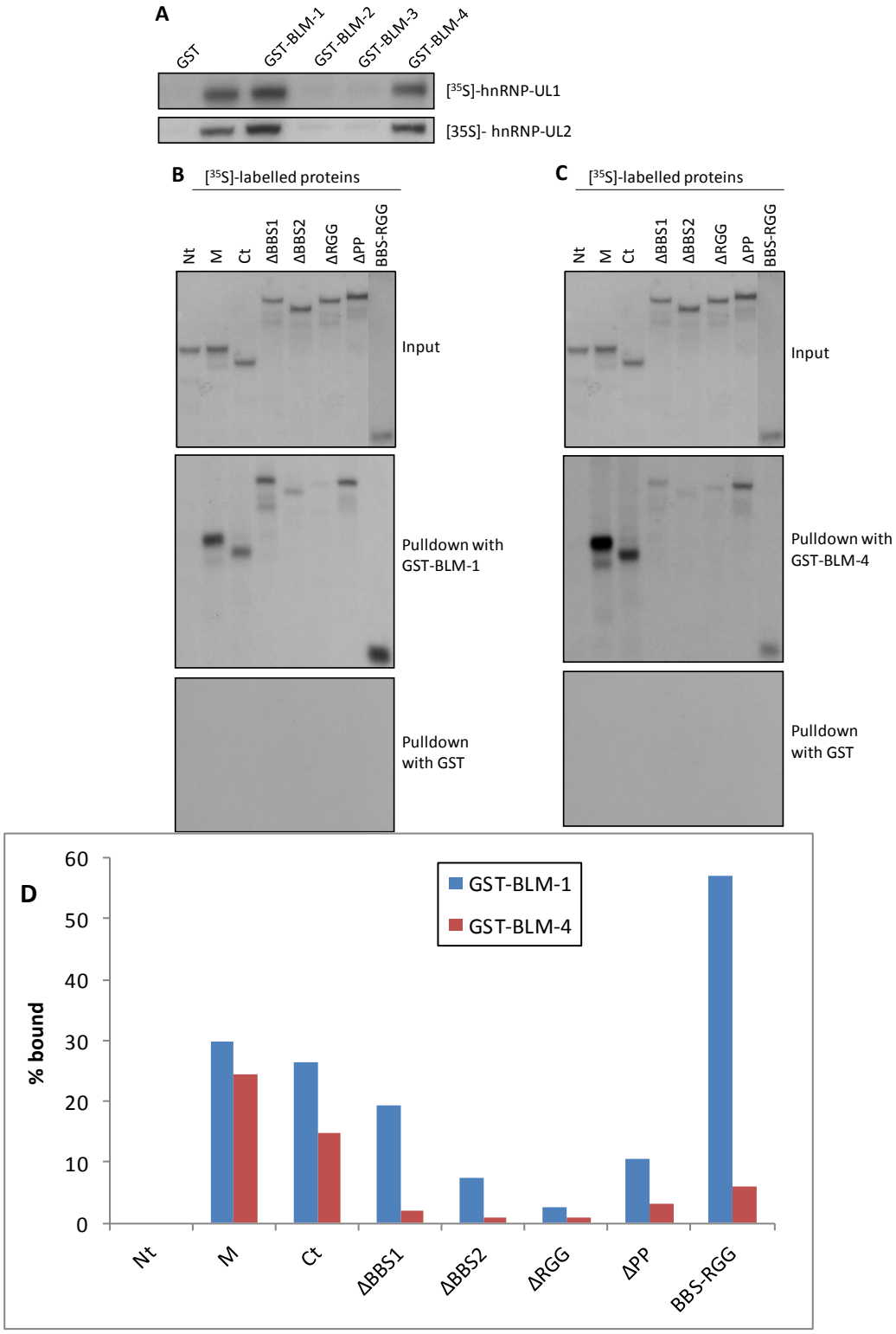

Figure 3.2c – The N-Terminal and C-Terminal Regions of BLM are Required to Interact with hnRNP-UL Proteins. A-C) [^{35}S]-labelled proteins were incubated with the indicated GST fusion proteins and protein complexes isolated with glutathione-agarose beads, before subsequent elution with glutathione. The eluted proteins were fractionated by SDS-polyacrylamide gel electrophoresis and revealed by autoradiography. **D)** Densitometric scanning was used to quantify the proportion of each of the proteins bound to the indicated GST-fusion protein.

3.3 – hnRNP-UL Proteins Homo- and Heterodimerize *In Vitro*

Within a previous study, depletion of either hnRNP-UL1 or -UL2 caused defects in DNA-end resection during DSB repair, showing they are not redundant in their actions despite sharing considerable amino acid sequence homology (Figure 1.2) [4]. Their recruitment to DSB sites was also shown to be largely interdependent, suggesting that they are probably recruited within the same protein complex. Therefore, we investigated the interaction of hnRNP-ULs with themselves and one another via the same method of GST pulldown, employing the use of GST-fusion proteins incubated with [^{35}S]-labelled *in vitro* translated forms of hnRNP-UL1, -UL2, and also various fragments of hnRNP-UL1. Results showed that hnRNP-UL1 homodimerizes and hnRNP-UL1 and –UL2 heterodimerize with one another (Figure 3.3). It appears that the RGG domain was most critical for interaction of hnRNP-UL1 both with itself and with hnRNP-UL2.

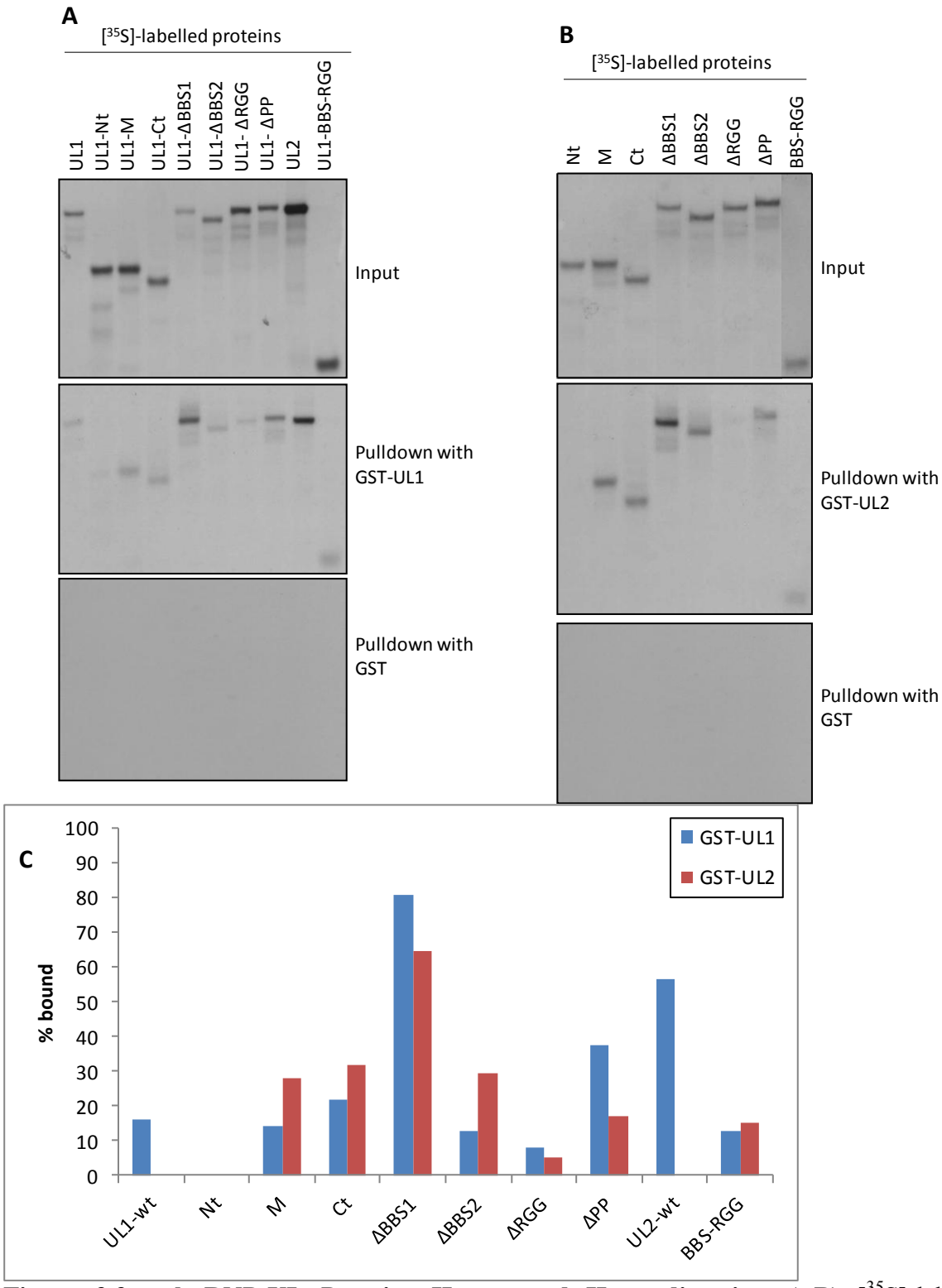

Figure 3.3 – hnRNP-UL Proteins Homo- and Heterodimerize. A-B) [^{35}S]-labelled proteins were incubated with the indicated GST fusion proteins and protein complexes formed isolated with glutathione-agarose beads, before subsequent elution with glutathione. The eluted proteins were fractionated by SDS-polyacrylamide gel electrophoresis and revealed by autoradiography. **C)** Densitometric scanning was used to quantify the proportion of each of the proteins bound to the indicated GST-fusion protein.

3.4 - p53, CtIP, BLM and PARP Interact with hnRNP-UL1 *In Vivo*

To confirm that p53, CtIP, and BLM associate with hnRNP-UL1 *in vivo*, co-immunoprecipitation assays were performed. Cell lysates were incubated with the appropriate antibodies and subsequent immune-complexes were isolated using Protein-G agarose beads and subjected to Western blotting for the indicated proteins (Figure 3.4a). Figure 3.7A shows that hnRNP-UL1 co-immunoprecipitated with antibodies against p53, CtIP and BLM confirming their *in vivo* association. A reciprocal experiment showed p53 co-immunoprecipitated with antibodies against hnRNP-UL1 (Figure 3.4a (B)).

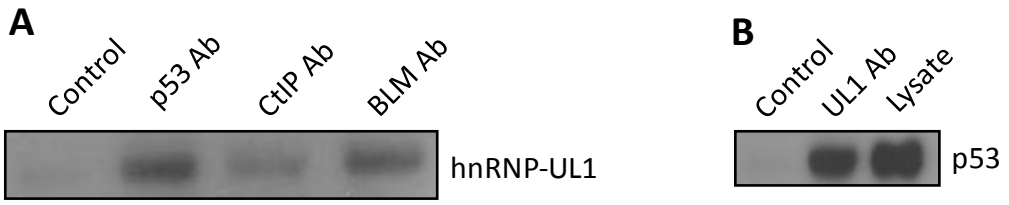

Figure 3.4a – p53, CtIP and BLM Interact with hnRNP-UL1 *In Vivo*. DLD1 cell lysates were incubated with the indicated antibodies, protein-protein complexes were isolated using Protein-G beads and subjected to Western blotting.

A further co-immunoprecipitation experiment employing an antibody against hnRNP-UL1 and subsequent immunoblotting for PARP showed their interaction with one another *in vivo* (Figure 3.4b (A)). A GST-pulldown experiment also showed PARP to interact with hnRNP-UL1, hnRNP-UL2 and a smaller fragment of hnRNP-UL1 (hnRNP-UL1-673) but not with the BBS-RGG fragment (Figure 3.4b (B)).

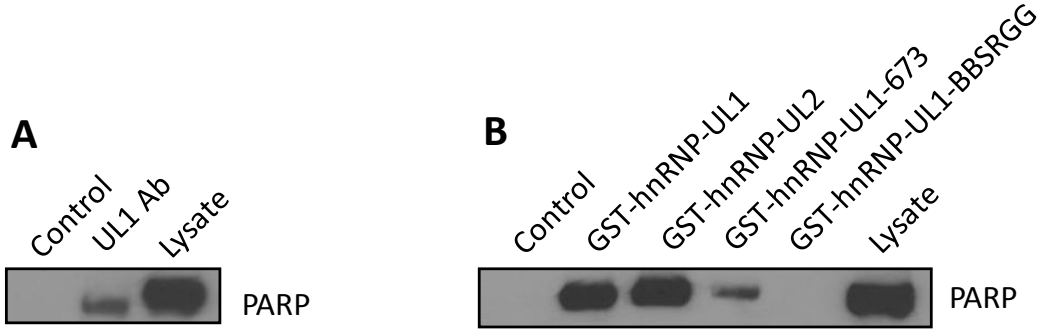

Figure 3.4b – PARP Interacts with hnRNP-UL1 *In Vivo*. A) U20S cell lysates were incubated with the indicated antibodies, protein-protein complexes were isolated using Protein-G beads and subjected to Western blotting. **B)** U20S cell lysates were incubated with the indicated GST-hnRNP-U-like fusion proteins. Protein complexes were isolated with the use of glutathione-agarose beads and subsequent elution with glutathione before being subjected to Western blotting for PARP.

3.5 - hnRNP U-like Proteins Bind Other hnRNPs *In Vivo*

Many studies have shown hnRNP proteins to interact with one another [36,37,38]. Within this study it has been shown that the hnRNP-UL proteins interact with one another and also homodimerize. GST-pulldown assays were performed to investigate whether other hnRNPs interact with the hnRNPUL proteins. Hela cell lysates were incubated with GST-fusion proteins and resulting protein complexes were isolated using glutathione-agarose beads before subjection to Western blotting for various proteins, along with GST protein alone and cell lysate alone as non-specific binding and positive controls, respectively. hnRNP-UL1 and –UL2 were shown to bind hnRNP-H, -K and -U(SAFA) (Figure 3.5 (A)). Figure 3.9B shows the BBS-RGG region being enough to pull down hnRNP-H and –U.

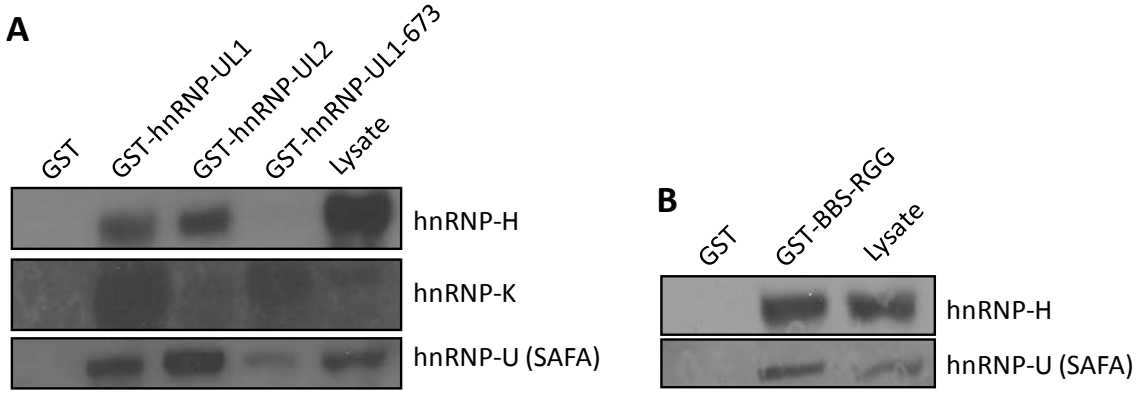

Figure 3.5 - hnRNP U-like Proteins Bind Other hnRNPs. Hela cell lysates were incubated with the indicated GST-hnRNP-U-like fusion proteins. Protein complexes were isolated with the use of glutathione-agarose beads and subsequent elution with glutathione before being subjected to Western blotting.

3.6 – Mass Spectrometry Tentatively Highlighted Some Other hnRNP-UL1 Interacting Proteins Involved in DNA Damage Repair/Processing

A pulldown assay was completed employing the GST-hnRNP-UL1-BBS-RGG fragment. Protein complexes formed were isolated and subjected to SDS-PAGE. Control and sample lanes within the gel were then sliced in to sections, digested with trypsin and the resulting peptides assessed by mass spectrometry. This tentatively identified other hnRNPs and various proteins involved in the DNA damage response (DDR) that associate with hnRNP-UL1. These included proteins already identified in the study, such as hnRNP-UL1, hnRNP-UL2 and hnRNP-U (SAFA), as well as hnRNPs: -D0, -R and -A/B. Further proteins included DNA-damage-binding protein 1, ATM, E3 ubiquitin-ligase SHPRH, E3 ubiquitin-protein ligase TTC_3 and E3 ubiquitin-protein ligase BRE_1A.

Chapter Four:

Discussion

4. Discussion

Previous studies carried out in conjunction with our laboratory had shown hnRNP-UL1 and hnRNP-UL2 to associate with various proteins with important roles within the DNA damage response [4]. These included direct binding of the NBS1 subunit of the MRN complex, as well as, the co-immunoprecipitation of CtIP and BLM helicase. The interaction with the MRN complex was crucial for their recruitment to DSB sites and association with BLM facilitated its recruitment to DSB sites to carry out its role in DNA-end resection. p53 has also been shown to interact with hnRNP-UL1 through pull-down and co-immunoprecipitation assays [7]. The co-immunoprecipitation of hnRNP-UL1 with CtIP in [4] did not necessarily mean the two species directly interact with one another. Like hnRNP-UL1, CtIP had been shown to directly bind the NBS1 subunit of MRN and co-immunoprecipitation of hnRNP-UL1 and CtIP could occur through these shared interactions with NBS1 [39]. Our study did confirm the *in vitro* interactions between hnRNP-UL1 and CtIP, as well as, with BLM and p53 through GST-pulldown experiments. The direct interaction of CtIP, BLM and p53 with hnRNP-UL2 was also shown, with p53 exhibiting two-fold better binding efficiency than CtIP and BLM.

The interaction of p53, CtIP and BLM was mapped to the middle and C-terminal portions of hnRNP-UL1, whilst an N-terminal fragment showed no interaction. A BBS-RGG domain fragment of hnRNP-UL1 was capable of strongly binding to p53. Whilst deletion of BBS and RGG independently highlighted their requirement for interaction with CtIP and BLM, the BBS-RGG domain fragment alone failed to show significant interaction with CtIP or BLM, however. This suggested interactions between CtIP and BLM with hnRNP-UL1 respectively, appear to require extensive interactions across the BBS and RGG domains and beyond. Interactions within the PP domain also appeared to be of significance as its deletion perturbed interaction. The requirement of the BBS domain in the interaction with BLM is consistent with functional studies carried out in [4]. That study showed hnRNP-UL1 depletion via siRNA treatment impaired BLM recruitment to sites of DNA resection during DNA repair. Whilst expression of a siRNA-resistant wild-type hnRNP-UL1 construct rescued recruitment, a ΔBBS mutant did not. Therefore, our *in vitro* studies confirmed the BBS region of hnRNP-UL1 to be required for the binding of BLM.

To extend the analysis of the BLM-hnRNP-UL1 binding, we then investigated which regions of BLM were required for hnRNP-UL1 interaction. Of the 4 GST-fragments of BLM, fragments 1 (N-terminal region, aa 1-212) and 4 (C-terminal region, aa 1001-1417) were able

to bind hnRNP-UL1 *in vitro*. The interactions of BLM and topoisomearases has been widely studied in the last 10 years and function together in a complex with RMI1 (RecQ-mediated genomic instability protein 1) to catalyze the dissolution of double Holliday junctions into noncrossover products, a process critical within DNA repair by HR [29]. The amino acids 489-587 of BLM were found to directly interact with topoisomerase IIα [40]. Our results show, this is a different region of BLM that is required to interact with hnRNP-UL1. Deletions within the BBS-RGG domain of hnRNP-UL1 were shown to be critical in the binding of BLM and a fragment of the BBS-RGG domain was sufficient independently to bind fragment 1 of BLM. Interestingly, whilst deleting the BBS and RGG domains perturbed binding to fragment 4 significantly, the BBS-RGG domain on its own showed very limited binding to fragment 4. This may be due to the binding of fragment 4 requiring other sections of hnRNP-UL1 outside of the BBS-RGG domain. It may also be due to the small fragments of the proteins (BBS-RRG of hnRNP-UL1 and aa 1001-1417 of BLM) failing to adopt the correct secondary structure (as seen in the intact protein) and this may inhibit interaction even though much of the binding site is present.

Previous studies showed that depletion of either hnRNP-UL1 or -UL2 caused defects in DNA-end resection during DSB repair, showing they are not redundant in their actions despite sharing considerable amino acid sequence homology (Figure 3.2) [4]. Their recruitment to DSB sites was also shown to be largely interdependent, suggesting that they are recruited as a complex. Our studies were able to confirm the direct binding of the hnRNP-U-like proteins to one another. hnRNP-UL1 was shown to homo-dimerize with itself and also hetero-dimerize with hnRNP-UL2. It appeared that the RGG domain was most critical for hnRNP-UL1's interactions both with itself and with hnRNP-UL2. HnRNPs form complexes together during their mRNA processing activities and many studies have shown them to hom- and hetero-dimerize [6,36,37,38].

All previous work within the study up to this point had been completed *in vitro*. Whilst confirming direct interaction between binding proteins, it did not address their interaction *in vivo*. Co-immunoprecipitation studies with cell lysates confirmed the *in vivo* association with p53, CtIP and BLM. It also interestingly revealed an interaction with poly (ADP-ribose) polymerase (PARP), a protein playing an essential role in the response to DNA damage [41]. PARP is rapidly recruited to sites of both double-strand and single-strand breaks and mediates poly(ADP-ribose) (PAR) modification of itself and histones. The poly(ADP-ribosyl)ation of histones mediates chromatin relaxation, which allows greater

accommodation of DNA repair factors at sites of damage [41]. PAR production also stimulates the recruitment of various DNA repair factors through their PAR-binding domains [42]. The discovery of the *in vivo* interaction between PARP and hnRNP-UL1 and hnRNP-UL2 came late within this study and further investigation was not possible. However, their interaction adds another level to the complexity of hnRNP-U-like proteins within the DDR.

As discussed above many previous studies had revealed hnRNPs to interact with one another in complexes. Indeed, within this study the two hnRNP-U-like proteins had been shown to hetero-dimerize and hnRNP-UL1 to homodimerize. *In vivo* interactions were confirmed between hnRNP-H, -K and –U and the hnRNP-U-like proteins, and the BBS-RGG domain of hnRNP-UL1 was sufficient for interaction with hnRNP-H and –U alone.

Towards the end of the study mass spectrometry was employed to highlight possible interacting partners for hnRNP-UL1 by analysing the GST-pulldown samples carried out with the BBS-RGG fragment. The results confirmed interacting partners already identified such as hnRNP-UL1, hnRNP -UL-2 and hnRNP –U. Other hnRNPs (hnRNP-D0, -R and –A/B) were also found. Further proteins identified with potential roles in the DDR were DNA-damage-binding protein 1, ATM, E3 ubiquitin-ligase SHPRH, E3 ubiquitin-protein ligase TTC_3 and E3 ubiquitin-protein ligase BRE_1A. It should be stressed, however, that such interactions are tentative and require confirmation through further work. For example, hnRNPs are very well known to occur in mass spectrometry analyses through non-specific interactions.

In conclusion, this study has confirmed the protein-protein interactions of various other studies which reveal a link between hnRNP-U-like proteins and the DNA damage response. The results have extended our knowledge of these interactions in terms of the distinct regions of the proteins required for binding, and PARP has also been identified as a novel interacting partner of hnRNP-UL1 and –UL2.

4.1 Limitations

The short duration of the study was a limiting factor to how far the study could go. Repeats of the GST-pulldown experiments conducted with *in vitro* translated proteins used for densitometric analysis in Figures 3.1, 3.2c and 3.3 would improve their reliability and the conclusions drawn from them. Similarly, it would be essential to repeat the mass spectrometry analysis. To explore the interaction with PARP would have been of great interest, however, this interaction was observed towards the end of the study and further

experiments were not possible. Antibodies against some of the hnRNPs were of poor quality and made confirming interactions between hnRNPs through GST-pulldown and co-immunoprecipitation assays difficult.

4.2 Future Work

As the binding site for hnRNP-UL1 on BLM was mapped using 4 GST-BLM fragments in GST-pulldowns with *in vitro* translated hnRNP-UL1 fragments, the same could be completed with CtIP employing the use of GST-CtIP fragments. In the long term, investigations in to the functionality of hnRNP-UL1 with the various mutated forms could be performed by knocking down endogenous hnRNP-UL1 and transfecting back the various fragments. Affects on the DDR could then be assessed via various methods.

It would also be of great interest to carry out further investigation of the interaction between hnRNP-UL1 and PARP. Acquiring a GST-labelled version of PARP to explore its interaction with hnRNP-UL1 through GST-pulldowns with the *in vitro* translated deletion variants and fragments of hnRNP-UL1 would be of great interest. Would the BBS-RGG domain be critical to their interaction, as it was with p53, CtIP and BLM? To investigate if the interaction was significant to the correct execution of the DDR would also be of great interest. DNA damage could be induced within cells (e.g. through ionizing irradiation, ultra-violet radiation or treatment with camptothecin) and the levels of hnRNP-UL1 and PARP interaction monitored at various time points by co-immunoprecipitation studies. This would give an indication to whether these proteins' interactions are increased or decreased during DNA damage response and if so this would suggest a role in the DDR. It would also be of interest to examine whether hnRNP-UL1 and -UL2 affect the enzymatic activity of PARP in both in vitro assays and in vivo (by looking at the PARylation of proteins in cells with hnRNP-UL1 and –UL2 knocked down). Finally, further investigation of some of the proteins pulled down with the GST-hnRNP-BBS-RGG fragment and identified by mass spectrometry could be made.

SIM:SUMO Interaction of the deSUMOylation Enzyme SENP7 and the SIMs Role in Protein Functionality

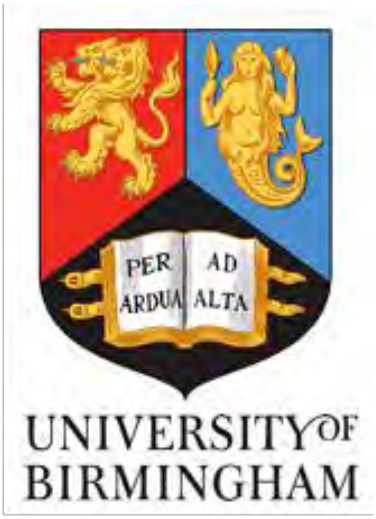

Submitted by Kenny Pratt

1198698

This project is submitted in partial fulfilment of the requirements for the award of the MRes

Supervisor: Dr Jo Morris

Abstract

The highly dynamic, post-translational protein modification, SUMOylation, has been identified as playing a key role in the DNA damage response (DDR). Given the highly reversible and dynamic nature of this modification it would appear logical that the deSUMOylation enzymes, SENPs (sentrin-specific proteases), would be critical for the correct execution of the DDR. Indeed, studies are now highlighting the requirement of SENPs within DNA repair mechanisms. Previous work in our laboratory had shown SENP7 to be recruited to sites of DNA repair and identified SENP7 as an essential factor for homologous recombination (HR).

To cleave poly-SUMO-2/3 chains as SENP7 is known to do, it was expected that the protein would employ SUMO-interaction motifs (SIMs) to bind SUMO. Analysis of the primary structure identified 7 potential SIMs within SENP7. Mutation of all or various combinations of these SIMs did not perturb localisation of SENP7 to regions of heterochromatin within the cell nucleus. Meanwhile, the SIMs were shown to be of critical importance both for interaction with SUMO-2-modified proteins and the functionality of the protein within its role in homologous recombination (HR). Of these 7 potential SIMs, those numbered 6 and 7 in this study were shown to be of greater importance than that of the other SIMs for SENP7 functionality. A clear correlation was also identified between the number of potential functional SIMs and the HR capability of the cells. However, this did not strictly correlate with the SUMO-binding capabilities of the SIMs, suggesting that SIMs 6 and 7 may deliver bound SUMO chains to the catalytic site of SENP7 more efficiently than others. During co-immunoprecipitation studies, KAP-1 (TIF1-β – transcription intermediary factor 1- β) was shown to interact with SENP7 and could be a potential substrate for deSUMOylation.

Acknowledgements

I would like to thank Dr Jo Morris and Dr Alex Garvin for their help, advice and guidance, both in the laboratory and in the writing of this project. I would also like to thank the other members of the Morris laboratory, past and present, including Dr Ruth Mensham, James Beesley, Helen Stone and Dr Junying Jia for their continual support.

List of Contents

List of Figures and Tables

Chapter One:

Introduction

1.1 Introduction

Many proteins are modified post-transcriptionally by various methods, including phosphorylation, acetylation, methylation and protein-based modification. Ubiquitination was the first protein-based modification to be described and in recent years many others have been discovered. SUMO (small ubiquitin-like modifier) as the name suggests is an ubiquitin-like protein (UBL) and can be covalently attached to target proteins to modify their dynamics and functions. Both modifiers, ubiquitin and SUMO, are typically attached to lysine residues of target proteins and can also be conjugated as monomers or as polymeric chains [43]. Like ubiquitylation before it, SUMOylation has emerged as a critical regulator of proteins involved in many biological processes, including the DNA damage response (DDR), which is of particular interest to our group [44].

1.2 SUMO and the SUMOylation Pathway

Three isoforms of SUMO are known to be conjugated to target proteins, SUMO-1, -2 and -3. The matured SUMO-2 and SUMO-3 differ by just 4 amino acids (~97% identical) and are roughly 50% identical in sequence to SUMO-1 [44]. Target proteins are SUMOylated via a sequential enzymatic process involving an activating enzyme (E1), a conjugating enzyme (E2) and a SUMO protein ligase (E3) [45]. Firstly, a heterodimer of SUMO-activating enzymes, SAE1 and SAE2, employs ATP to adenylate the C-terminal glycine of SUMO. The second reaction involves the transfer of SUMO from the E1 enzyme to a cysteine residue within the E2-conjugating enzyme, Ubc9 (ubiquitin-conjugating enzyme 9). The Ubc9-SUMO conjugate then catalyses the formation of an isopeptide linkage between the C-terminal carboxyl group of SUMO and the ε-amino group of a lysine residue within the substrate (Figure 1.2). This lysine residue most commonly lies within a consensus motif ψKX(D/E), (where ψ is a large hydrophobic amino acid and X is any amino acid), however, modification has been found to occur at non-consensus sites [46]. Ubc9 does have the capability to carry out the addition of SUMO to its target on its own, however, E3 ligases are commonly employed and appear to provide substrate specificity and enhance reaction efficiency [45].

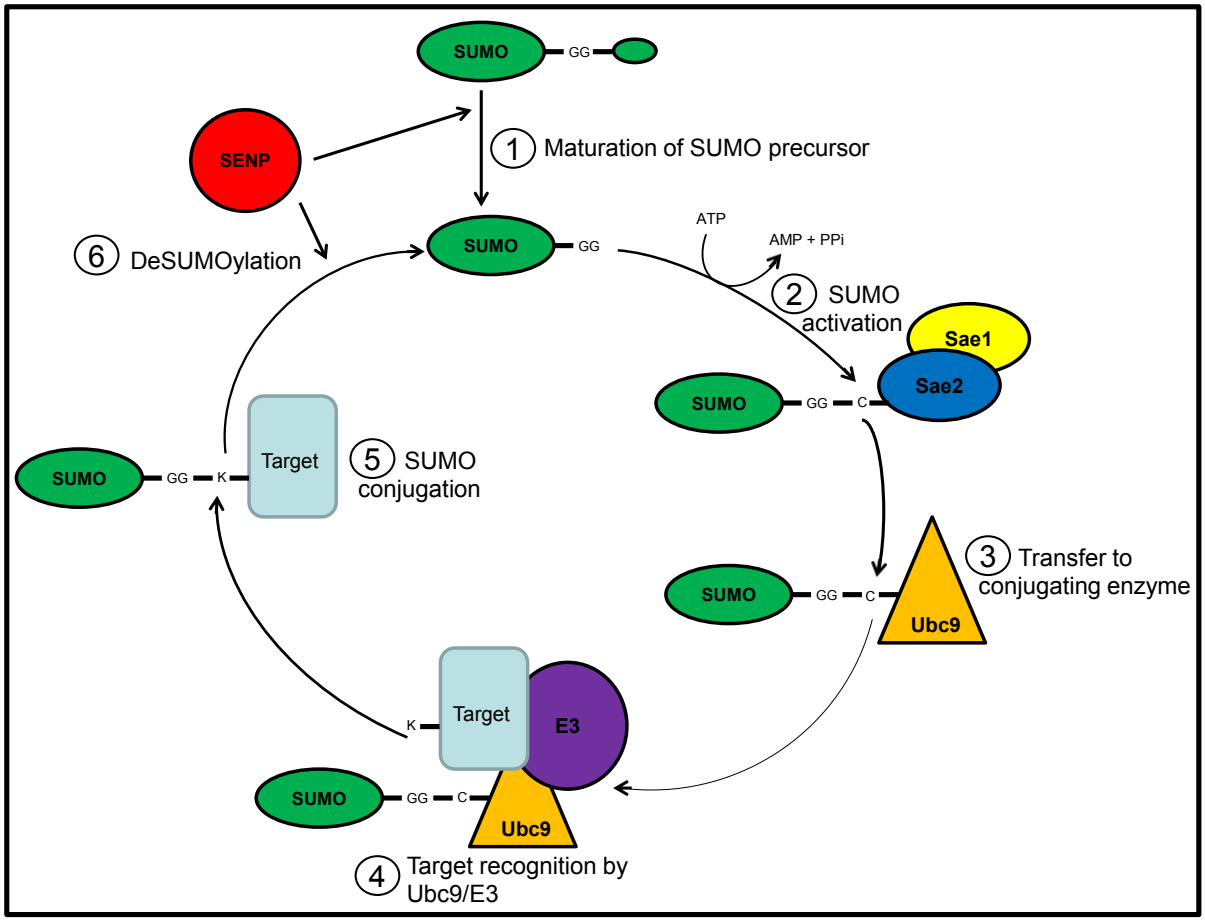

Figure 1.2 – The SUMO Pathway. Specific SENPs (sentrin-specific proteases) are first required to process specific precursor forms of SUMO (1), before they are activated by Sae1 and Sae2. SUMO is then conjugated to the E2, Ubc9 (3), which along with an E3 ligase recognises a specific target protein (4) and catalyses SUMO conjugation (5). SENPs are then also required for deSUMOylation of target proteins (6) (Adapted from [13]).

SUMO-2 and SUMO-3 have the capability to form polymeric chains through a conserved lysine (K11) embedded within a typical consensus modification site. SUMO-1 does not have such a capability, but it has been reported to be linked to the end of a poly-SUMO-2/3 chain causing termination of chain growth [47]. SUMOylation of target proteins is reversible and often an extremely dynamic process with SUMO modifications being made and removed in quick succession [48]. SUMOylation is regulated in part by their target, SUMO-modified proteins, which contain ψKX(D/E) consensus motifs enabling direct interaction with Ubc9. Thus, the target for SUMOylation plays an essential role in the stability of the interaction between the E2 enzyme and the substrate [44]. DeSUMOylation is carried out by a family of cysteine proteases called SENPs (SUMO-1/sentrin/SMT3-specific peptidases), which is discussed in greater detail in section 1.4 [45].

1.3 SUMO-Interaction Motifs (SIMs)

SUMOylation of proteins can regulate their protein-protein interactions. This is largely due to the presence of SUMO-interaction motifs (SIMs), most typically characterised by a short stretch of hydrophobic amino acids [(V/I)X(V/I)(V/I)] flanked by acidic residues, which show specificity for SUMO. When complexed to SUMO, the SIM adopts a parallel or antiparallel β-strand conformation, which allows the hydrophobic pocket of the SUMO surface to interact with the hydrophobic side chains of the SIM [49,50]. It has been hypothesised that the flanking acidic residues of the SIM can form salt bridges or hydrogen bonding interactions with the conserved basic residues on the SUMO surface and in doing so help determine the polarity of a SIM-SUMO interaction [44]. SIMs have been discovered in a wide range of proteins, including SUMO enzymes, SUMO substrates, SUMO-binding proteins and SUMO-targeted ubiquitin ligases [44]. Some examples include the base excision repair enzyme thymine DNA glycosylase (TDG), promyelocytic leukemia protein (PML) and the transcription factor DAXX [51,52]. The SIMs within the above mentioned proteins do not appear to confer specificity for a particular SUMO isoform, however, this is not always the case as seen with ubiquitin-specific protease 25 (USP25), which exhibits a preference for modification by SUMO-2/3 [53]. Whilst it appears that the architecture of a SIM can determine SUMO-interaction specificity the molecular determinants that underlie this specificity are yet to be eluded [44].

1.4 SENPs (SUMO-1/Sentrin/SMT3-Specific Peptidases)

There are six SENPs in humans (SENP1-3 and SENP5-7), which show sequence homology to two proteins executing similar roles in yeast cells (Ulp1 and Ulp2). Localisation of the human SENPs within the cell differs; SENP-2 is localised to the nuclear core complex, SENP-1, -6, and -7 are localised to the nucleoplasm, and SENP-3 and -5 to the nucleolus. SENPs fulfil two essential functions: the processing of precursor SUMO to its mature form (C-terminal hydrolase activity) and of interest to this study, the cleavage of isopeptide bonds between SUMO and its target protein (isopeptidase activity) [45].

SENP1 and SENP2 both exhibit greater isopeptidase activity than hydrolase activity with SENP1 removing SUMO-1 and SUMO-2/3 conjugates with equal efficiency from target proteins. SENP2, however, has shown a preference for deconjugation of SUMO-2/3 from target proteins. Studies have also revealed SENP3 and SENP5 to have greater isopeptidase activity on SUMO-2/3-conjugated targets than SUMO-1-modified species. Meanwhile,

SENP6 and SENP7 have repeatedly shown a preference for deconjugating poly-SUMO-2/3 chains over singularly-attached SUMO moieties (Figure 1.4) [54,55].

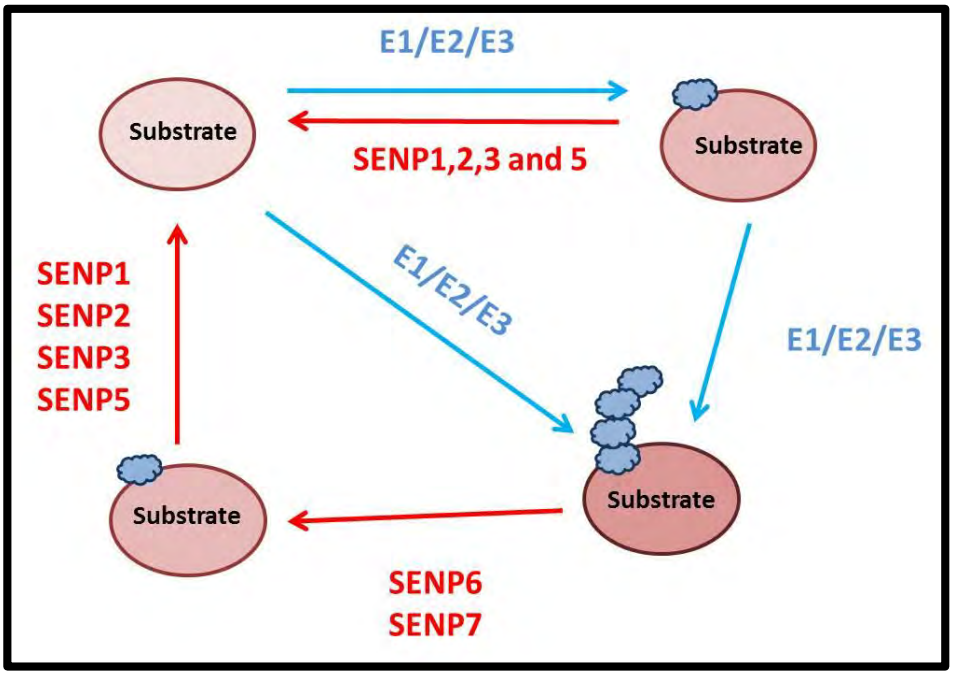

Figure 1.4 – The Varying Isopeptidase Activities of the Various SENPs within the SUMO Pathway. E1, E2 and E3 enzymes are required for the SUMOylation of substrates and synthesis of poly-SUMO chains. Whilst SENPs 1,2, 3, and 5 are responsible for deSUMOylation of mono-SUMOylated substrates, SENPs 6 and 7 have shown specificity for deconjugating poly-SUMO chains.

1.5 The DNA Damage Response (DDR)

Cells have hugely complex mechanisms to deal with the continuous damage the DNA undergoes from both exogenous and endogenous sources, which can result in single-strand lesions, double-strand breaks and inter-strand crosslinks. Critical regulators of DNA damage response (DDR) pathways are the PI3K (phosphatidylinositol 3 kinase) proteins, ATM (ataxia telangiectasia) and ATR (ataxia telangiectasia and RAD3 related) proteins, and their activation can trigger activities such as cell cycle inhibition, DNA repair or even apoptosis. ATM is activated in response to double-stranded DNA breaks (DSBs) commonly caused by ionising radiation (IR), cellular stress and prolonged stalling of replication forks. Meanwhile ATR is activated in response to single-stranded DNA lesions induced by ultra-violet (UV) radiation [10].

Of focus to this investigation is the repair of double-strand breaks (DSBs). DSBs are commonly repaired via two mechanisms; homologous recombination (HR) and non-

homologous end joining (NHEJ). The cells choice of repair mechanism is dependent upon the stage of the cell cycle as HR requires a section of homologous DNA in order to complete error-free repair. However, the sister chromatids required for such repair are only available during the S and G2 phases of the cycle. During other phases of the cell cycle NHEJ must be employed which is error-prone meaning the DNA sequence is often altered during repair [12].

To repair a DSB by HR, a cascade of tightly controlled protein signalling must be achieved to firstly recognise the DNA break, recruit repair factors and then execute accurate repair. The following details just a few of the main players within the initial response to a DSB by HR to create a distinct focal point around the location of the break, often referred to as Ionizing Radiation-Induced Foci (IRIF) [13]. The MRN complex is able to sense DSBs and is able to stimulate ATM, which activates itself by autophosphorylation at S1981 [14]. These proteins are recruited to DSB sites and ATM is able to phosphorylate a large number of proteins contributing to cell-cycle arrest, DNA repair and apoptosis (Figure 1.5). One such protein is the histone H2AX, whose phosphorylation mediates interaction with the scaffold protein MDC1. MDC1 acts as a hub for many proteins involved in the DDR to attach and form repair foci, including the ubiquitin ligases RNF8, RNF168 and BRCA1. As detailed in Figure 1.5, the ubiquitylation of histones H2A and H2AX, as well as other substrates, by ubiquitin ligases is critical for recruitment and correct function of proteins within the DDR to DSBs [15]. In recent years, SUMOylation within the DDR has been increasingly recognised as crucial for controlled regulation and correct execution of DSB repair.

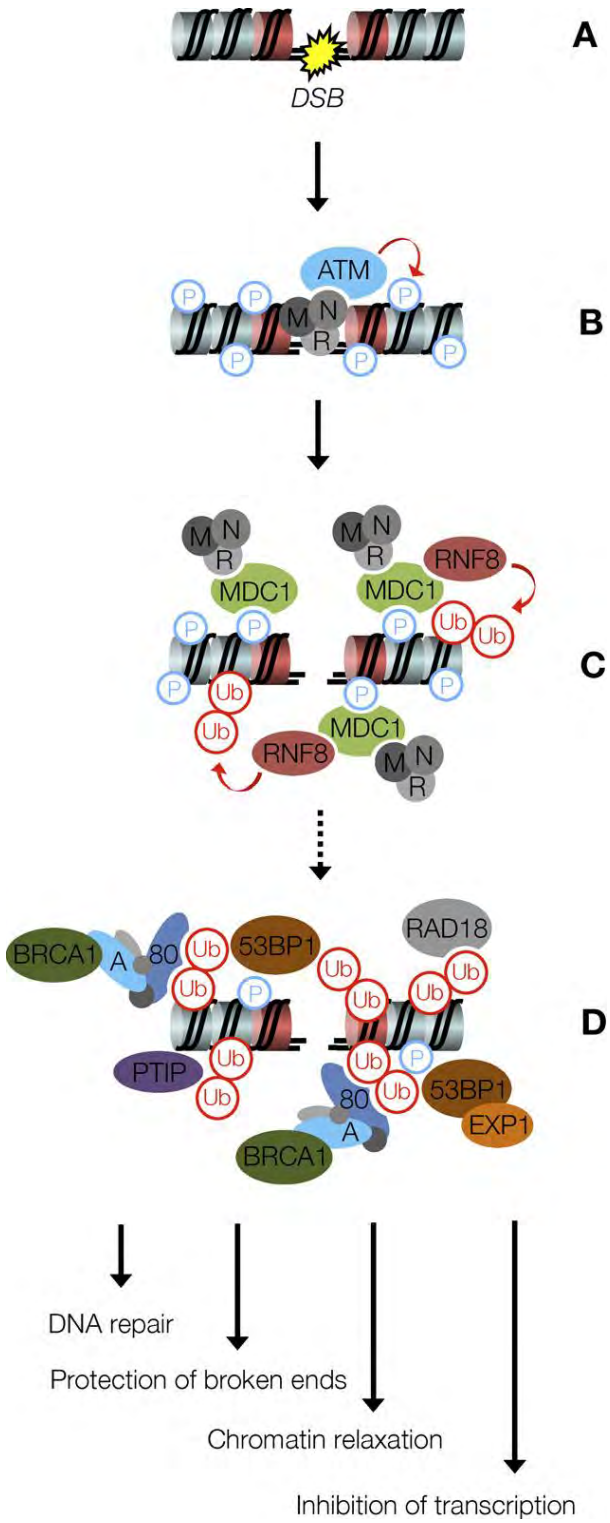

Figure 1.5 – The Early Responses to DSBs Resulting in the Highly Hierarchical Assembly of IRIF. The DSB is sensed by the MRN (MRE11-RAD50-NBS1) complex, which recruits the ATM kinase (A) resulting in turn in the recruitment of the scaffold protein MDC1 via phosphorylation of the histone H2AX. MDC1 recruits many proteins including the ubiquitin ligase RNF8, which ubiquitylates histones (C) to further recruit a second wave of repair factors such as 53BP1, the BRCA1 A complex and so on. The assembly of these repair proteins controls various DNA and chromatin transactions, ultimately leading to repair of the DSB. P: phosphate, M: MRE11, N: NBS1, R: RAD50, Ub: Ubiquitin, A: Abraxas (ABRA1), 80: Rap80, EXP1: EXPAND1 [16].

1.6 Ubiquitylation and SUMOylation in the DDR

The cascade of DDR signalling described above involves the timely and spatially specific assembly and disassembly of large protein complexes, which must be stringently controlled [43]. The specific orchestration of their localisation, interactions, activities and so on, is hugely aided by post-translational modifications. In recent years, modification by ubiquitylation has been revealed to be far from a simple marker for degradation, but instead a highly versatile modification with increasingly broader implications. The popularity of the ubiquitylation and SUMOylation stories has led to much increased study and it appears they have roles in many nuclear functions, including DNA repair mechanisms and checkpoint responses [56]. Given the highly reversible and dynamic nature of the two modifications it is unsurprising that they appear to be of such critical importance to the DDR as it is such a complex and highly regulated process. It also seems logical that the de-SUMOylation enzymes, SENPs, would be of critical importance to the correct execution of the DDR, as will be briefly explored within this study with regards to SENP7.

Several examples of the importance of ubiquitylation and SUMOylation modifications within the DDR have been shown in recent years. As touched on earlier, the ubiquitin ligases RNF8 and RNF168 form lysine (K) 63-linked chains, which act to anchor the adaptor protein RAP80 through its ubiquitin-interaction motif (UIM) domain, and RAP80 in turn recruits BRCA1 to repair foci [15]. PIAS1 and PIAS4 are E3 SUMO ligases required for promotion of BRCA1 accumulation at sites of repair, as well as, stimulate SUMOylation of BRCA1, which is crucial for its own ubiquitin-ligase activity. Cells also exhibit increased sensitivity to DNA damaging agents and fail to carry out efficient HR and NHEJ when PIAS1 and PIAS4 expression is depleted [57,58]. This suggests a cross-link between SUMOylation and ubiquitylation in DNA repair pathways.

SUMO/Ub cross-talk within the DDR is perhaps no more evidently displayed than in the modification of the proliferating cell nuclear antigen (PCNA) at the evolutionary conserved lysine 164 [59]. PCNA ubiquitylation is induced by DNA damage and required for DNA repair. Mono-ubiquitylation facilitates tranlesion DNA synthesis (TLS) via mediating interaction with TLS polymerases through their UIMs. However, K-63 linked poly-ubiquitylation directs repair through HR [60]. SUMOylation of PCNA on the other hand, inhibits repair by recombination through recruitment of the SIM-containing protein, Srs2 [61].

1.7 SENPs (Sentrin-Specific Proteases) in the DDR

RPA70 is the major ssDNA-binding subunit of the replication protein A (RPA) complex, which plays a critical role in the DDR. RAP70 associates with SENP6 during the S phase of the cell cycle to maintain RPA70 in a hypo-SUMOylated state [62]. However, in times of induced replication stress, the two proteins dissociate allowing SUMOylation of RPA70 by SUMO-2/3. This initiates DNA repair through HR via recruitment of Rad51 to the repair foci. Consistent with these results, γ-H2AX, RPA, and Rad51 foci are unperturbed by SENP6 knockdown, suggesting a role downstream of the early responses to DNA damage [62]. With regard to mammalian cells this is the only published work currently showing a direct link between SENPs and the DDR. However, work in yeast with Ulp2 (the yeast homolog to SENP 6 and 7) also showed a requirement in the later stages of the DDR and possible involvement in the restart of the cell cycle following termination of the DNA damage checkpoint [63].

Previous work in our laboratory had shown knockdown of SENP6 and SENP7 to cause large defects in HR repair capability. This could be conceived to be due to a loss of availability of SUMO-2/3 in the cell as deSUMOylation of poly-SUMO-2/3 chains is not possible in their absence. Indeed, unpublished work within our laboratory showed over-expression of RFP-SUMO rescued HR in SENP6-depleted cells, however, it did not do so in SENP7-depleted cells suggesting a more direct role in HR.

Further work upon SENP7 showed it to be recruited to sites of DSBs and co-localise with γ-H2AX in response to damage mediated by hydroxyurea. SENP7 was found to be chromatin bound through its interaction with heterochromatin protein-1-α (HP1-α) [64]. A HP1 box comprising of 7 amino acids (I,P,R,V,I,L,T) mediated interaction with HP1-α, and mutation of this domain disrupted binding and localisation of SENP7 to chromatin. Depletion of SENP7 was also found to reduce poly-Ub chain enrichment at sites of damage, as well as, disrupting Rad51 kinetics.

1.8 SENP7 and its SUMO-Interaction Motifs

A large part of this project was to look at the SUMO interaction properties of SENP7. Whilst SIM:SUMO interactions are known to be critical in the conjugating of SUMO to its targets, it is not known if they are involved in deconjugation. By studying the amino acid sequence of SENP7 and looking for the SIM consensus of amino acids [(V/I)X(V/I)(V/I)], 10 potential

SIMs were identified (Figure 1.8a). Three of these potential SIMs fell within the N-terminal catalytic domain and due to knowledge of the crystal structure of the domain it appeared that these were very unlikely to be of importance as they were located within well-formed secondary structures [55].

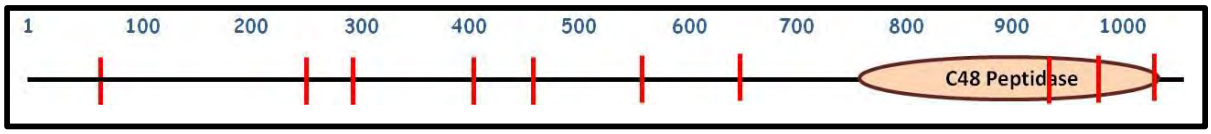

Figure 1.8a – Schematic of the SENP7 Protein. Red lines indicate the 10 SIMs identified within the coding sequence of SENP7. The c48 peptidase (catalytic domain) is also indicated. The numbers above represent amino acid number.

Crystallographic studies and computational modelling studies have shown SENP7 and SENP6 to have greater structural similarities to one another, whilst exhibiting significant differences to the other members of the SENP family [55]. These changes are likely to play a role in their preference for poly-SUMO-2/3 chains. Indeed, the identification of four sequence insertions (Loop-1 through to Loop-4) within SENP6 and SENP7 are thought to permit greater interaction with SUMO chains which have more flexible isopeptide linked substrates [55].

Another protein found to preferentially bind poly-SUMO-2/3 chains is the SUMO-targeted ubiquitin ligase, Ringer finger protein 4 (RNF4). This preferentiality has been shown to be due to a set of tandem SIMs that can recognise two or more SUMO-2/3 molecules in a chain [65]. SENP7's 7 potential SIMs (outside of the catalytic domain) may also be critical for its poly-SUMO-2/3 specificity [55]. However, the SIMs do not appear in tandem (Figure 1.8a) and it is unclear which of the SIMs are critical for SUMO binding. Figure 1.8b shows the amino acid sequences of the 7 potential SIMs of SENP7. To test their importance in SUMO interaction a construct of SENP7 was synthesised with these 7 potential SIMs made dysfunctional by changing their 4 amino acid SIM consensus (Figure 1.8c). This created a SIMless mutant of SENP7 to work with within the study.

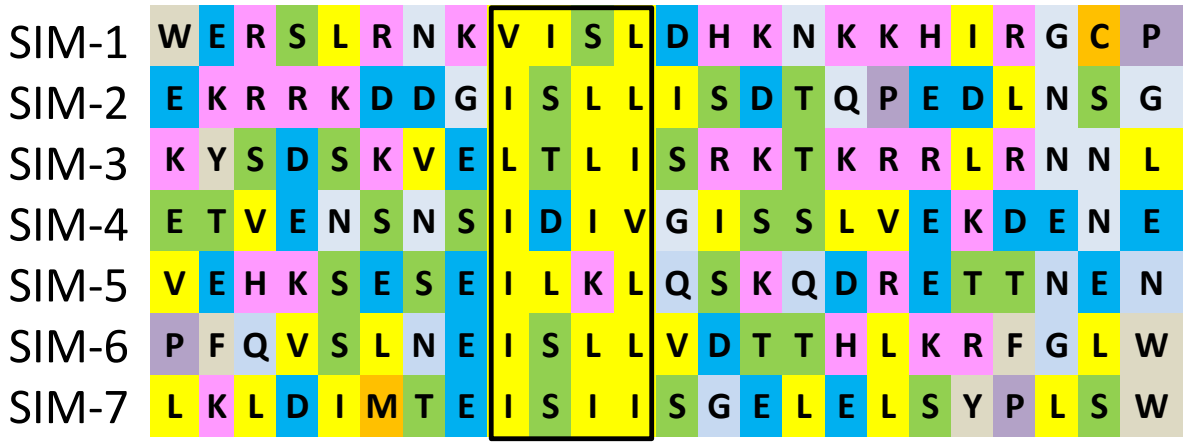

Figure 1.8b – The 7 Potential SIMs of SENP7. Numbered 1 to 7 in the order in which they appear in the primary sequence of the protein's amino acids. The 4 amino acids making up the recognised SIM sequence [(V/I)X(V/I)(V/I)] is boxed.

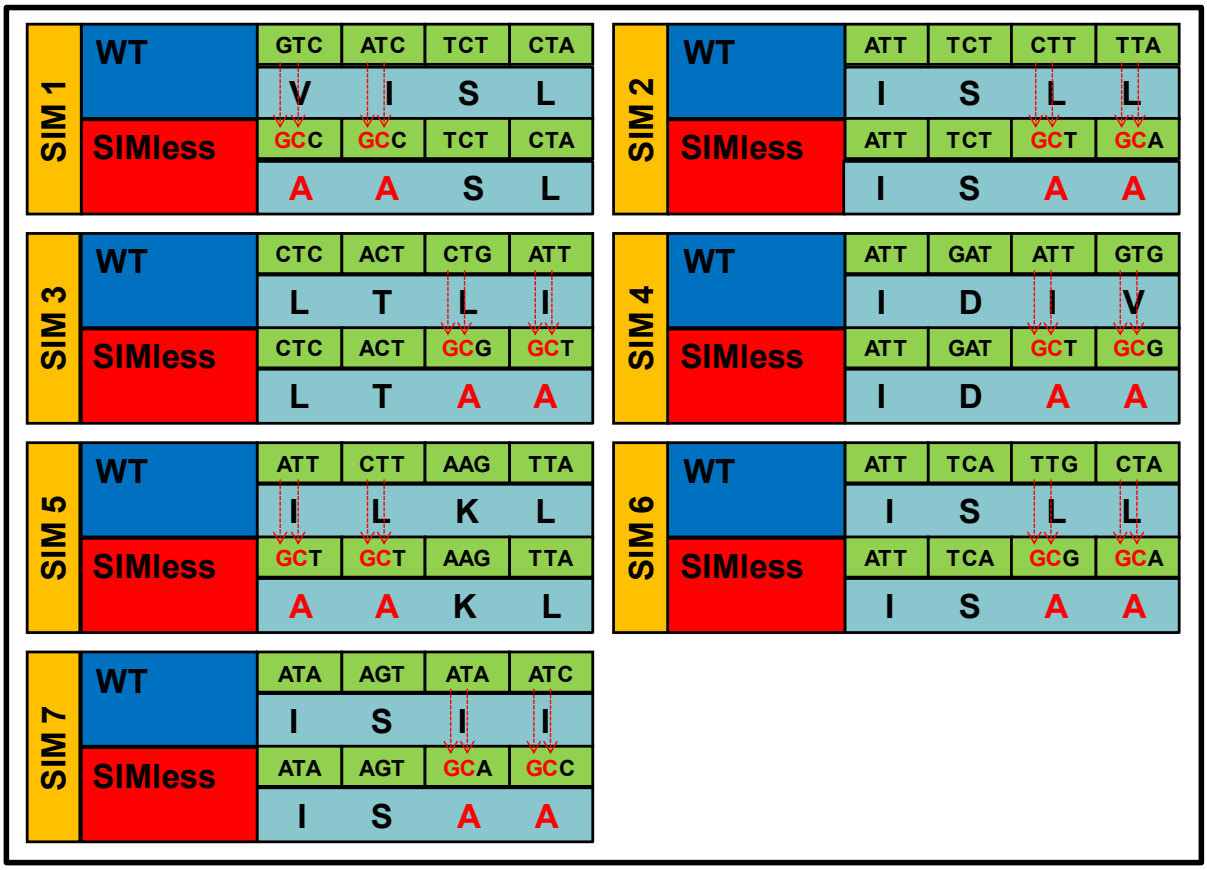

Figure 1.8c – The 7 Potential SIMs of SENP7 shown in their Wild-Type (WT) and SIMless Forms. The DNA sequence triplet codes and the amino acid sequences they encode are shown for WT SENP7 and SIMless SENP7 for each potential SIM. The nucleotide changes required to alter the translated amino acid sequence are shown in red, as are the changes to the amino acid sequence.

1.9 Aims

Based upon the studies and previous work conducted within the Morris laboratory discussed above and knowledge of SENP7's SUMO-binding activity and primary structure (i.e. the 7 potential SIMs), the principle aims of this study were outlined as the following:

1. To investigate which of the potential SIMs within SENP7 have SUMO-binding activity.
2. To investigate the importance of the potential SENP7 SIMs in homologous recombination (HR) and therefore, assess their importance for functionality of the protein.
3. To address whether SIM:SUMO binding and HR activity show correlation to one another.

Chapter Two:

Materials and Methods

2. Materials and Methods

2.1 Tissue Culture Techniques

2.1.1 Maintenance of Human Cell Lines

Cell lines were maintained in a 5% CO_2 incubator at 37ºC (Table 2.1). Cell lines were sustained in Dulbecco's modified Eagle's medium (DMEM) (Sigma), supplemented with 7% v/v foetal calf serum (FCS) (PAA Laboratories) and penicillin (+100 units/ml)/streptomycin (+100µg/ml) (Life Technologies).

FlpIn cells, and the stable cell lines created from the FlpIn cell line (see section 2.2.3) used for inducible expression of various Flag-SENP7 constructs, were maintained in tetracycline-free DMEM.

Table 2.1 Human Cell Lines Used in the Study.

Cell line	ATCC number	Additional Information
U20S	HTB-96	Human epithelial osteosarcoma cell line (origin = bone).
DR3 (Hela)	CCL-2 (Parent cell line)	Human epithelial adenocarcinoma cell line (origin = cervix). Contains human papilloma virus.
293T	CRL-11268	Human epithelial kidney cell line (origin = kidney).
FlpIn-TREx-293	CRL-1573 (Parent cell line)	A tetracycline-regulated expression cell line stably expressing the tetracycline repressor. Transfection of the cell line with pcDNA5/TO FRT plasmid expression construct containing a gene of interest, allows selection with hygromycin and induction of expression with doxycycline.

2.1.2 Human Cell Culture

The passage of adherent cell lines was achieved by washing twice with PBS (phosphate buffered saline) (Sigma), trypsinisation using 5 mls of 1% trypsin-ethylenediaminetetraacetic acid (EDTA) (PAA Laboratories) and incubated at 37ºC until cells lost adherence to the tissue culture dish. 10 mls of media was added to deactivate the trypsin, followed by

centrifugation at 1,400 revolutions per minute (rpm) at room temperature for 4 minutes. The cell pellet was resuspended in media and re-plated at required density.

2.1.3 Bacterial Cell Culture

pcDNA3.1(-) *E. Coli* bacteria (α-select competent cells) (BioLine) were grown on LB agar plates (containing 10g/L Tryptone, 10g/L NaCl, 5g/L yeast extract, 15g/L agar, and 1.5g/L Tris/TrisHCl) (Fisher Scientific), supplemented with 100 ng/ml ampicillin or 50ng/ml kanamycin to select for those bacteria that had successfully been transformed with the vector of interest, and incubated at 37ºC overnight. When growth of the bacteria was required on a larger scale, colonies were placed in Luria broth (LB) (containing 10g/L Tryptone, 5g/L NaCl, 5g/L yeast extract, and 1.5g/L Tris/TrisHCl) (Fisher Scientific) and grown under agitation at 37ºC overnight.

2.2 Cell Biology Techniques

2.2.1 – Knockdown of Gene Expression using Small-Interfering RNAs (siRNAs)

siRNA was prepared for transfection by adding to OptiMEM media (Gibco) and mixing with Dharmafect transfection reagent (Thermo Scientific) (1µl per well to be transfected) also in OptiMEM media (of an equal volume). The Dharmafect/OptiMEM solution was then added dropwise to the siRNA/OptiMEM solution and incubated for 30 minutes at RT. This was then added dropwise to the media covering the cells and the media swirled to ensure even coverage of the well.

Table 2.2.1 siRNAs Used in this Study. The siRNAs used in this study are shown, along with siRNA type, sense sequence and source.

Target protein	siRNA	Source
Non-targeting	Non-targeting siRNA #1	ThermoScientific
SENP7	SENP7.2	Sigma

2.2.2 – DNA Transfection of Human Cell Lines

DNA was prepared for transfection by adding to OptiMEM media and mixing with Fugene transfection reagent (Promega) also in OptiMEM media (of an equal volume). The Fugene

and DNA solutions were vortexed thoroughly and allowed to incubate at RT for 30 minutes before adding drop-wise to media and gently swirling to ensure even coverage of the plate.

2.2.3 – Creation of Stable Cell Lines, Selection with Hygromycin and Induction of Expression with Doxycycline

FlpIn-TREx-293 cells were transfected with 2 µg of the pcDNA5/TO FRT plasmid DNA construct to be inserted and 1µg of the plasmid vector pOG44 was also used. This contains a sequence encoding the restriction enzyme, pOG44, required for recombination of the DNA construct in to the Frt site of the FlpIn cells. Stable cell lines were selected by treatment with 200 µg/ml hygromycin B (Calciochem) and the induction of protein expression was made with 2µg/ml doxycycline (Sigma) supplementation of media.

2.3 Protein Chemistry Techniques

2.3.1 Harvesting Human Adherent Cells

For harvesting cells for co-immunoprecipitation assays, media was removed and cells washed twice in cold 0.15M saline. Cells were incubated in 300mM nuclear buffer (10mM HEPES pH 7.6, 300mM NaCl, 1.5mM $MgCl_2$, 10% glycerol, 0.2mM EDTA, and 0.1% Triton), supplemented with DNase (26.4 µg/ml) (Sigma), phosphatase inhibitor (X1) (Roche), protease cocktail inhibitor (X1) (Roche) and *N*-ethylmaleimide (NEM) (Sigma) at 4°C for 3 minutes before pipetting the lysate in to Eppendorf tubes. Lysates were then incubated at 4ºC for 2 hours under gentle agitation. Lysates were subsequently centrifuged at 15,000 rpm for 15 minutes and the pellet discarded.

2.3.2 Sodium Dodecyl Sulphate-Polyacrylamide Gel Electrophoresis (SDS-PAGE)

Proteins were separated according to molecular weight via SDS-PAGE. 10% polyacrylamide gels were made using the following components: 30% w/v acrylamide (37:5:1 BIS-acrylamide) (Severn Biotech), 0.1M Tris (Melford)/ 0.1M Bicine (pH8.3) (Severn Biotech), 0.1% SDS (Severn Biotech), 0.3% N, N, N', N'-Tetramethylethylenediamine (TEMED) (Sigma), 0.6% ammonium persulphate (APS) (Sigma) and deionised water. Gels were cast in an assembled apparatus (BioRad) and wells filled with running buffer (0.025M Tris, 1.92M Glycine, and 0.1% w/v SDS) (GeneFlow). Cell lysate and co-immunoprecipitation samples were prepared for running on polyacrylamide gels by adding an equal amount of Laemmli

sample buffer (25% v/v glycerol (BDH Laboratories), 5% β-mercaptoethanol, 2% w/v SDS, 0.01% w/v bromophenol blue (BDH Laboratories) and 65nM Tris (pH 6.8)). Samples were then heated at 95ºC for 5 minutes, spun down, and loaded in to the gel wells along with PageRuler Prestained Protein Ladder (Thermo Scientific). Gels were run at 150V typically for a time period of 80 to 110 minutes.

2.3.3 Visualisation of Proteins on Nitrocellulose Membranes

Proteins transferred from polyacrylamide gels on to polyvinylidene fluoride (PVDF) membranes (Millipore) were stained with Ponceau-S Stain (consisting of 0.1% w/v Ponceau-S and 5% v/v acetic acid) (Sigma) for 30 seconds. Membranes were then thoroughly washed with deionised water for visualisation and then further washed in Phosphate-Buffered Saline Tween-20 (PBST) (containing PBS (Sigma) and 1% Tween-20 (Fisher Scientific)), to remove the remaining stain.

2.3.4 Separation of DNA by Agarose Gel Electrophoresis

5-7µl of sample DNA was added to 2-3µl of X5 GelPilot Loading Dye (Qiagen) before loading on to an agarose gel (consisiting of 0.8% w/v agarose (Sigma) and 0.0001% v/v ethidium bromide (Fisher Scientific), along with Hyper DNA ladder (Bioloine). Gels were typically run at 130V for 60-90 minutes, before visualisation via ultra-violet (UV) spectroscopy (Syngene G:BOX).

2.4 Immunological Techniques

2.4.1 Western Blotting

Following molecular size separation of proteins by SDS-PAGE, proteins were transferred on to PVDF membrane via the following method. Transfer cassettes were assembled containing the following layers: a sponge, Whatmann 3MM blotting paper, PVDF membrane (firstly immersed in 100% methanol (ProLabo) to activate it prior to transfer), SDS-PAGE gel, Whatmann blotting paper and a sponge (all equipment was pre-immersed in transfer buffer containing 20% v/v methanol, 0.192M glycine and 0.025M Tris). The cassette was then placed in a transfer tank filled with transfer buffer and 100 volts run across it for 1 hour. Membranes were then blocked by placement in 5% skimmed dried milk (Marvel) in PBST for 30 minutes. Primary antibodies (Table 2.4.1a) were diluted in 5% skimmed dried milk in

PBST and incubated with the membranes for a suitable time period (typically overnight) at 4ºC. The membranes were then washed 3 times for 15 minutes in PBST, before incubation with secondary antibodies (Table 2.4.1b) conjugated to horseradish peroxidise (HRP) in 5% skimmed dried milk in PBST for 2 hours at RT under gentle agitation. Membranes were washed again in PBST 6 times for 5 minutes each time, before being placed in enhanced chemiluminescence (ECL) reagent (consisting of 0.1M Tris-HCl pH 8.5, 1.25mM Luminol (Sigma), 0.81mM Coumaric acid (Sigma), 0.018% (w/v) hydrogen peroxide (Sigma)) and deionised water) for 1 minute and exposed to autoradiography film (Fujifilm) for a suitable time period.

Table 2.4.1a – Primary Antibodies Used in this Study. Indicated are the primary antibodies used in this study, their antigens, dilution, use, species of origin and source.

Antibody	**Antigen**	**Dilution**	**Use**	**Species**	**Company/Source**
Flag (M2)	Flag	1 in 1000	WB, IP, Confocal microscopy	Mouse	Sigma
RFP	RFP	1 in 1000	WB	Rabbit	Sigma
KAP1	KAP1	1 in 1000	WB	Goat	Abcam
Beta-actin	Beta-actin	1 in 1000	WB	Rabbit	Abcam
HP1-alpha	HP1-alpha	1 in 1000	Confocal microscopy	Rabbit	Cell Signalling Technology

(N.B. WB – Western blot; IP – immunoprecipitation)

Table 2.4.1b – Secondary Antibodies Used in this Study. Indicated are the secondary antibodies used in this study, their antigens, dilution, use, species of origin and source.

Antibody	Antigen	Dilution	Use	Species	Company/Source
Mouse	Mouse IgG	1 in 5000	WB	Rabbit	Dako Laboratories
Rabbit	Rabbit IgG	1 in 5000	WB	Swine	Dako Laboratories
Goat	Goat IgG	1 in 5000	WB	Rabbit	Dako Laboratories
Mouse AlexaFlour-488 Ab	Mouse IgG	1 in 2000	Confocal microscopy	Goat	Invitrogen
Rabbit AlexaFlour-555 Ab	Rabbit IgG	1 in 2000	Confocal microscopy	Goat	Invitrogen

(N.B. WB – Western blot; IP – immunoprecipitation)

2.4.2 – Co-Immunoprecipitation (Co-IP)

293T cells were cotransfected with the various mutant SENP7 constructs and RFP as a control or with the RFP-SUMO-2 (Q90P mutant variant). When SUMO-conjugated proteins interact with Flag-SENP7 through SUMO interaction in which the Q90P variant of SUMO-2 is involved, the interacting protein is not released from SENP7 as this mutant variant is not cleavable.

Cell lysates, as prepared in Section 2.2.1, were incubated with 5-10µl (packed volume) of Anti-Flag (M2) Affinity Gel Beads (Sigma) on rotation at 4ºC overnight. Samples were then centrifuged at 3,000rpm, 4ºC for 1 minute and supernatant discarded. 1 ml of phosphate-buffered saline (PBS) (Sigma) was then added to the pellet, vortexed and spun again at 3,000rpm, 4ºC for 1 minute. This wash step was repeated a further 3 times. Supernatant was removed and 10µl Laemmli buffer (25% v/v glycerol (BDH Laboratories), 5% β-mercaptoethanol, 2% w/v SDS, 0.01% w/v bromophenol blue (BDH Laboratories) and 65mM Tris (pH 6.8)) added to the pellet. This is subsequently heated to 95ºC for 5 minutes and supernatent resolved by SDS-PAGE.

2.5 Molecular Biology Techniques

2.5.1 – Polymerase Chain Reaction (PCR)

The following reactants are added to a PCR tube: dNTPs (typically 0.2-0.4mM) (BioLine), the plasmid vector (a concentration typically of 0.02mM), the forward (F) primer and the reverse (R) primer (typically at concentrations of 0.3-0.5mM), and a DNA polymerase (Pfu enzyme (Sigma) or Pfusion polymerase (Promega) within a buffer (X10 buffer) (Promega). Suitable heat cycles for the required PCR were then undertaken.

Table 2.5.1a – Primers Used in this Study. Indicated are the primers used in this study, the gene they target, their sequence and source.

Gene being targeted	Primer	Sequence	Source
SENP7	SENP7 F	_____	Sigma
SENP7	158 F	5'-CTCAGAACGCTGGACTCTCC	Sigma
SENP7	545 F	5'-CCCACCTGTAACTGAGGGAAG	Sigma
SENP7	824 F	5'-TCATCTCGAACAGGAAAGCAG	Sigma
SENP7	1133 F	5'-GAGTAATGCCACCAAAAGTGC	Sigma
SENP7	1284 F	5'-AAGGGAACCAATCACTGATCTC	Sigma
SENP7	1492 F	5'-GCCCATATAATCCTGTCATGG	Sigma
SENP7	1700 F	5'-TAAAGCGGTTTGGGTTATGG	Sigma
SENP7	322 R	5'-CCGTCCATCGGACATTCGTC	Sigma
SENP7	790 R	5'-CCACTGTTAAGGTCTTCAGG	Sigma
SENP7	1025 R	5'-GGCTTTTCAAACTCAGTGG	Sigma
SENP7	1360 R	5'-CTGCTTGGTAACCCCCAG	Sigma
SENP7	1456 R	5'-TCAATGGTAGTTCTAACAATGCT	Sigma
SENP7	1690 R	5'-CAAACCGCTTTAAATGTGTGG	Sigma
SENP7	2050 R	5'-CAACACCAGCAGGGAAAG	Sigma

(N.B. F – forward primer; R – reverse primer)

2.5.4 – Transformation

Typically, 2-3µl of the plasmid DNA construct of interest was added to 50µl of competent pcDNA3.1(-) *E. Coli* bacteria and incubated on ice for 30 minutes. The cells were heat-shocked for 45 seconds at 42ºC, placed back on ice for 5 minutes before adding 250µl of LB

broth under aseptic conditions and incubating at 37ºC for 1 hour. Cells were grown overnight on, a single colony picked and placed in to 400mls of LB and grown under gentle agitation at 37ºC overnight.

2.5.5 – Isolating DNA from Bacteria

For maxi-preps, bacterial cell culture was centrifuged at 3,500rpm for 15 minutes at 4ºC and the supernatant discarded. For mini-preps, 1ml of bacterial cell culture grown overnight was placed in to a 1.5ml Eppendorf tube, centrifuged at 13,000rpm for 1 minute and the supernatant removed. A further 1ml of cell culture was added to the tube, spun again and supernantent discarded. Extractment of DNA from the bacterial cell pellet employed the use of the Machery-Nagel Nucleobond Xtra Maxi kit (maxi-prep) and the Machery-Nagel Plasmid DNA Purification kit (mini-prep). DNA was dissolved in sterile distilled water and concentration measured with the use of a Nanodrop spectroscopy machine. The DNA was stored at -20ºC until further required.

2.5.6 – Sequencing of DNA

The sequencing of DNA to confirm successful creation of various constructs was completed by an external source. DNA was prepared to a concentration of 100ng/µl and primers to a concentration of 3.2pmol/µl and outsourced to SourceBioscience (Lifesciences) for sequencing.

2.5.7 – Preparation and Viewing of Samples by Confocal Microscopy

U2OS cells were plated on to a 24-well plate in which small, circular, glass slides had been placed for the cells to adhere too. Cells were transfected with 1µg of DNA for each of the individual SENP7 construct plasmids used. After a period of 48 hours post-transfection, media was removed and the wells washed with 1ml of PBS. PBS was removed and cells fixed via incubation in 250µl of 4% w/v paraformaldehyde (PFA) (Sigma) for 10 minutes at RT. The 4% PFA was removed and cells incubated in 250µl 10% Triton (Fischer Chemicals) for 5 minutes at RT to allow cells to be permeable to antibodies. Triton was removed and the fixed cells left in PBS, covered in parafilm (Bemis) and left at 4°C until required for staining.

PBS was removed and the cells incubated for 24hrs with polyclonal rabbit anti-HP1-α Ab (1:1000) and for 1 hour with polyclonal mouse anti-Flag (M2) Ab (1:1000) within 200µl fetal calf serum (FCS) at 4°C. The FCS was removed and a four PBS washes made before subsequent incubation anti-rabbit 555 Ab (1:2000) and anti-mouse 488 Ab (1:2000) within

200µl FCS for 1 hour at 4°C. The FCS was once again removed and the cells washed two times in PBS, before addition of 0.4 µg/ml Hoescht stain (Sigma) in PBS for two minutes at RT. This was removed, the cells washed with PBS and the glass slides carefully removed from the wells and fixed cell-side-down upon a microslide via the use of Immunomount gel (Thermo Scientific).

Cells were examined using a Zeiss LSM 510 confocal microscope with three lasers giving excitation lines at 633, 543 and 488nm. Data from channels was collected with 8-fold averaging at a resolution of 1024x1024 pixels, using an optical slice of between 0.5 and 1mm using a 63x objective with the Zeiss Axioplan-II microscope.

2.5.8 – Preparation of Samples for the Homlogous Recombiantion (HR) Assay and Analysis via Flourescent-Associated Cell Sorting (FACs)

DR3 (Hela) cells were grown within 12-well plates. Endogenous SENP7 was knocked down via the use of a SENP7 specific siRNA (50nM per well) (SENP7.2) (Sigma). For control wells a non-targeting siRNA was employed (50nM per well) (Sigma). After 24 hours, media was removed and replaced with fresh media. Cells were subsequently cotransfected with various SENP7 mutant constructs, an RFP-encoding vector and a SceI recombinase-encoding vector (all at 1µg per well). The RFP expression of the cells is used to identify those cells who have been successfully transfected when analysing via FACs. The SceI recombinase-encoding vector contains two inactive alleles of GFP (Figure 2.5.8). The first is inactive because within its coding sequence it contains the 18 base-pair (bp) restriction enzyme recognition site for the I-SceI recombinase. The second GFP allele is inactive due to truncation. SceI recombinase is a rare-cutting endonuclease derived from Saccharomyces cerevisiae and is therefore, very unlikely to cut the human genome. When the plasmid is transfected in to a cell and the SceI recombinase cleaves the first GFP allele a double-strand break (DSB) is created. Accurate repair of this DSB is only possible through HR by employing the second ‘donor’ GFP allele as a template for repair (as the cell uses the sister chromatid for HR during the S phase of the cell cycle). Once repaired, the cell expresses GFP. Therefore, the proportion of RFP positive cells exhibiting GFP expression during FACs analysis can be used to determine the HR capability of the cells. With reference to this study, the effect of the various SENP7 mutations upon the functionality of the proteins compared to WT SENP7 in terms of HR rescue can be assessed.

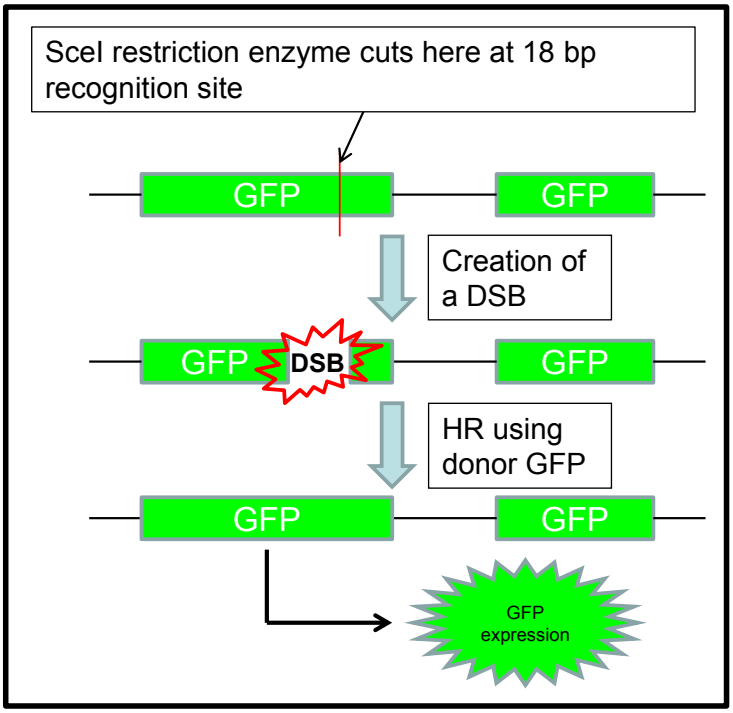

Figure 2.5.8 – HR Repair of GFP Allele After Cleavage by SceI. A schematic showing the repair of one GFP allele via employing a donor GFP allele during HR repair in response to a DSB after cleavage at a specific-site within the coding region of the first GFP allele.

48 hours after cotransfection the media is removed, the cells washed with PBS and detached by trypsinisation. 1ml of PBS was then added and the cells transferred to FACs tubes. These are centrifuged at 1500rpm for 5minutes at 4°C and supernatant removed. 250µl of 4% w/v PFA is then added, the tubes vortexed to resuspend the cells and incubated at RT for 30 minutes under gentle agitation. The tubes are then spun again at 1500rpm for 5minutes at 4°C, supernatant removed and 250µl of PBS is added. Samples can be stored at 4°C until ready for analysis by FACs. Prior to analysis on an Accuri C6 Flow Cytometer cells are resuspended by vortexing.

2.6 Statistical Methods

2.6.1 Paired Two-Sided T-Test for Comparison of Means Derived From Small Samples

T-tests were performed to evaluate the statistical significance between two groups of data for the HR assay. All t-tests were performed at a P-value of 0.05 using percentage points based on 'student's' *t*-distribution.

Chapter Three:

Results

3.1 – The Creation of Various SIM Mutant Versions of SENP7

Employing the synthesised SIMless version of Flag-SENP7, various SIM mutants (Table 3.1) were created via two sets of PCRs. The first utilised primers specific for sequences either side of the SIM(s) of interest to create a PCR product of known size with either wild-type (WT) functional SIMs or mutated non-functional SIMs. For example, to create an intermediate section of DNA including the coding region for WT SIM1 a forward primer would be used that binds upstream of SIM1 on one strand and a reverse primer that binds downstream of SIM1 on the other strand whilst employing the Flag-WT-SENP7 vector (Figure 3.1a(A)). Alternatively, to create an intermediate section of DNA including the coding region for mutated SIMs 4 and 5 a forward primer would be used that binds upstream of SIM4 on one strand and a reverse primer that binds downstream of SIM5 on the other strand whilst employing the Flag-SIMless-SENP7 vector (Figure 3.1a(B)). Successful production of the intermediates from PCR1 was confirmed by agarose-gel electrophoresis allowing analysis of the intermediate sizes (Figure 3.1b).

This ‘intermediate’ section of DNA was then used as the primers for a second PCR employing the reciprocal SENP7 vector (WT or SIMless) from the first PCR (details in Table 3.1). Removal of methylated template DNA was achieved via enzymatic digestion with the restriction enzyme, Dpn1.Transformation in to competent bacteria and subsequent culture growth allows the purification of concentrated plasmid DNA containing the recombinant DNA of interest. Finally, sequencing of selected regions within the SIM mutant constructs confirmed their correct synthesis.

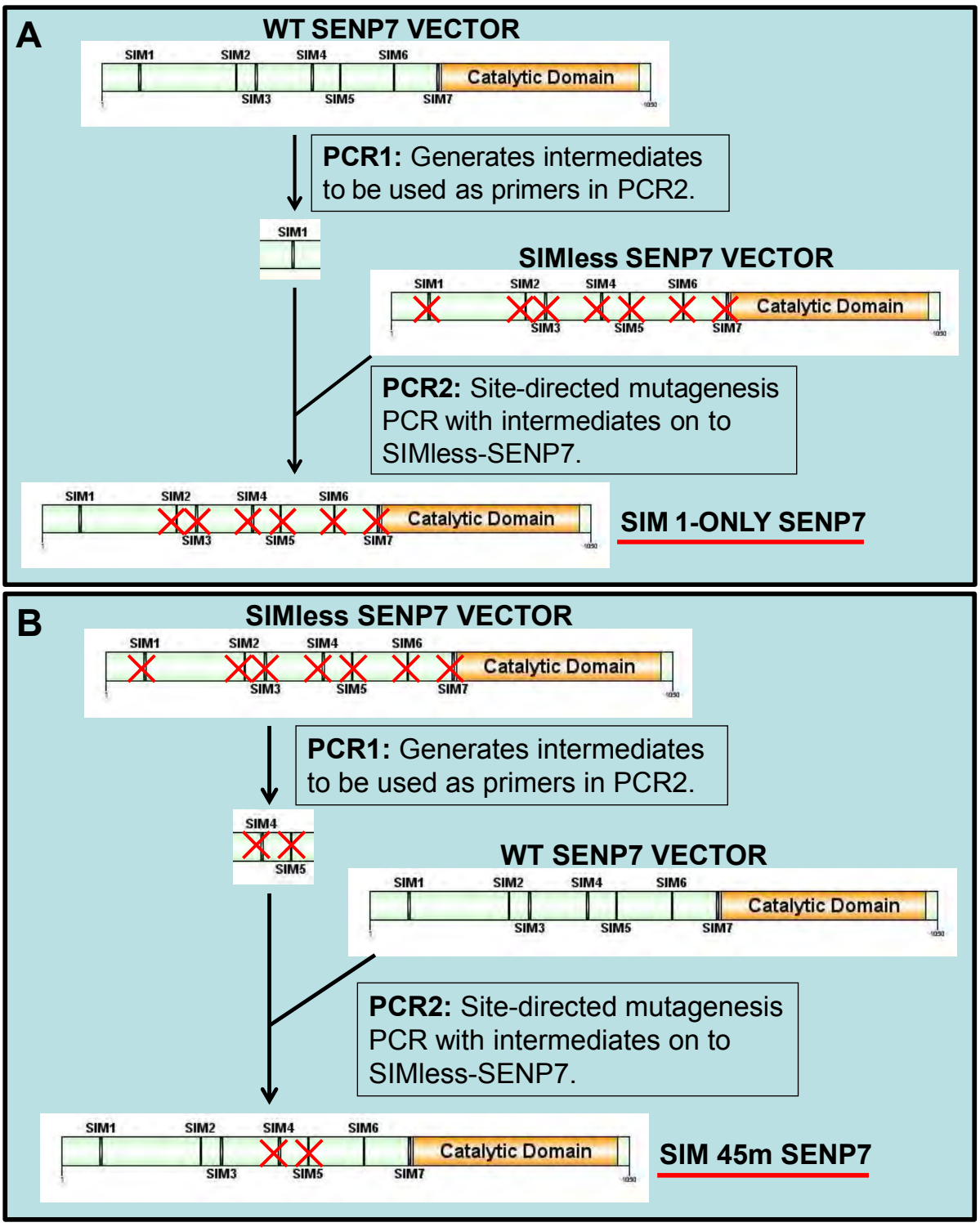

Figure 3.1a – Schematic Highlighting the Steps Required to Produce the Various SIM Mutants of SENP7. A) The creation of a SIM 1-only mutant via the production of an intermediate section of wild-type (WT) SENP7 encompassing SIM 1 in its WT form. This is then used as a primer in a site-directed mutagenesis PCR with the SIMless SENP7 vector to produce the final vector carrying a Flag-SENP7 SIM 1-only recombinant section of DNA. B) The creation of a SIM 45-mutated mutant via the production of an intermediate section of SIMless SENP7 encompassing SIM 4 and SIM 5 in their mutated form. This is then used as a primer in a site-directed mutagenesis PCR with the WT SENP7 vector to produce the final vector carrying a Flag-SENP7 SIM 45-mutated recombinant section of DNA.

Table 3.1 – Details of the PCRs Required in Making the Various SIM Mutant Constructs of SENP7.

Mutant SENP7 construct	Forward Primer	Reverse Primer	Size of intermediate piece of DNA	Vector for PCR1	Vector for PCR2	Primer for sequencing
SIM 1-O	158 F	322 R	164	WT	SIMless	SENP7 F
SIM 23m	545 F	1025 R	480	SIMless	WT	545 F
SIM 45m	1133F	1456 R	326	SIMless	WT	824 F
SIM 45m	1492 F	2050 R	558	SIMless	WT	1492 F
SIM 23-O	545 F	1025 R	480	WT	SIMless	545 F
SIM 45-O	1133F	1456 R	326	WT	SIMless	824 F
SIM 67-O	1492 F	2050 R	558	WT	SIMless	1492 F
SIM 4567-O (i)	158 F	1025 R	867	SIMless	WT	SENP7 F
SIM 4567-O (ii)	1133 F	2050 R	917	WT	SIMless	824 F
SIM 167-O	545 F	1456 R	911	SIMless	WT	545 F
SIM 123-O (i)	1133 F	2050 R	917	SIMless	WT	SENP7 F
SIM 123-O (ii)	158 F	1025 R	867	WT	SIMless	SENP7 F
SIM 2345-O	545 F	1456 R	911	WT	SIMless	545 F

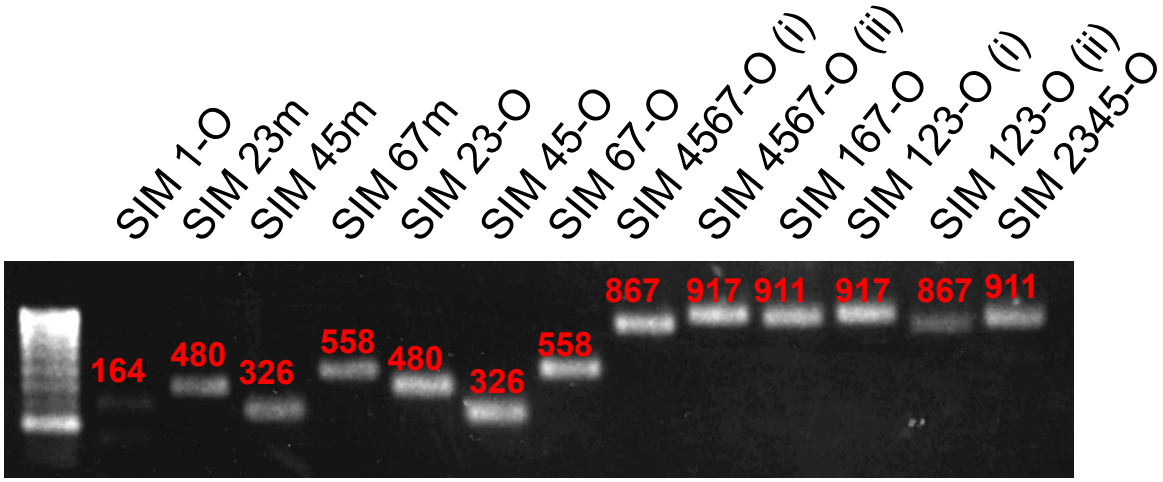

Figure 3.1b – PCR1 Produced Intermediates of the Expected Size for each of the Various SIM Mutants to be made. PCR product from PCR1 was subjected to ethidium bromide-supplemented agarose-gel electrophoresis and viewed via UV spectroscopy.

3.2 – The Creation of Stable Cell Lines for Inducible Expression of Various SENP7 Constructs

It was realised that the creation of stable cell lines for the inducible production of Flag-tagged SENP7 protein of the WT, catalytic (CA), SIMless, and SIMless-catalytic (SIMlessCA) variants would be very useful for this study. WT and CA stables already existed in the laboratory, whilst the SIMless and SIMlessCA did not. Firstly, the SIMlessCA construct was made via site-directed mutagenesis of the SIMless vector to introduce a cysteine to alanine amino acid substitution at residue 992 (C992A) within the catalytic domain.

To create stable cell lines the section of recombinant DNA encoding the Flag-tagged SENP7 construct must be inserted in to the 5.1 kb inducible expression vector pcDNA5/FRT/TO. Over a period of weeks, stable cells were selected through hygromycin supplementation of media (see section 2.2.3 for further details). Treatment with doxycycline allowed the inducible expression of the protein encoded by the inserted gene, i.e. Flag-SIMless SENP7 or Flag-SIMlessCA SENP7, and confirmed the successful creation of stable cell lines (Figure 3.2).

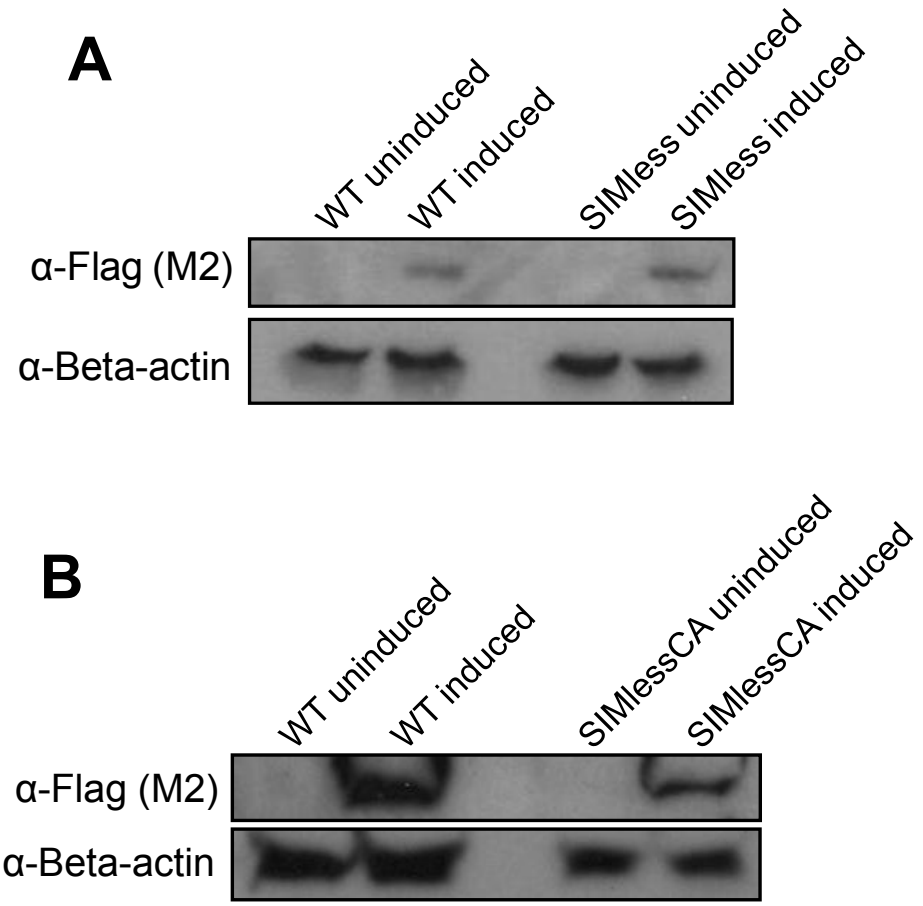

Figure 3.2 – Successful Creation of Stable Cell Lines for Inducible Production of Flag-SIMless SENP7 and Flag-SIMlessCA SENP7. A-B) Cell lines were induced or not induced with 2µg/ml doxycycline two days prior to taking cell lysates and subjecting to Western blotting.

3.3 – The Cellular Localisation of SENP7 and HP1-α is Not Affected by the Various SENP7 Mutations

SENP7 had previously been shown both in our own laboratory and in [64] to co-localise with HP1-α to heterochromatin within the cell nucleus. Confocal microscopy was employed to investigate whether any of the various mutated forms of SENP7 localise differently within the cell as compared to WT. It was shown that localisation is not effected within any of the mutants and co-localisation with HP1-α is unperturbed. This is somewhat expected as SENP7 has been shown to interact with HP1-α through its HP1 box with no SIM involvement, as discussed in section 1.7.

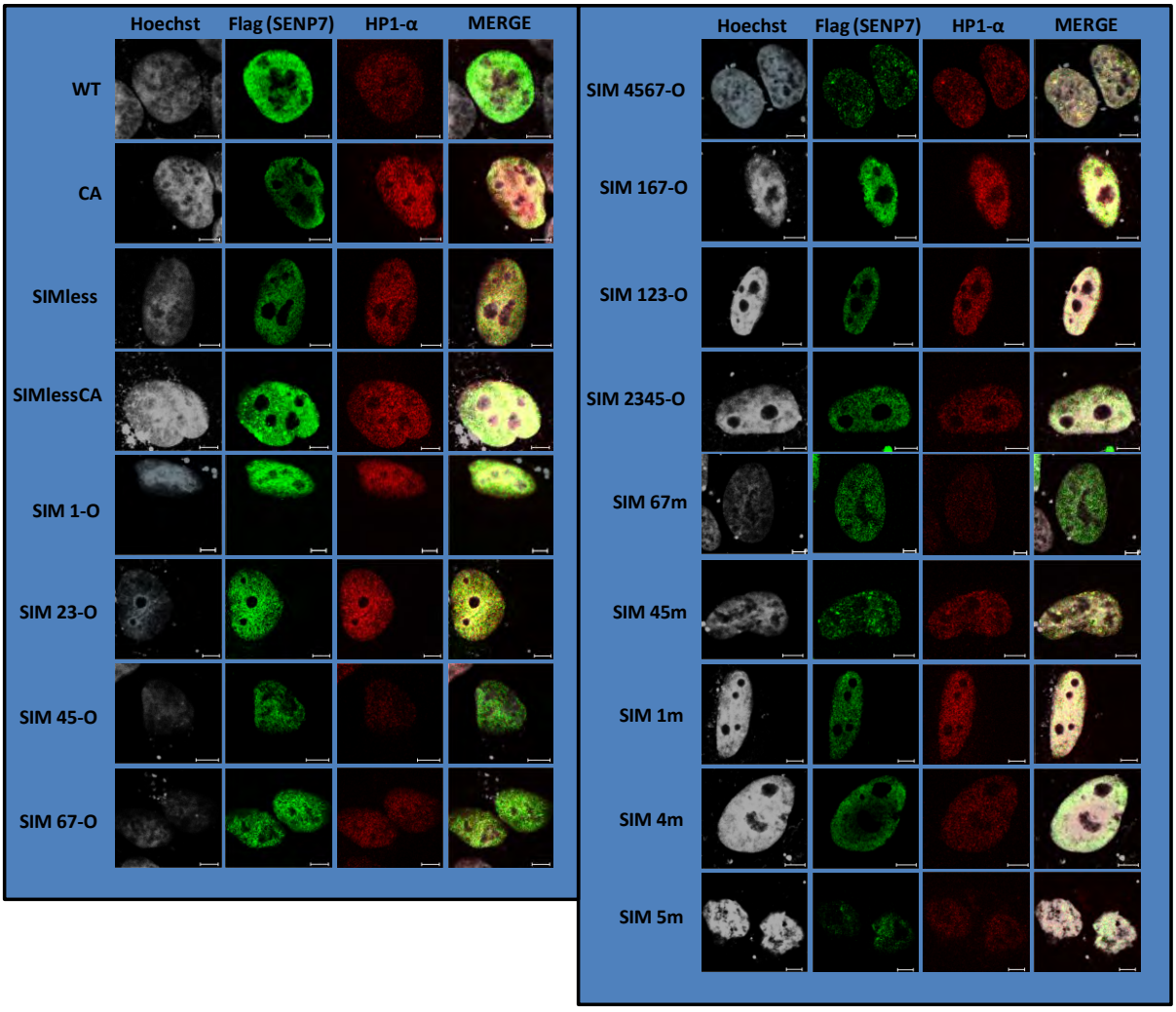

Figure 3.3 – All the Various SENP7s Localise to the Nucleus. U2OS cells were transfected with 1µg of DNA for each SENP7 construct indicated. After 48 hours cells were fixed using 4% paraformaldehyde (PFA) and treated with 10% Triton to allow cells to be permeable to antibodies. Cells were then incubated for 24hrs with polyclonal rabbit anti-HP1-α Ab (1:1000) and for 1 hour with polyclonal mouse anti-Flag (M2) Ab within fetal calf serum (FCS). Cells were then washed and incubated with anti-rabbit 555 Ab and anti-mouse 488 Ab within FCS. Cells were washed once again and stained with Hoechst for 2 minutes, before further washing, mounting on to microslides and viewing via confocal microscopy.

3.4 – SENP7 Interacts with SUMO-2 and the Various Mutated Forms of SENP7 Investigated in this Study Exhibit Different Strengths of Binding

Many previous studies have shown SENP7 to interact with SUMO-2/3 preferentially over SUMO-1 [54,55]. Via immunoprecipitation methods, the various Flag-SENP7 proteins (WT and mutated) were isolated from cell lysates, along with any interacting partners. Through transfection of RFP and RFP-SUMO-2-Q90P (a catalytic resistant variant of SUMO-2 – see section 2.4.2 for details), when Western blotting, probing membranes for RFP allowed identification of any proteins with SUMO-2 modifications which interact with SENP7. Figure

3.4a shows that WT SENP7 interacted with SUMO-2 modified proteins, whilst the SIMless and SIMlessCA exhibited far less interaction, suggesting the SIMs are required for interaction with SUMO-2 moieties. Meanwhile, the CA SENP7 variant exhibited greater interaction with SUMO-2 moieties than WT. Whilst neither form of SENP7, CA or WT, can cleave the Q90P variant SUMO-2, it would be expected that poly-SUMO-2/3 chains existing in the cells at the time of cell lysis would consist of both of the Q90P variant SUMO-2 and also endogenous SUMO-2/3. WT SENP7 has the capability to cleave these residues releasing the attached SUMO-modified protein. However, the CA mutant does not have this capability and therefore, is expected to exhibit more interaction with SUMO-2-modified proteins.

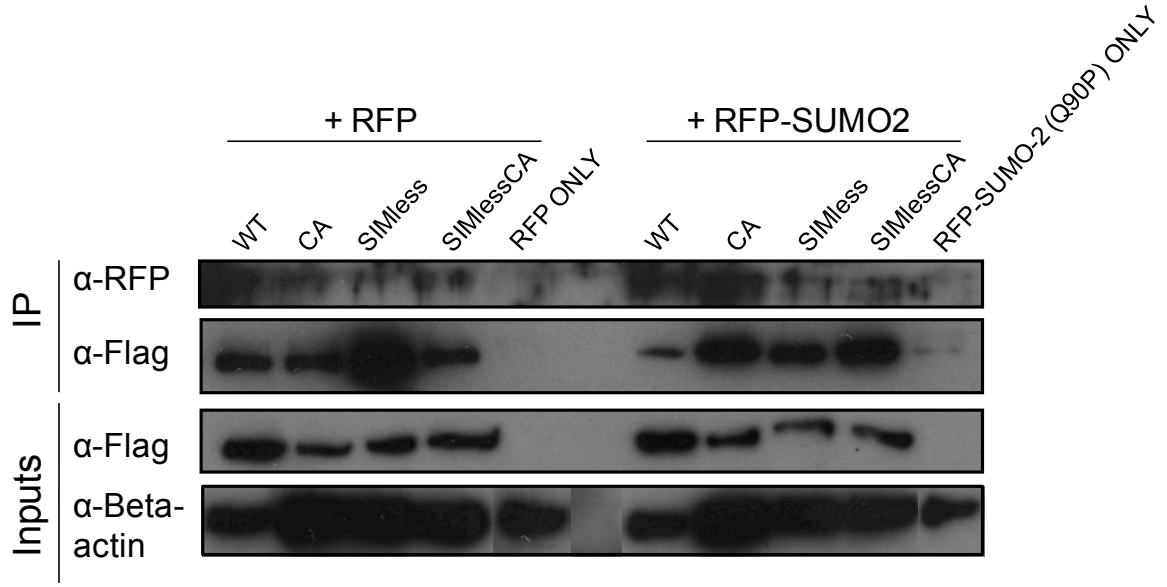

Figure 3.4a - The Catalytic, SIMless and SIMless-Catalytic Mutants of SENP7 Exhibit Different Strengths of Interaction with SUMO-2/3 *in Vitro* Compared to WT. The various stable SENP7 cell lines were induced with 2µg/ml doxycycline and transfected with either RFP or RFP-SUMO-2/3 two days prior to making cell lysates. Note that uninduced WT SENP7 cells were transfected with RFP or RFP-SUMO-2/3 as a control. Lysates were then incubated with Flag(M2) Ab-coated beads for 24 hours at 4°C. A series of PBS washes were made, before addition of Laemmli buffer, heating at 95°C and subjecting to Western blotting.

Immunoprecipitation experiments to investigate the SUMO-2 binding capabilities of the various SIM mutant constructs revealed some interesting results. SIM 67-only, SIM 4567-only, SIM 167-only, SIM-123-only and SIM 2345-only exhibited good binding to RFP-SUMO-2 (Q90P). SIM 1-only surprisingly showed some binding also, however, the densitometry readings are a little skewed by smudges on the IP blot for RFP making interpretation difficult. Meanwhile, SIM 23-only and SIM 45-only exhibited little to no

interaction with RFP-SUMO-2 (Q90P) when compared to control (RFP-SUMO-2-Q90P only).

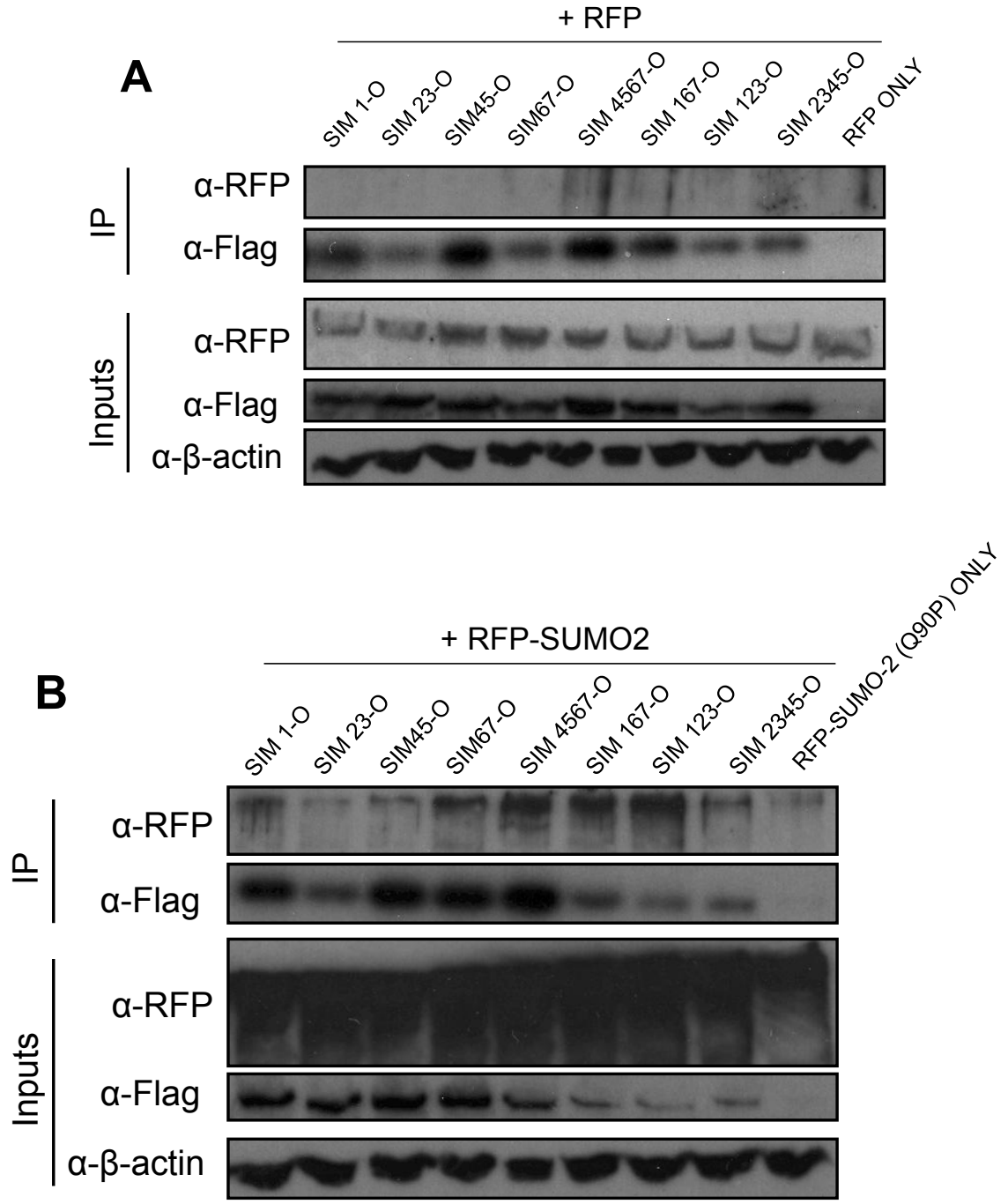

Figure 3.4b - The Various SIM Mutants of SENP7 Exhibit Different Strengths of Interaction with SUMO-2 *in Vitro*. 293T cells were cotransfected with the various SIM mutant constructs indicated and either RFP **(A)** or RFP-SUMO-2-Q90P **(B)** two days prior to making cell lysates. Transfection with RFP **(A)** or RFP-SUMO-2/3 **(B)** alone was used as a control. Lysates were then incubated with Flag(M2) Ab-coated beads for 24 hours at 4°C. A series of PBS washes were made, before addition of Laemmli buffer, heating at 95°C and subjecting to Western blotting. **C)** Densitometric scanning was used to quantify the proportion of RFP-SUMO-Q90P bound by the various SIM mutants relative to the amount of Flag-SENP7 immunoprecipitated.

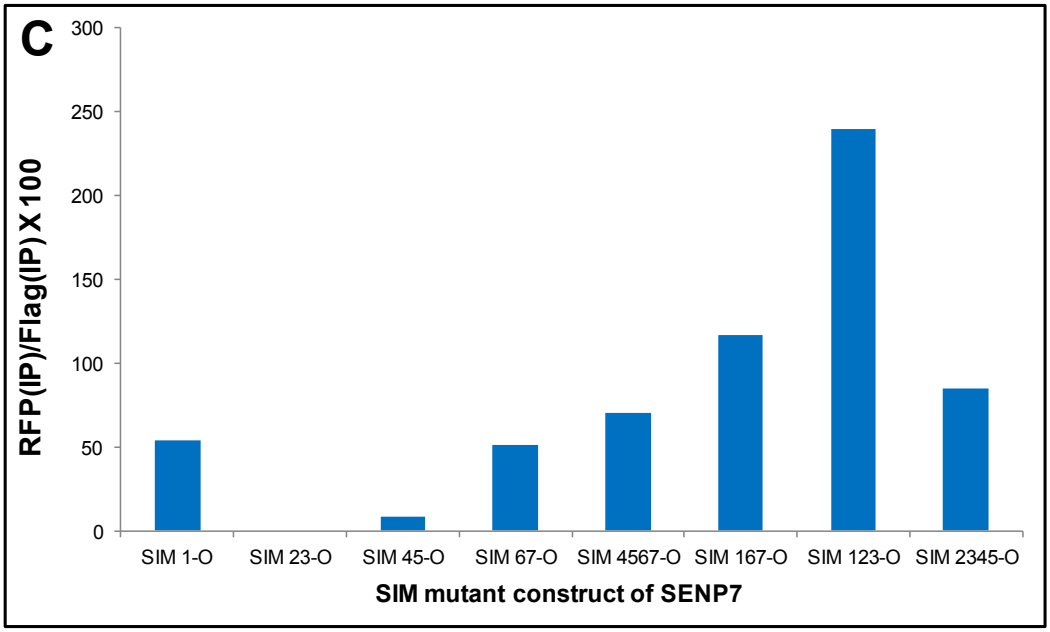

Figure 3.4b continued - The Various SIM Mutants of SENP7 Exhibit Different Strengths of Interaction with SUMO-2 *in Vitro*. 293T cells were cotransfected with the various SIM mutant constructs indicated and either RFP **(A)** or RFP-SUMO-2-Q90P **(B)** two days prior to making cell lysates. Transfection with RFP **(A)** or RFP-SUMO-2/3 **(B)** alone was used as a control. Lysates were then incubated with Flag(M2) Ab-coated beads for 24 hours at 4°C. A series of PBS washes were made, before addition of Laemmli buffer, heating at 95°C and subjecting to Western blotting. **C)** Densitometric scanning was used to quantify the proportion of RFP-SUMO-Q90P bound by the various SIM mutants relative to the amount of Flag-SENP7 immunoprecipitated.

3.5 – The Activity of the Various SENP7 Mutants Measured in Terms of the Cells Ability to Perform Homologous Recombination (HR)

To investigate whether the SUMO binding efficiency of the various SENP7 mutants affects their function, the ability of the cells to perform homologous recombination (HR) was assessed (see section 2.5.8 for details). As expected, DR3 cells expressing endogenous SENP7 (treated with non-targeting siRNA and transfected with empty vector) were capable of carrying out HR close to the efficiency of those cells expressing WT Flag-SENP7 (treated with SENP7 siRNA and WT Flag-SENP7 vector transfected) (Figure 3.5a). In cells expressing no SENP7 (treated with SENP7 siRNA and only empty vector pcDNA5.0 transfected) the percentage of HR relative to WT was less than 40%. In all other samples, endogenous SENP7 was knocked down and various mutants of SENP7 were transfected in. The CA, SIMless and SIMlessCA mutants failed to rescue the HR ability of the cells.

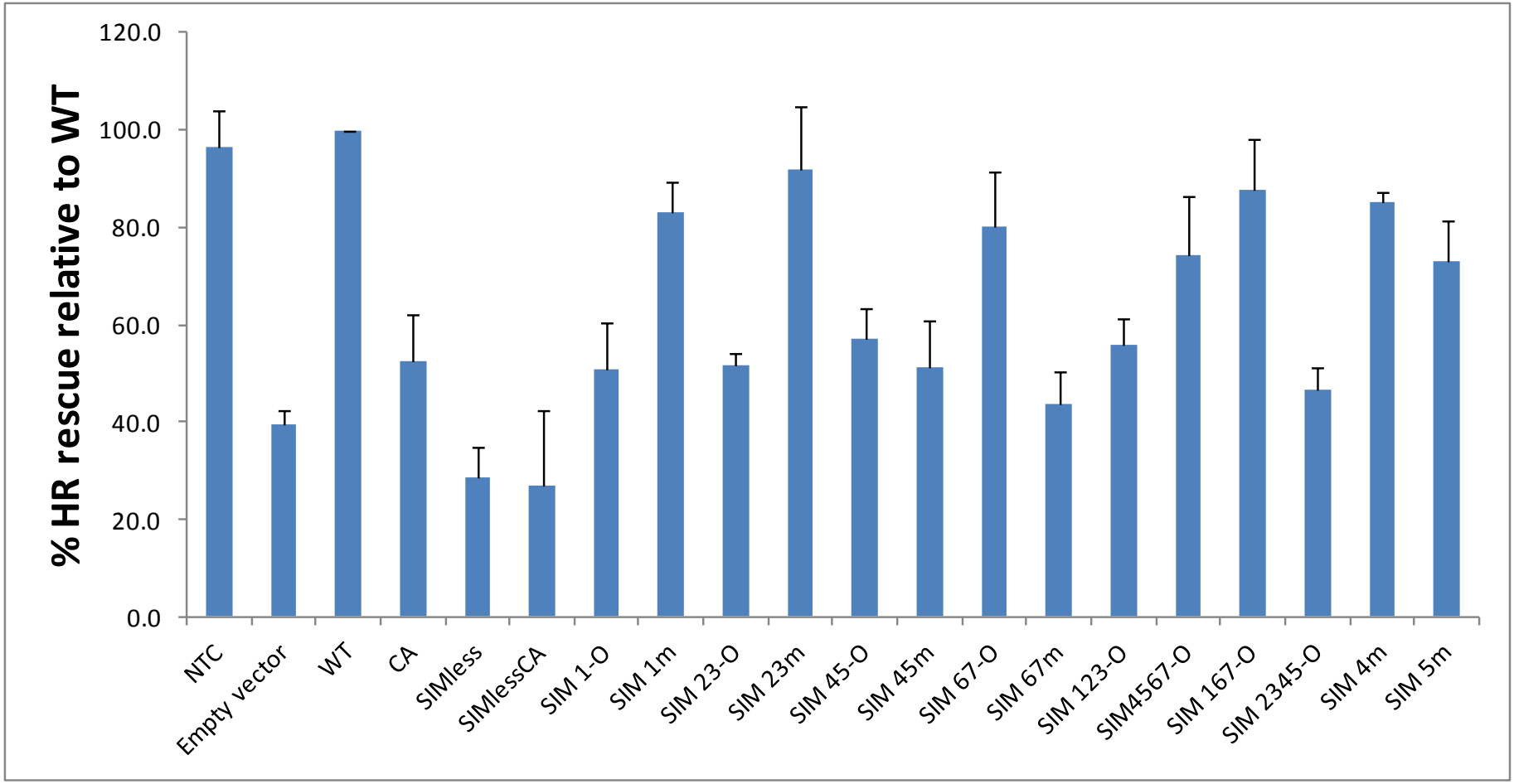

Figure 3.5a – Some SIM Mutants are able to Rescue the Cells Ability to Perform Repair of DSBs via Homologous Recombination Better than Others. DR3 (Hela) cells had their endogenous SENP7 knocked down via siRNA. Control cells were instead exposed to non-targeting siRNA. After 24 hours the media was changed and the cells were cotransfected with the various SIM mutant constructs (or empty vector) as indicated, an RFP vector and a SceI recombinase encoding vector. After a further 48 hours, cells were harvested and fixed using 4% PFA. PFA was subsequently removed and cells resuspended in PBS, before analysis by fluorescent cell sorting (FACs). N.B. These results are representative of at least 3 separate experiments, each performed with 3 repeats for each sample. Error bars are shown for standard error.

Table 3.5 – SIM Mutants Statistical Difference to SIMless SENP7 in HR Capability. A paired, two-sided, Student's t test was used to statistically analyse the change in HR capability of the cells when transfected with the various SIM mutants in comparison to SIMless SENP7.

	% HR rescue relative to WT	SD	df	t value	Statistical significance? (where P<0.05)
SIM 1-O	50.8	14	4	1.93	No
SIM 1m	83.0	10.7	4	6.20	Yes
SIM 23-O	51.5	8.3	4	3.36	Yes
SIM 23m	92	16.2	4	4.80	Yes
SIM 45-O	56.9	10.9	4	3.18	Yes
SIM 45m	51.1	14.4	4	1.91	No
SIM 67-O	80.3	15.7	4	4.02	Yes
SIM 67m	43.6	11.4	4	1.60	No
SIM 123-O	55.9	9.4	5	3.77	Yes
SIM 4567-O	74.1	16.9	4	3.30	Yes
SIM 167-O	87.7	15.0	4	4.82	Yes
SIM 2345-O	46.7	9.3	4	2.36	No
SIM 4m	85.0	8.4	4	8.24	Yes
SIM 5m	73.2	12.4	4	4.38	Yes

No statistical difference was observed when comparing the average % HR rescue (relative to WT) of SIMless SENP7 to SIM 1-O, 45m, 67m and 2345-O (Table 3.5). If the % of HR rescue observed with the SIMless construct of SENP7 is taken as non-rescuing, then it is possible to say that at the 5% level of significance from the Null hypothesis, the SIM mutants mentioned above are also non-rescuing. Meanwhile, the other SIM mutants indicated in Table 3.5 show some level of significant HR rescue in comparison to SIMless SENP7. The SIM mutants 1m, 23m, 67-O, 167-O, 4m, and 5m show the highest t values (Table 3.5) and therefore greater degrees of significant difference from the non-rescuing SIMless. They are also shown to have the highest % HR rescue relative to WT SENP7 in Figure 3.5a. This statistically highlights some mutants as having greater HR capability than others.

To identify if some of the potential SIMs appear to be more important for SENP7 functionality than others, the mutants have been paired in Figure 3.5a

according to the functional SIMs they possess in an attempt to make comparison easier. SIM 1-only has been shown to not rescue HR whilst SIM 1m rescues HR to over 80% of that of WT SENP7. As SIM 1 mutated still contains 6 functional SIMs this result was to be expected. Similar results are seen with the 23-O and 23m mutant, respectively. This suggests a possible hypothesis of the number of functional SIMs left within a mutant correlating to protein function and such a theory would appear logical. However, the trend does not continue with regards to the mutants 45-only and 45-mutated, and also the 67-O and 67m. Neither 45-O or 45m rescued HR. Considering the 67-O mutant rescued HR to almost 80% of WT SENP7, it would be expected that the SIM 45mutated would be capable of such a level of rescue also, as it obviously contains two functional 6 and 7 SIMs. When comparing the rescue seen with the 67-O and 67m alone, it would be possible to argue that SIMs 6 and 7 seem particularly important for SENP7 function. This hypothesis also remains true when considering the high levels of rescue seen with 4567-O and 167-O. Their respective reciprocal SIM mutants, 123-O and 2345-O, do not exhibit significant levels of rescue and coincidently do not contain SIMs 6 and 7. The mutants 4m and 5m also show good levels of HR rescue relative to WT, both of which contain 6 functional SIMs out of 7, including numbers 6 and 7.

As SENP7 has been shown to be preferential to binding to poly-SUMO-2/3 chains it is conceivable and would appear logical, as mentioned above, that the greater the number of functional SIMs left within any SIM mutant the greater the ability to bind poly-SUMOylated proteins. To test this hypothesis the % HR rescue results for each SIM mutant containing the same number of functional SIMs as an average was plotted against the number of functional SIMs (Figure 3.5b). A relatively strong correlation can be seen between the number of functional SIMs and HR rescue. Whilst a clear correlation is visible, it is also clear that simply the number of functional SIMs remaining within SENP7 does not explain all the results seen. This is expected, as some SIMs may be of more importance for SUMO interaction and protein function than others, which has been eluded to already with SIMs 6 and 7. The greater importance of some SIMs over others can explain the relatively big standard error bars observed in Figure 3.5b. For example, whilst the 67m variant has 5 functional SIMs out of 7 it does not rescue HR. This could be due to it missing the two SIMs which appear to be more crucial than any of the others and therefore, the

standard error bar seen for 5 functional SIMs is large and the average skewed below the trendline (Figure 3.5b).

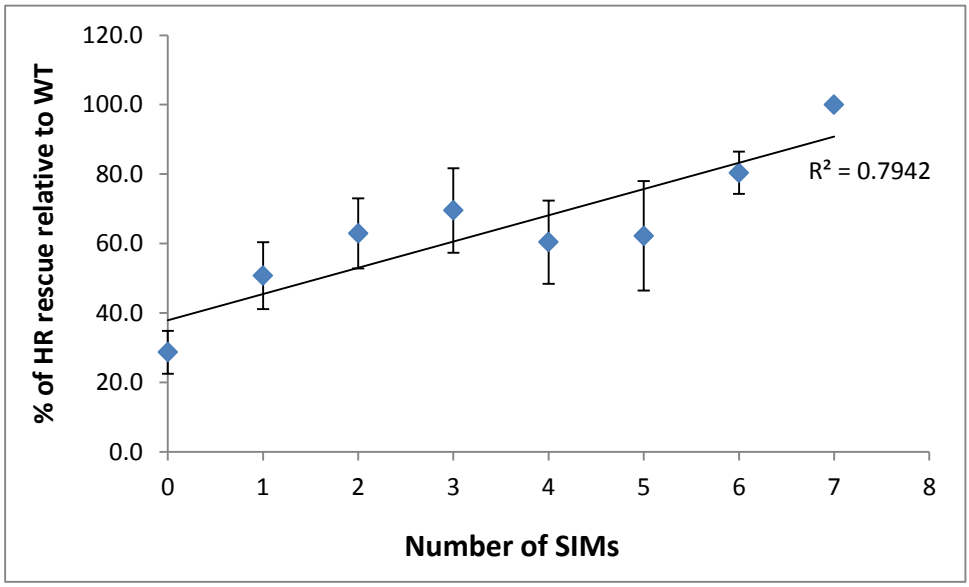

Figure 3.5b – Averaged Results for the Number of Non-Mutated SIMs Present within SENP7 Correlates with Function of the Protein. A scatter graph plotting percentage of HR rescue relative to WT against the number of functional SIMs within the SENP7 construct (averaged results for all variants with the same number of variant SIMs). N.B. Error bars are shown for standard error.

Using the densitometry readings from the IP showing the various SIM mutants interacting with SUMO2-Q90P, it is possible to investigate a relationship between strength of SUMO-binding and HR capability. The two variables do not appear to show correlation (Figure 3.5c). SIM mutants 4567-O, 67-O and 167-O show both good SUMO2-binding and HR rescue ability, whilst SIM mutants 123-O and 2345-O also exhibit good SUMO2-binding ability but their HR rescue capabilities are limited. Therefore, the story of SIM:SUMO interaction within SENP7 is probably a rather complex one. Whilst some trends have been observed in the results, no SIM can be defined as completely redundant or completely essential in SUMO binding or SENP7 function.

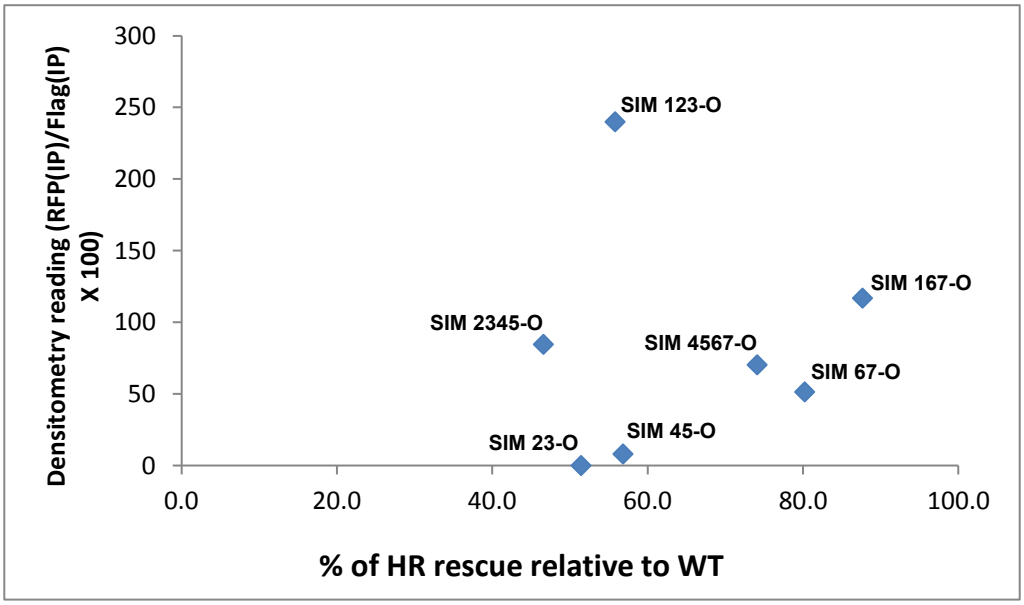

Figure 3.5c – Binding Capability of the SIM Mutants to SUMO Does Not Correspond to HR Activity. A scatter graph plotting the binding capabilities of various SIM mutants (densitometry reading) versus the percentage of HR rescue relative to WT SENP7. (N.B. Note that SIM 1-O has not been included as its densitometry reading was falsified due to the smudging of the blot).

3.6 – SENP7 Interacts with KAP-1

KAP-1 (TIF1-β – transcription intermediary factor 1- β) coimmunoprecipitated with SENP7 (Figure 3.6). KAP-1 is known to be modified by SUMOylation and co-localise with other numerous DNA damage response factors at DNA lesions [66,67]. KAP-1 is therefore very likely a substrate for deSUMOylation by SENP7. It also contains a HP1 box, like that of SENP7, and has been shown to interact with HP1-α [68]. Therefore, these 3 proteins probably interact as part of a complex. Across the 3 repeat blots, WT showed little to no interaction with KAP-1, whilst CA and SIMless exhibited good interaction and SIMlessCA significantly less than these two. It should be noted that the inputs for the WT SENP7 extract are down in comparison to the other extracts which does make interpretation a little difficult.

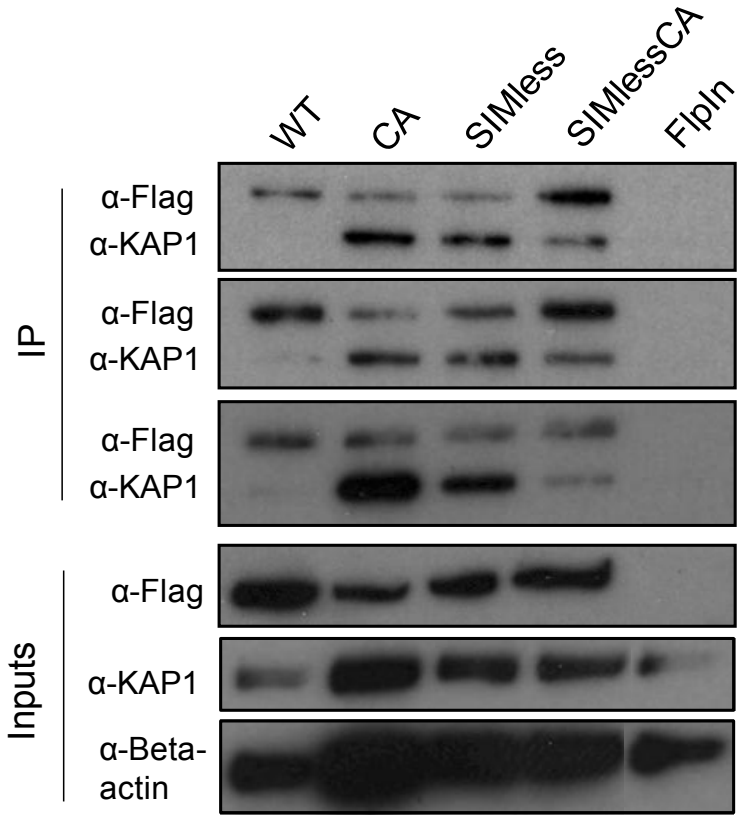

Figure 3.6 – SENP7 Interacts with KAP1 *in Vivo*. The various stable SENP7 cell lines were induced with 2µg/ml doxycycline two days prior to making cell lysates. Regular untreated FlpIn cells were used as a control. Lysates were then incubated with Flag(M2) Ab-coated beads for 24 hours at 4°C. A series of PBS washes were made, before addition of Laemmli buffer, heating at 95°C and subjecting to Western blotting.

Chapter Four:

Discussion

4. Discussion

Previous work in this laboratory had shown both SENP6 and SENP7 to be required for efficient repair of DSBs by HR. The effects of knocking down SENP6 could be rescued by over-expression of RFP-SUMO suggesting it was a decrease in availability of SUMO due to lack of SENP6 that caused the HR defect. However, such rescue was not observed in SENP7-depleted cells, preluding to a more direct role for SENP7 in HR. In addition, it was found to be recruited to sites of DNA repair and co-localise with γ-H2AX in response to damage mediated by hydroxyurea. Other studies had shown SENP7 to preferentially cleave poly-SUMO-2/3 chains [54,55]. Therefore, it was expected that the protein would employ SUMO-interaction motifs (SIMs) to bind SUMO and analysis of primary structure identified 7 potential SIMs within SENP7 outside of catalytic domain.

The creation of various SIM mutants allowed the investigation of which of the potential SIMs of SENP7 exhibited SUMO-binding activity and were required for efficient functionality of the protein. The methods of which are explained in section 3.1 and the results were a series of Flag-tagged-SENP7 constructs with only a selected number of the 7 potential SIMs retaining function (Table 3.1).

Both in previous, unpublished work within our laboratory and within [64], SENP7 was shown to co-localise to heterochromatin within the nucleus through its interaction with HP1-α. The work presented in this study showed that none of the mutant variants of SENP7, including CA, SIMless, SIMlessCA and all of the SIM mutant variants, perturbed this co-localisation. This was expected as SENP7 was shown to bind HP1-α through a HP1 box domain with no relation to the SIMs of SENP7. With localisation of all the mutants confirmed to be the same as WT, the SUMO-binding and functionality of these proteins could be investigated in the knowledge that cellular localisation was not affecting the results.

Employing the use of a catalytic-resistant variant of SUMO-2 (RFP-SUMO-2-Q90P), co-immunoprecipitation studies revealed the interaction of WT and CA SENP7 with SUMO-2 modified proteins. Critically important to this study was the observation that the SIMless and SIMlessCA mutants (devoid of all functional SIMs) exhibited a greatly significant decrease in interaction with SUMO-2 (Figure 3.4a). This confirmed the requirement of the SIMs for interaction with SUMO-2 modified

proteins. It was now possible to pursue an answer to the question: which of the potential SIMs possess SUMO-binding activity?

Further co-IP studies revealed that some SIM mutant variants bound to SUMO-2 modified proteins with greater efficiency than others. The mutants SIM 67-only, SIM 4567-only, SIM 167-only, SIM 123-only and SIM 2345-only all exhibited good interaction with SUMO-2, whilst the mutants SIM 23-O and SIM 45-O did not (Figure 3.4b). It was now of interest to investigate if this binding capability of the SIM mutants correlated with the functionality of these proteins. This was assessed in terms of the cells ability in which these mutants were being expressed (with endogenous SENP7 knocked down) to carry out DSB DNA repair by HR.

As already known due to previous work completed in the laboratory, the CA and SIMless mutants were unable to perform HR to the levels of that of WT SENP7. These results were duplicated within this study and confirmed the requirement of SENP7 for effective execution of HR repair. SIMlessCA SENP7 produced similar results to that of the SIMless, as expected. Meanwhile, the various SIM mutants were shown to have varying levels of HR rescue relative to WT SENP7. Firstly, a clear trend could be seen in that all SIM mutants retaining functional SIMs 6 and 7 (SIM 1m, SIM 23m, SIM 67-O, SIM 4567-O, SIM 167-O, SIM 4m and SIM 5m), with the exception of SIM 45m, rescued HR to above 73% relative to WT (Figure 3.5a). This highlighted these SIMs as of greater importance for protein function over the other SIMs. Whilst the SIM mutants above did show good levels of HR rescue, none rescued to the same level as that of WT, including those with just one SIM mutated. This highlights the fact that whilst SIMs 6 and 7 do appear to be of more importance for SENP7 function, they are not capable of fully rescuing the protein's functionality on their own. The mutation of SIM 1, 4 or 5 alone also had an affect on HR capability, as none of these mutants rescued HR to the levels of WT, suggesting no single SIM is completely redundant. However, to make this conclusion definite, investigations would be needed with single SIM mutants for each individual SIM.

A correlation was also observed between the number of functional SIMs retained within the protein and HR capability (Figure 3.5b). This would appear logical when considering the known preference of SENP7 for binding to poly-SUMO-2/3 chains [55]. Another protein found to preferentially bind poly-SUMO-2/3 chains is the SUMO-targeted ubiquitin ligase, Ringer finger protein 4 (RNF4). This preferentiality has been shown to be due to a set of tandem SIMs that can recognise

two or more SUMO-2/3 molecules in a chain [65]. SENP7's 7 potential SIMs do not appear in tandem (Figure 1.8a), however, due to the known flexibility of the protein in the region of these SIMs their somewhat scattered location upon the primary structure of the protein may not be of importance. The results of this study do suggest that the more functional SIMs available to interact with the SUMOs of the chain the greater the strength of binding and better functionality of the protein.

Surprisingly, there did not appear to be a relationship between strength of SUMO-binding and protein function (HR capability) of the various mutants investigated (Figure 3.5d). Whilst mutants 4567-O, 67-O and 167-O showed both good SUMO-2 binding and HR rescue ability, mutants 123-O and 2345-O exhibited good SUMO-2 binding with only limited HR rescue capabilities. A potential explanation for this anomaly may lie within the structure of SENP7. Whilst it has been shown that SENP7 is highly flexible outside of its N-terminal catalytic domain, it is possible that the 123-O and 2345-O mutants can bind SUMO effectively, but cannot efficiently deliver it to the catalytic site for cleavage. Conversely, when SIMs 6 and 7 bind SUMO they may be able to deliver SUMO to the catalytic site with greater efficiency. SIMs 6 and 7 being in closer proximity to the catalytic domain in terms of primary amino acid sequence although applicably logical to such a theory, is probably of little significance as SENP7 is thought to be highly flexible outside of the catalytic domain. Only structural analysis of the whole protein in conjugation to SUMO-conjugated proteins will resolve such a theory, which to date has been beyond the reach of crystallographic studies. It therefore seems the story of SIM:SUMO interaction within SENP7 is probably a rather complex one. Whilst some trends have been observed in the results, no SIM can be defined as completely redundant or completely essential in SUMO binding or SENP7 function.

Finally, our study was able to reveal a possible substrate of SENP7's for deSUMOylation, KAP-1. KAP-1 is a nuclear protein, which amongst its known roles in the regulation of transcriptional repression and activation, has been shown to be involved in the DDR [69]. It co-localises with 53BP1, H2AX, BRCA1, and TopBP1 (DNA damage response proteins) at DNA lesions [67]. KAP-1 is also known to interact with HP1-α through the presence of a HP1 box, like that of SENP7 [68]. The differences in KAP-1 interaction seen with the various forms of SENP7 could be explained as follows. The little to no interaction of WT SENP7 with KAP-1 is explained by the fact that SENP7 will be binding and cleaving the SUMO chains

attached to KAP-1 very dynamically. CA SENP7 shows strong interaction as the two will bind, but no cleavage activity is possible to release KAP-1. SIMless SENP7 shows similar levels of interaction to the CA mutant. This is not through SENP7's interaction with the SUMO-modified KAP-1, but instead due to SENP7 and KAP-1 remaining in a complex through their independent HP1-α binding. The reduced interaction seen with the SIMlessCA mutant cannot yet be explained, however, it is possible that this could be explained by further complexities and interactions not yet known within the complex.

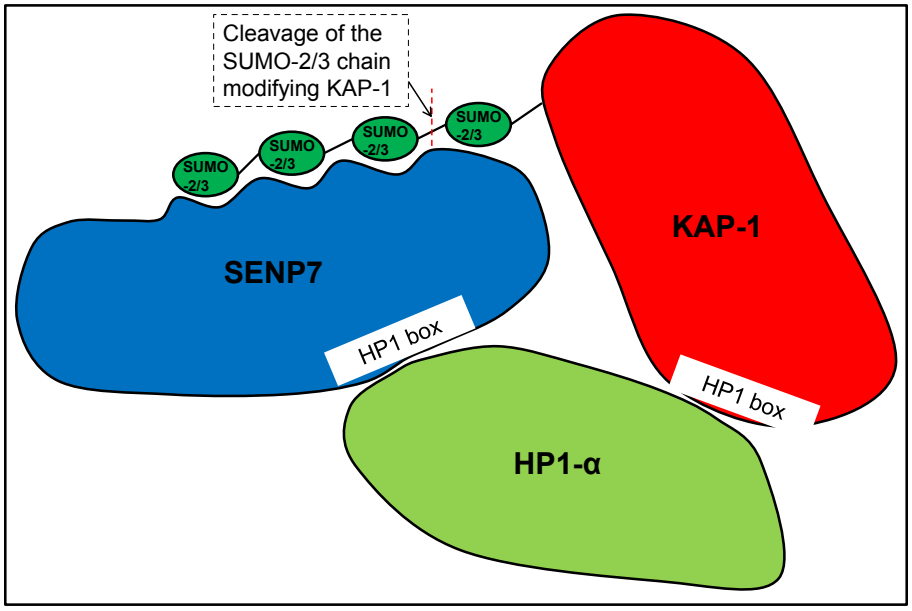

Figure 4.0 – Schematic Detailing the Possible Interactions of SENP7, KAP-1 and HP1-α. SENP7 interacts with the poly-SUMO-2/3 chain modifying KAP-1 through its SIMs and can cleave the chain. The HP1 boxes of SENP7 and KAP-1 allow interaction with HP1-α.

4.1 Limitations

To further analyse the requirement of each individual SIM for protein function SENP7 constructs in which SIM 2, SIM 3, SIM 6 and SIM 7 were mutated alone would have been useful in determining whether any SIM is completely redundant. Conversely, it would also have allowed the analysis of SIM 6 and SIM 7 individually. These SIMs were shown to be of greater importance than others, however, in all of the mutants constructed they existed as a pair (either both being mutated, or both being functional). Unfortunately, these mutants could not initially be made due to the limited availability of forward and reverse SENP7 primers required in their synthesis.

When it came to the point in which their importance was realised not enough time remained within the project to construct these mutants and analyse their behaviour. Indeed, the length of the 3 month short project was a limiting factor within the study.

Whilst stable lines were eventually available for the WT, CA, SIMless and SIMlessCA constructs of SENP7, they were not for all of the SIM mutants. Stable cell lines would have eased the production of large amounts of SENP7 protein required for the co-IP experiments.

4.2 Future Work

To order the required forward and reverse primers required to create the single SIM mutants would circumvent the limitations of this study mentioned above. The making of stable cell lines for the SIM mutants constructs had started before the end of my project, however, not in time for my use. Successful creation of these cell lines would have been very useful. Further repeats of the HR assay would verify the data already collected and help make stronger conclusions upon which SIMs were most important for SUMO-binding and function of SENP7.

It would also be of great interest to carry out further investigation of the interaction between SENP7 and KAP-1 and particularly if it is significant to the DDR. DNA damage could be induced within cells (e.g. through ionizing irradiation) and the levels of SENP7 and KAP-1 interaction monitored at various time points by co-immunoprecipitation studies. This would give an indication to whether these proteins' interactions are increased or decreased during DNA damage response and if so this would suggest a role in the DDR.

Chapter Five:

References

[1] Haley B., Paunesku T., Protić M., et al.. Response of heterogeneous ribonuclear proteins (hnRNP) to ionizing radiation and their involvement in DNA damage repair. *Int J Radiat Biol*. 2009;85:643-655.

[2] Dreyfuss G., Matunis M.J., Pinol-Roma S., et al.. hnRNP Proteins and the Biogenesis of mRNA. *Annual Review of Biochemistry*. 2003;62:289-321.

[3] Gabler, S., Schutt, H., Groitl, P., et al.. E1B 55-kilodalton-associated protein: a cellular protein with RNA-binding activity implicated in nucleocytoplasmic transport of adenovirus and cellular mRNAs. *J. Virol*. 1998;72;7960-7971.

[4] Polo S., Blackford A., Chapman J. et al. Regulation od DNA-End Resection by hnRNPU-like Proteins Promotes DNA Double-Strand Break Signaling and Repair. *Mol Cell*. 2012;45:1-12.

[5] Asparuhova M.B., Ferralli J., Chiquet M. et al.. The transcriptional regulator megakaryoblastic leukemia-1 mediates serum response factor-independent activation of tenascin-C transcription by mechanical stress. *The FASEB Journal.* 2011;25:3477-3488.

[6] Chaudhury A., Chander C. and Howe P.H. Heterogeneous nuclear ribonucleoproteins (hnRNPs) in cellular processes: Focus on hnRNP E1's multifunctional regulatory roles. *RNA*. 2010;16:1449-1462.

[7] Barral P.M., Rusch A., Turnell A.S., et al.. The interaction of the hnRNP family member E1B-AP5 with p53. *FEBS Letters*. 2005;579:2752-2758.

[8] Kzhyshkowska J., Rusch A., Wolf H., et al.. Regulation of transcription by the heterogenous nuclear ribonucleoprotein E1B-AP5 is mediated by complex formation with the novel bromodomain-containing protein BRD7. *Biochem. J*. 2003;371:385-393.

[9] Bruton R.K., Rasti1 M., Mapp K.L., et al.. C-terminal-binding protein interacting protein binds directly to adenovirus early region 1A through its N-terminal region and conserved region 3. *Oncogene*. 2007;26:7467-7479.

[10] Jackson S. and Bartek J. The DNA-damage response in human biology and disease. *Nature*. 2009;461:1071-1078.

[11] Vousden K.H. and Prives C. Blinded by the Light: The Growing Complexity of p53. *Cell*. 2009;137:413-431.

[12] Mao Z., Bozzella M., Seluanov A., et al.. DNA repair by nonhomologous end joining and homologous recombination during cell cycle in human cells. *Cell Cycle*. 2008;7:2902-2906.

[13] Anderson D.B., Wilkinson K.A. and Henley J.M. Protein SUMOylation in neuropathological conditions. *Drug News Perspect*. 2009;22:255-265.

[14] Derheimer F.A. and Kastan M.B. Multiple roles of ATM in monitoring and maintaining DNA integrity. *FEBS Letters*. 2010;584:3675–3681.

[15] Stewart G.S., Panier S., Townsend K., Al-Hakim A.K., et al.. The RIDDLE Syndrome Protein Mediates a Ubiquitin-Dependent Signaling Cascade at Sites of DNA Damage. *Cell*. 2009;136:420-434.

[16] Bekker-Jensen S. and Mailand N. Assembly and function of DNA double-strand break repair foci in mammalian cells. *DNA Repair*. 2010;9:1219–1228.

[17] Sartori A.A., Lukas C., Julia Coates J., et al.. Human CtIP promotes DNA end resection. *Nature*. 2007;450:509-515.

[18] Filippo J.S., Sung P., and Klein H. Mechanism of Eukaryotic Homologous Recombination. *Annu. Rev. Biochem*. 2008;77:229-257.

[19] Schaeper U., Subramanian T., Lim L., et al.. Interaction between a cellular protein that binds to the C-terminal region of adenovirus E1A (CtBP) and a novel cellular protein is disrupted by E1A through a conserved PLDLS motif. *J Biol Chem*. 1998;273:8549-8552.

[20] Yu X., Fu S., Lai M., et al.. BRCA1 ubiquitylates its phosphorylation-dependent binding partner CtIP. *Genes Dev*. 2006;20:1721-1726.

[21] Yun M.H. and Hiom K. CtIP2BRCA1 modulates the choice of DNA double-strand-break repair pathway throughout the cell cycle. *Nature*. 2009;459:460-464.

[22] You Z. and Bailis J.M. DNA damage and decisions: CtIP coordinates DNA repair and cell cycle checkpoints. *Trends in Cell Biology*. 2010;20:402-409.

[23] Wu L., Bachrati C.Z., Ou J., et al.. BLAP75/RMI1 promotes the BLM-dependent dissolution of homologous recombination intermediates. Proc. Natl. Acad. Sci. USA. 2006;103:4068-4073.

[24] Bugreev D.V., Yu X., Egelman E.H., et al.. Novel pro- and anti-recombination activites of the Bloom's syndrome helicase. *Genes Dev*. 2007;21:3085-3094.

[25] Karow J.K., Constantinou A., Li J.L., et al.. The Bloom's syndrome gene product promotes branch migration of Holliday junctions. *PNAS*. 2000;97:6504-6508.

[26] Ellis N.A., Sander M., Harris C.C., et al.. Bloom's syndrome workshop focuses on the functional specificities of RecQ helicases. *Mechanisms of Ageing and Development*. 2008;129:681-691.

[27] Payne M. and Hickson I.D. Genomic instability and cancer: lessons from analysis of Bloom's syndrome. *Biochem. Soc. Trans*. 2009;37:553-559.

[28] Nimonkar A.V., Ozsoy A.Z., Genschel J., et al.. Human exonuclease 1 and BLM helicase interact to resect DNA and initiate DNA repair. *Proc. Natl. Acad. Sci. USA*. 2008;105:16906-16911.

[29] Yang J., Bachrati C.Z., Ou J., et al.. Human Topoisomerase IIIα Is a Single-stranded DNA Decatenase That Is Stimulated by BLM and RMI1. *The Journal of Biological Chemistry*. 2010;28:21426-21436.

[30] Iwanaga K., Sueoka N., Sato A., Hayashi S., et al.. Heterogeneous nuclear ribonucleoprotein B1 protein impairs DNA repair mediated through the inhibition of DNA-dependent protein kinase activity. *Biochemical and Biophysical Research Communications*. 2005;333:888-895.

[31] Zhang S., Schlott B., Gorlach M., et al.. DNA-dependent protein kinase (DNA-PK) phosphorylates nuclear DNA helicase II/RNA helicase A and hnRNP proteins in an RNAdependent manner. *Nucleic Acids Research*. 2004;32:1-10.

[32] Moumen A., Masterson P., O'Connor M.J., et al.. hnRNP K: An HDM2 Target and Transcriptional Coactivator of p53 in Response to DNA Damage. *Cell*. 2005;123:1065-1078.

[33] Blackford A.N., Bruton R.K., Dirlik O., et al.. A Role for E1B-AP5 in ATR Signalling Pathways during Adenovirus Infection. Journal of Virology. 2008;82:7640-7652.

[34] Sengupta S., Robles A.I., Linke, S.P., et al.. Functional interaction between BLM helicase and 53BP1 in a Chk1-mediated pathway during S-phase arrest. *The Journal of Cell Biology*. 2004;166:801-813.

[35] Srivastava V., Modi P., Tripathi V. et al. BLM helicase stimulates the ATPase and chromatin-remodelling activites of RAD54. *J Cell Sci*. 2009;122:3093-3103.

[36] Chou M.Y., Underwood J.G., Nikolic J., et al.. Multisite RNA Binding and Release of Polypyrimidine Tract Binding Protein during the Regulation of *c-src* Neural-Specific Splicing. *Molecular Cell*. 2000;5:949–957.

[37] Kim D.H., Langlois M.A., Lee K.B., et al.. HnRNP H inhibits nuclear export of mRNA containing expanded CUG repeats and a distal branch point sequence. *Nucleic Acids Research*. 2005;33:3866-3874.*Acids Research*. 2005;33:3866-3874.

[38] Torosyan Y., Dobi A., Glasman M., et al.. Role of multi-hnRNP nuclear complex in regulation of tumor suppressor ANXA7 in prostate cancer cells. *Oncogene.* 2010;29:2457-2466.

[39] Chen L., Nievera C.J., Yueh-Luen Lee A., et al.. Cell cycle-dependent complex formation of BRCA1/CtIP/MRN is important for DNA double-strand break repair. *Journal of Biological Chemistry.* 2008;283:7713-7720.

[40] Russell B., Bhattacharyya S., Keirsey J., et al.. Chromosome Breakage Is Regulated by the Interaction of the BLM Helicase and Topoisomerase IIα. *Cancer Research.* 2011;71:561-571.

[41] De Vos M., Schreiber V. and Francoise Dantzer F. The diverse roles and clinical relevance of PARPs in DNA damage repair: Current state of the art. *Biochemical Pharmacology*. 2012;84:137-146.

[42] Krishnakumar R. and Kraus WL. The PARP side of the nucleus: molecular actions, physiological outcomes, and clinical targets. *Mol. Cell*. 2010;39:8-24.

[43] Van Wijk S.J.L., Muller S. And Dikic I. Shared and unique properties of ubiquitin and SUMO interaction networks in DNA repair. Genes Dev. 2011;25:1763-1769.

[44] Gareau J.R. and Lima C.D.. The SUMO pathway: emerging mechanisms that shape specificty, conjugation and recognition. *Nature Reviews*. 2010;11:861-871.

[45] Melchior F., Schergaut M. And Pichler A. SUMO: ligases, isopeptidases and nuclear pores. *TRENDS in Biochemical Sciences.* 2003;28:612-618.

[46] Rodriguez M.S., Dargemont C. and Hay R.T. SUMO-1 conjugation *in vivo* requires both a consensus modification motif and nuclear targeting. *J. Biol. Chem.* 2001;276:12654–12659.

[47] Matic I., van Hagen M. and Schimmel J. In vivo identification of human SUMO polymerization sites by high accuracy mass spectrometry and an in vitro to in vivo strategy. *Mol. Cell. Proteomics.* 2007;7:132-144.

[48] Hay R. SUMO-specific proteases: a twist in the tail. *TRENDS in Cell Biology.* 2007;17:370-376.

[49] Reverter D. And Lima C.D. Insights into E3 ligase activity revealed by a SUMO-RanGAP1-Ubc9-Nup358 complex. *Nature.* 2005;435:687-692.

[50] Song J., Zhang Z., Hu W. et al. Small ubiquitin-like modifier (SUMO) recognition of a SUMO binding motif: a reversal of the bound orientation. *J. Biol. Chem.* 2005;33:201-208.

[51] Kerscher O. SUMO junction-what's your function? New insights through SUMO-interacting motifs. *EMBO Rep.* 2007;8:550-555.

[52] Bernardi R. and Pandolfi P.P. Structure, dynamics and functions of promyelocytic leukaemia nuclear bodies. *Nature Rev. Mol. Cell Biol.* 2007;8:1006-1016.

[53] Meulmeester E., Kunze M., Hsiao H.H. et al. Mechanism and consequences for paralog-specific sumoylation of ubiquitin-specific protease 25. *Mol. Cell.* 2008;30:610-619.

[54] Mukhopadhyay D., Ayaydin F., Kolli N. et al. SUSP1 antagonizes formation of highly SUMO2/3-conjugated species. *J. Cell. Biol*. 2006;174:939-949.

[55] Lima C.D. and Reverter D. Structure of the human SENP7 catalytic domain and poly-SUMO deconjugation activities of SENP6 and SENP7. *J. Biol. Chem*. 2008;46:32045-32055.

[56] Bergink S. and Jentsch S. Principles of ubiquitin and SUMO modifications in DNA repair. *Nature.* 2009;458:461-467.

[57] Morris J.R., Boutell C., Keppler M. et al. The SUMO modification pathway is involved in the BRCA1 response to genotoxic stress. *Nature.* 2009;462:886-891.

[58] Galanty Y., Belotserkovskaya R., Coates J. Mammalian SUMO E3-ligases PIAS1 and PIAS4 promote responses to DNA double-strand breaks. *Nature*. 2009;462:935-939.

[59] Moldovan G.L., Pfander B. and Jentsch S. PCNA, the maestro of the replication fork. *Cell*. 2007;129:665–679.

[60] Hoege C., Pfander B., Moldovan G.L.. RAD6-dependent DNA repair is linked to modification of PCNA by ubiquitin and SUMO. *Nature*. 2002;419:135-141.

[61] Pfander B., Moldovan G.L., Sacher M. SUMO-modified PCNA recruits Srs2 to prevent recombination during S phase. *Nature*. 2005;436:428-433.

[62] Dou H., Huang C., Nguyen T.V. et al. SUMOylation and de-SUMOylation in response to DNA damage. *FEBS Letters*. 2011;585:2891-2896.

[63] Felberbaum R. and Hochstrasser M. Ulp2 and the DNA damage response: Desumoylation enables safe passage through mitosis. *Cell Cycle*. 2008;7:52-56.

[64] Maison C., Romeo K., Bailly D. et al. The SUMO protease SENP7 is a critical component to ensure HP1 enrichment at pericentric heterochromatin. *Nature Structural and Molecular Bilogy. 2012*;19:458-460.

[65] Tatham M.H., Geoffroy M.C., Shen L. et al. RNF4 is a poly-SUMO-specific E3 ubiquitin ligase required for arsenic-induced PML degradation. *Nature Cell Biology.* 2008;10:538-546.

[66] Li X., Lee Y.K., Jeng J.C. et al.. Role for KAP1 serine 824 phosphorylation and sumoylation/desumoylation switch in regulating KAP1-mediated transcriptional repression. *J. Biol. Chem*. 2007;282:36177-36189.

[67] White D.E., Negorev D., Peng H. et al.. KAP1, a novel substrate for PIKK family members, colocalizes with numerous damage response factors at DNA lesions. *Cancer Res*. 2006;66:11594-11599.

[68] Peng H., Gibson L.C., Capili A.D. et al.. The structurally disordered KRAB repression domain is incorporated into a protease resistant core upon binding to KAP-1-RBCC domain. *J. Mol. Biol*. 2007;370:269-289.

[69] Ryan R.F., Schultz D.C., Ayyanathan K., et al.. KAP-1 corepressor protein interacts and colocalizes with heterochromatic and euchromatic HP1 proteins: a potential role for Kruppel-associated box-zinc finger proteins in heterochromatin-mediated gene silencing. *Mol. Cell. Biol*. 1999;19:4366-4378.